2017-12-01

Acoustic Intensity of Narrowband Signals in Free-Field Environments

Kelli Fredrickson Succo
Brigham Young University

Acoustic Intensity of Narrowband Signals in Free-Field Environments

Kelli Fredrickson Succo

A thesis submitted to the faculty of
Brigham Young University
in partial fulfillment of the requirements for the degree of

Master of Science

Scott D. Sommerfeldt, Chair
Kent L. Gee
Tracianne B. Neilsen

Department of Physics and Astronomy

Brigham Young University

ABSTRACT

Acoustic Intensity of Narrowband Signals in Free-Field Environments

Kelli Fredrickson Succo
Department of Physics and Astronomy, BYU
Master of Science

The phase and amplitude gradient estimator (PAGE) method has proven successful in improving the accuracy of measured energy quantities over the p-p method, which has traditionally been used, in several applications. One advantage of the PAGE method is the use of phase unwrapping, which allows for increased measurement bandwidth above the spatial Nyquist frequency. However, phase unwrapping works best for broadband sources in free-field environments with high coherence. Narrowband sources often do not have coherent phase information over a sufficient bandwidth for a phase unwrapping algorithm to unwrap properly. In fact, phase unwrapping processing can cause significant error when there is no coherent signal near and above the spatial Nyquist frequency. However, for signals at any frequencies up to the spatial Nyquist frequency, the PAGE method provides correct intensity measurements regardless of the bandwidth of the signal. This is an improved bandwidth over the traditional method. For narrowband sources above the spatial Nyquist frequency, additional information is necessary for the PAGE method to provide accurate acoustic intensity. With sufficient bandwidth and a coherence of at least 0.1 at the spatial Nyquist frequency, a relatively narrowband source above the spatial Nyquist frequency can be unwrapped accurately. One way of using extra information, called the extrapolated PAGE method, uses the phase of a tone below the spatial Nyquist frequency and an assumption of a propagating field, and therefore linear phase, to extrapolate the phase above the spatial Nyquist frequency. Also, within certain angular and amplitude constraints, low-level broadband noise can be added to the field near a source emitting a narrowband signal above the spatial Nyquist frequency. The low-level additive broadband noise can then provide enough phase information for the phase to be correct at the frequencies of the narrowband signal. All of these methods have been shown to work in a free-field environment.

Keywords: acoustic intensity, narrowband, phase unwrapping, sine wave, sawtooth wave, fan noise, spatial Nyquist frequency, bandwidth extension

ACKNOWLEDGMENTS

When people used to ask me why I chose the Physics Department at BYU for graduate school, I used to tell them that it came down to the 3 F's: faculty, funding, and food (thanks, Nan!). Later, a fourth F, family, made me really glad I stuck around in Provo.

In all seriousness, I am beyond grateful for the education I have received here. All of the acoustics faculty—Dr. Sommerfeldt, Dr. Gee, Dr. Neilsen, Dr. Leishman, Dr. Anderson, and Dr. Blotter—have helped me and significantly contributed to my learning. Not only were the classes they taught incredibly valuable, but they were always willing to help me with research. I am especially grateful to Dr. Gee for encouraging me on the path of acoustics when I was an undergraduate in PHSCS 461, and for Dr. Sommerfeldt for being my advisor. I truly would not have gotten to this point without the help of every single acoustics professor.

Next, I have an immense amount of gratitude for the people who helped me enjoy graduate school the most: my officemates and fellow acoustics graduate and undergraduate students, many of whom have become good friends. I especially feel the need to thank Sarah Young and Joseph Lawrence, who were great friends to me and were always willing to help with a "quick" question or listen to a "quick" story. Endless thank yous also go out to my other fellow graduate students throughout the years: Matthew Calton, Joshua Bodon, Travis Hoyt, Michael Denison, Mylan Cook, Jenny Whiting, Eric Whiting, Kyle Miller, Blaine Harker, Brent Reichman, Kevin Leete, Brian Patchett, Caleb Goates, Michael Rose, Nathaniel Wells, Hales Swift, and Pegah Aslani. Thank you for all the help you have given me and all of the kindness I have felt as I have been here as a graduate student. Also, a huge thank you to all former BYU students who have worked on this project and paved the way for continued research.

I am endlessly grateful to my family as well for the part they played in helping me get here. Thank you to my husband, Christian, for his patience when I had late nights on campus and for his comforting words when I was unsure what to do next. Also, a big thank you goes to my sister, Amy, for her encouragement and friendship throughout graduate school and my whole life. Thank you to my parents, who are not only my neighbors and fellow supporters of BYU sports, but some of my biggest cheerleaders as well. My other siblings, though not quite as involved in this process, also deserve mention for their continued love and good example to me.

I am very grateful for the funding I received through the National Science Foundation and the Physics Department.

Table of Contents

List of Figures

List of Tables:

Chapter 1

Introduction

1.1 Acoustic intensity

Energy-based methods in acoustics can provide novel ways of analyzing acoustic fields. The main energy-based quantities are acoustic intensity, acoustic energy density, and specific acoustic impedance. Acoustic intensity is a vector, so it can provide not only the magnitude information that could be found from pressure measurements, but also provide a direction. For active intensity, this direction can aid in finding propagation directions. Direction of propagation can also be helpful for characterizing a source by identifying which regions of the source are radiating more dominantly.[1] Intensity also can be used to find the sound power of a source.[2-5] Several methods for these sound power calculations as well as other applications of intensity have become published standards.[6-13] In addition, intensity can be useful in nearfield acoustical holography, which is a way to use pressure and/or particle velocity measurements at one location to visualize the field at another location.[14-19] Energy density, though not a vector, varies differently throughout a sound field than pressure and can therefore be useful in applications such as active noise control[20-22] and room acoustics,[23] in addition to providing another way of calculating sound power.[24] Specific acoustic impedance describes the medium through which the wave is propagating by relating the ratio of pressure and particle velocity. The measurement of these quantities can provide additional information about a sound field or source than pressure

measurements can alone. For the purposes of this thesis, acoustic intensity is explored, but many of the principles could be applied to the calculation of other energy quantities.

Complex acoustic intensity can be expressed in the frequency domain as:

$$\boldsymbol{I}_{\mathrm{c}} = \frac{1}{2} p \boldsymbol{u}^{*}, \qquad (1)$$

where p refers to pressure, u refers to particle velocity, vector quantities are in bold, and the * denotes a complex conjugate. The active intensity, expressed as $\boldsymbol{I}$, is the real part of $\boldsymbol{I}_{\mathrm{c}}$; the reactive intensity is expressed as $\boldsymbol{J}$ and is the imaginary part of $\boldsymbol{I}_{\mathrm{c}}$. It is shown in Eq. (1) that the calculation of $\boldsymbol{I}_{\mathrm{c}}$ requires both pressure and particle velocity. Particle velocity can be directly measured using a particle velocity probe such as the Microflown[25-27], but such probes are very sensitive to air flow in the acoustic field. Alternatively, when Euler's equation is used to relate particle velocity to the gradient of pressure, we can rewrite the complex acoustic intensity as:

$$\boldsymbol{I}_{\mathrm{c}} = j \frac{1}{\rho_0 \omega} p \nabla p. \qquad (2)$$

Acoustic intensity can be measured in several ways based on Eq. (2). One of the most prevalent ways is what is referred to in the literature as the p-p method, in which a probe with multiple microphones is used to estimate the gradient of pressure by using the change in the real and imaginary parts of pressure divided by the microphone spacing.[28-30] This p-p method is hereafter referred to as the traditional method.

The traditional method has several limitations of varying degree. One significant limitation is that estimating the gradient as the change in the real and imaginary parts of pressure over a distance between microphones is only a good estimation when the microphone spacing is small relative to a wavelength. This causes an underestimation of particle velocity when the microphone spacing begins to be sufficiently large relative to a wavelength. At much lower

frequencies, any inherent phase mismatch can cause significant errors because when the microphone spacing is very small relative to a wavelength, the actual phase difference being measured is small, and therefore the sensor phase mismatch becomes a relatively larger error. Between these two main types of errors, there is only a fairly limited bandwidth over which the traditional method can be adequately used. These and other errors have been discussed at length in the literature,[4,31-37] and many have tried to overcome the errors using varying experimental placement or processing.[38-41]

1.2 The PAGE method

To overcome some of the problems of the traditional method, especially for high-amplitude jet and rocket noise, the phase and amplitude gradient estimator (PAGE) method was developed at Brigham Young University (BYU).[42,43] Instead of using formulations which split the complex pressure into real and imaginary parts, as is done in the traditional method, the formulations for the PAGE method represent the complex pressure as magnitude and phase, based on expressions from Mann et. al.[44] and Mann and Tichy[1,45]. The expressions for active and reactive intensity in the PAGE method are:

$$\boldsymbol{I} = \frac{1}{\rho_0 \omega} P^2 \nabla \phi \tag{3}$$

and

$$\boldsymbol{J} = -\frac{1}{\rho_0 \omega} P \nabla P. \tag{4}$$

Here, P represents the pressure magnitude and ϕ represents the pressure phase. These expressions are advantageous, especially in propagating fields, because the magnitude and phase of pressure vary less spatially than the real and imaginary parts of pressure, which allows for a more accurate estimation of the particle velocity across a wider range of frequencies.

1.2.1 The spatial Nyquist frequency

One limitation of many multi-microphone processing techniques is the spatial Nyquist frequency. The spatial Nyquist frequency, or f_N, is defined as the frequency at which half a wavelength is equal to the spacing between the microphones. The traditional method starts to underestimate the particle velocity before this frequency, so it is not the limiting factor in that processing method. However, since the PAGE method can be accurate to higher frequencies, the spatial Nyquist frequency is a limiting factor on the bandwidth for which PAGE calculations can be accurate.

1.2.2 Phase unwrapping

In certain conditions, phase unwrapping can be used in the PAGE method to obtain meaningful particle velocity estimates above the spatial Nyquist frequency. The phase of a transfer function between microphones, an important element in obtaining the particle velocity estimate in the PAGE method, starts to be erroneous above the spatial Nyquist frequency due to a phenomenon known as phase wrapping. In this phenomenon, the phase difference between microphones reaches $-\pi$ or π at the spatial Nyquist frequency and multiples of it, at which points the phase makes a 2π jump. These jumps make the phase inaccurate above that frequency. With phase unwrapping,[46] all of the jumps are removed to obtain a continuous phase relationship, as demonstrated in Figure 1.1. Thus, phase unwrapping can provide correct particle velocity estimation and therefore accurate calculations of energy quantities above the spatial Nyquist frequency.

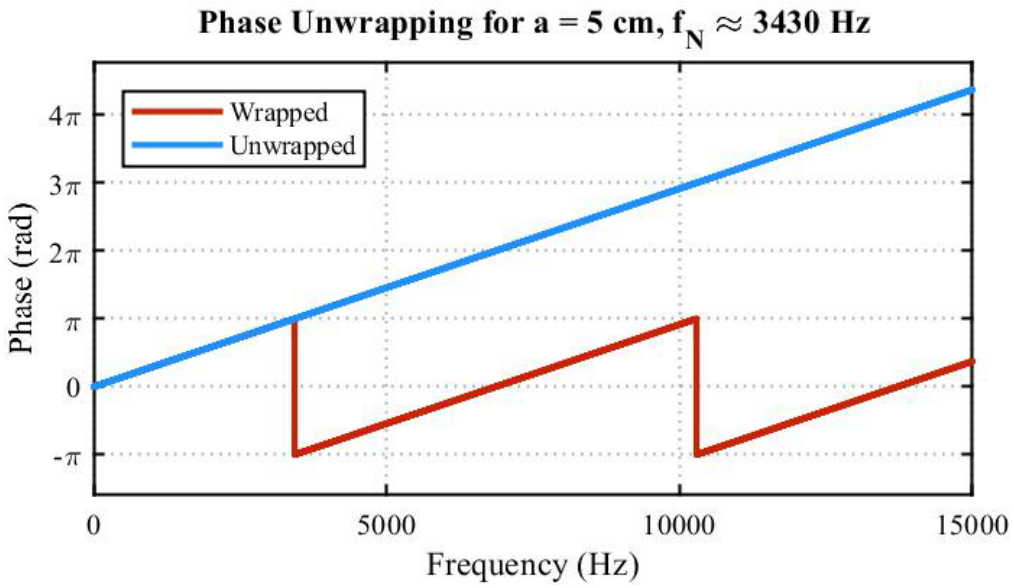

Figure 1.1: An illustration of phase unwrapping for two microphones with 5 cm spacing and therefore a spatial Nyquist frequency of 3430 Hz. Each 2π jump in the wrapped phase occurs at an integer multiple of the spatial Nyquist frequency.

Phase unwrapping, and therefore energy quantity calculation above the Nyquist frequency, consistently works only under specific conditions. The first requirement is that the phase be linear, or at least locally linear. This requires a field that is at least mostly propagating. Also, the signal must have sufficient frequency information for an unwrapping algorithm to resolve how to properly remove jumps and obtain an accurate continuous phase relationship. For example, phase unwrapping works well for broadband noise because there is phase information at every frequency. The use of phase unwrapping has been effective at increasing the bandwidth of PAGE calculations of jet noise, rocket noise, and other broadband sources in fields that are at least mostly propagating.[47- 51]

1.3 Comparison of methods for broadband noise

An illustrative example of acoustic intensity calculation using both the traditional and PAGE methods is seen in Figure 1.2.[49] In order to have a propagating field, the experiment was done in a plane wave tube with an anechoic termination and with microphones spaced at 5 cm,

30 cm, and 90 cm apart. These three spacings correspond to spatial Nyquist frequencies of about 3430 Hz, 572 Hz, and 191 Hz, respectively. An illustration of this setup is in Figure 1.2(a). The benchmark for accurate sound intensity level, L_I, was calculated from the theoretical active intensity for a plane wave: $\boldsymbol{I} = \frac{p_{rms}^2}{\rho_0 c}$. Intensity calculated using the traditional method is shown in Figure 1.2(b), where it can be observed that the intensity begins to be underestimated well below the spatial Nyquist frequency, and deep nulls occur at integer multiples of the spatial Nyquist frequency for each spacing. For the 5 cm spacing, which has a spatial Nyquist frequency of 3430 Hz, it can be seen that at 2 kHz the traditional calculation is already underestimating the benchmark by several dB. In Figure 1.2(d), the intensity calculated using the PAGE method is shown to overlay almost perfectly with the benchmark for all spacings. This result is accomplished using phase unwrapping, which is shown in Figure 1.2(c).

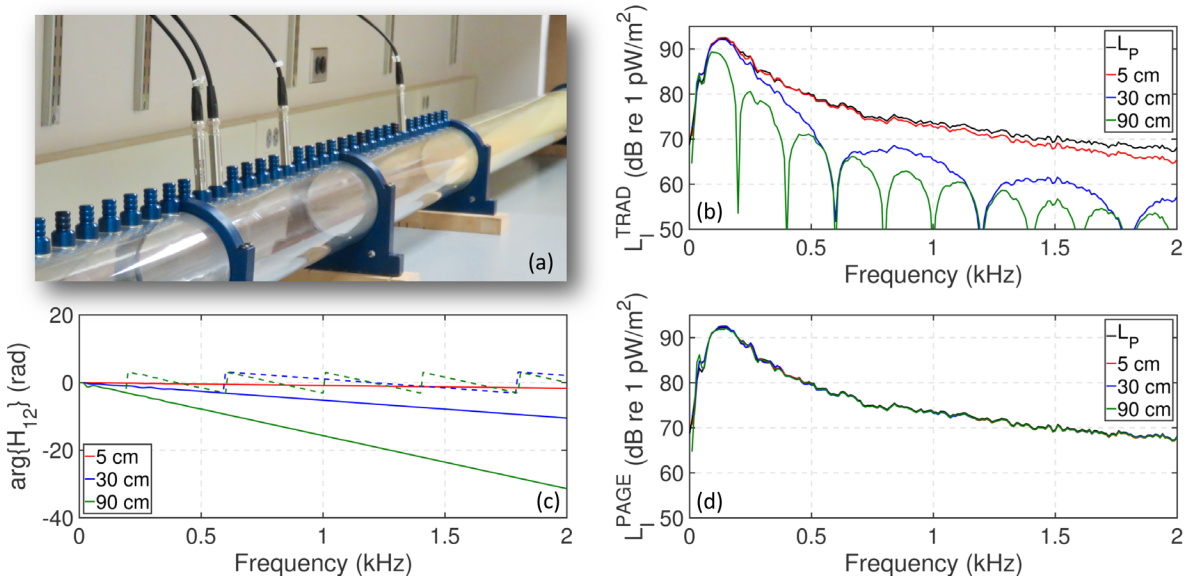

Figure 1.2: (a) Anechoic plane-wave tube experiment with downstream microphones placed at 5, 30, and 90 cm from the first microphone. (b) Traditional-method intensity levels, L_I^{TRAD}, and L_P. (c) Wrapped (dashed) and unwrapped transfer function phases. (d) PAGE-calculated levels, L_I^{PAGE}, along with L_P. (From Fig. 1 on page 3 of Gee et. al.[49])

For broadband noise cases, several other papers have been published about the PAGE method. These papers help to outline a more complete picture of appropriate uses of the PAGE method[52-55] and some of the applications of phase unwrapping[55,56] to acoustics applications.

1.4 The narrowband problem

Although phase unwrapping and the PAGE method have been shown to work well for broadband sources, problems arise when the source is not broadband. In narrowband signals, such as a sawtooth wave, there is only coherent phase information at very specific frequencies corresponding to the peaks in the sawtooth wave. Therefore, phase unwrapping is unable to piece together a correct phase for the portions of the signal above the spatial Nyquist frequency because it does not have phase information at enough frequencies.

For each narrowband signal case, the main question explored in this thesis is: How well does the PAGE method do for this case, and is it an improvement over the traditional method? Then, the main follow-up question for most cases is: Is there any way to accurately obtain correct intensity above the spatial Nyquist frequency, through phase unwrapping or other means?

First, in Chapter 2, these questions are explored in a roughly one-dimensional field using a one-dimensional probe. This is accomplished by testing different narrowband signals in a plane wave tube.

In Chapters 3 and 4, these questions are explored for experiments in an anechoic chamber using a 5-microphone planar probe. Chapter 3 contains results for tests including repeating the test cases in Chapter 2 in a multi-dimensional field and exploring how angle of incidence and multiple sources can affect the PAGE calculation. In Chapter 4, the results are shown of experiments which test the idea of adding phase information in the form of broadband noise at a low level in order to provide sufficient phase information for phase unwrapping.

Chapter 2

One-dimensional narrowband cases

2.1 Experimental setup

Narrowband signals were explored in a roughly one-dimensional field. This was done using a plane-wave tube. Four phase-matched Type I microphones were placed at varying spacings along the tube to allow for one test to yield different results based on the microphone pair used for processing. This was especially useful since the spatial Nyquist frequency is an important measure in this work, and different microphone spacings yield different spatial Nyquist frequencies. Although the spacings sometimes varied between experimental cases, the setup was the same as that in Figure 1.2(a).

Three main signals were used in the plane wave tube testing: sine waves, sawtooth waves, and bandlimited white noise. Bandlimited white noise involved using high-pass and low-pass filters on a broadband white noise signal. The band of each signal is defined by the cutoff frequencies used, which does not describe the entire bandwidth of useful phase information due to the roll off of the filter.

In each case, a benchmark curve calculated from $\boldsymbol{I} = \frac{p_{rms}^2}{\rho_0 c}$ is used to verify the accuracy of the PAGE method calculations. However, the benchmark is the intensity for an ideal plane wave and the waves in the tube may not be perfect plane waves due to factors such as a termination that is not absolutely 100% anechoic. From previous work with this plane wave tube, the absorption coefficient is known to be between 0.998 and 1.000 across the frequencies of

interest for these experiments. However, an absorption coefficient of 0.999 corresponds with a pressure reflection coefficient, or R, of 0.0316, which can result in as much as a 0.25 dB variation in intensity level. Based on this, a value of 0.25 dB in intensity level between the PAGE calculation and the benchmark at the frequencies of interest was considered to be a successful measurement and calculation by the PAGE method. Some error may also come from deviation from the sound speed of 343 m/s used for the calculations.

2.2 Sine waves

First, experiments with sine waves were conducted to determine limits of the PAGE method. Since sine waves only have accurate phase information at a single frequency, it was not expected that there would be any chance of successful phase unwrapping. The main goal of these experiments was to find the high-frequency limit for the accuracy of the PAGE method when only a single frequency is present. Several iterations were performed, each with the sine wave at a different frequency. The frequencies of the sine waves in the testing included frequencies above and below the spatial Nyquist frequency for each spacing. In this case, spacings of d = 10, 15, and 20 cm were used to correspond to spatial Nyquist frequencies of 1715 Hz, 1143.3 Hz, and 857.5 Hz, respectively (see Table 2.1).

Table 2.1: Spatial Nyquist frequencies for the spacings used for sine wave testing in plane wave tube

d: Microphone Spacing (cm)	f_N: Spatial Nyquist Frequency (Hz)
10	1715
15	1143.3
20	857.5

As expected, the traditional method begins to underestimate the intensity magnitude below the spatial Nyquist frequency and the PAGE method does not. It was found that the PAGE method was able to accurately match the expected intensity magnitude and direction of the sine

wave up to the spatial Nyquist frequency, as can be seen in Figure 2.1 and Figure 2.3. In Figure 2.2 and Figure 2.3 the difference between the PAGE and traditional calculation close to the spatial Nyquist frequency can be seen, and it can be observed that the direction is correct in both cases, but the magnitude is underestimated by the traditional method by a little over 10 dB.

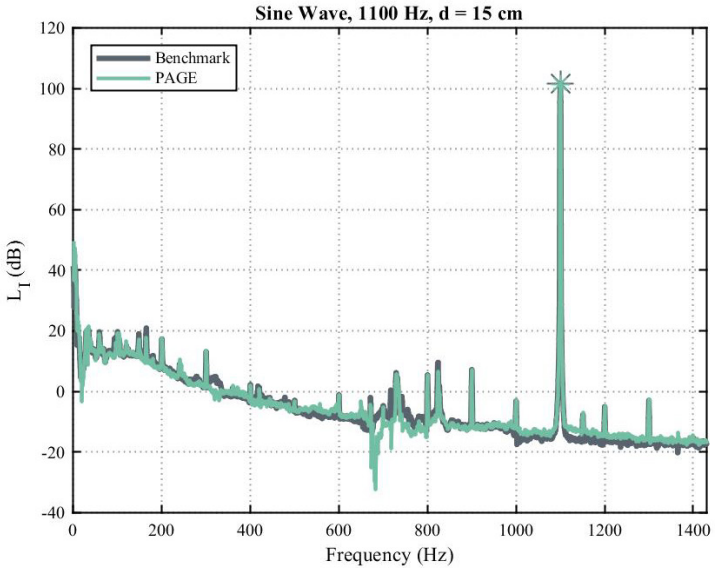

Figure 2.1: For an 1100 Hz sine wave in the plane wave tube, a benchmark of $\boldsymbol{I} = \frac{p_{rms}^2}{\rho_0 c}$ *is compared to the PAGE calculation of active intensity. Markers on each curve are at the frequency of the sine wave.*

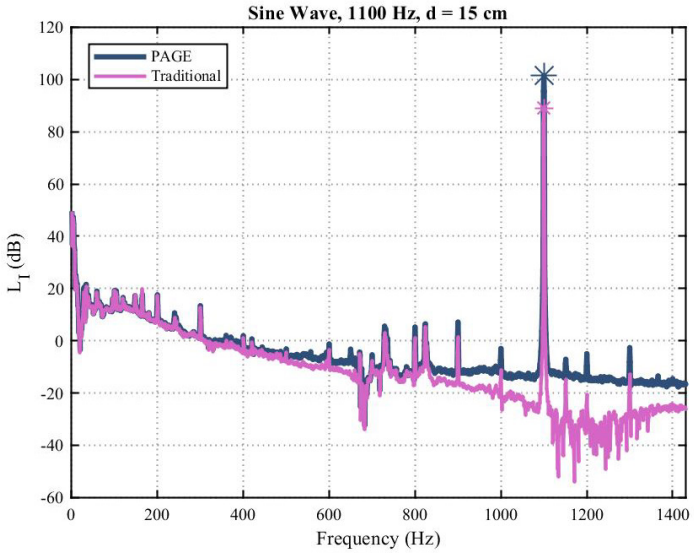

Figure 2.2: For an 1100 Hz sine wave in the plane wave tube, the active intensity calculated using the PAGE method is compared to the active intensity calculated using the traditional method. Markers on each curve are at the frequency of the sine wave.

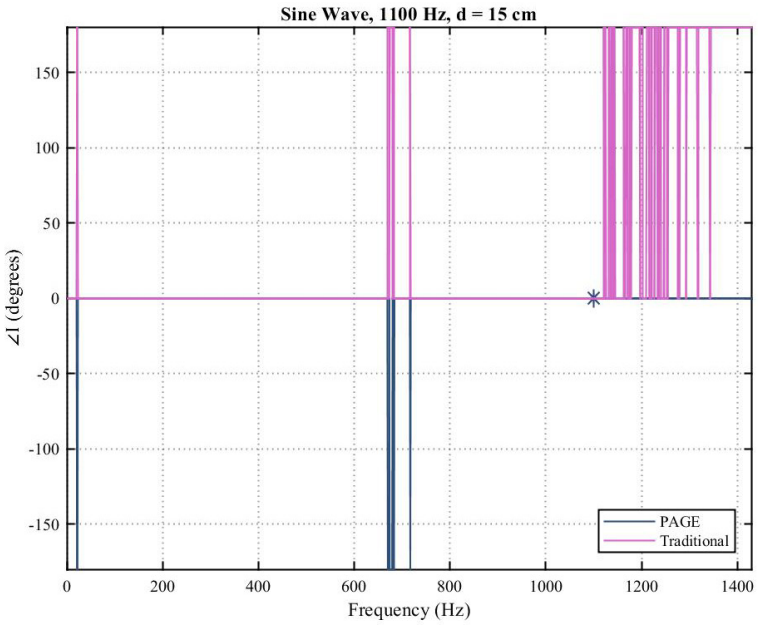

Figure 2.3: For an 1100 Hz sine wave in the plane wave tube, the intensity direction calculated using the PAGE method is compared to the intensity direction calculated using the traditional method. Markers on each curve are at the frequency of the sine wave.

It was expected that because there was only phase information at the frequency of the sine wave, the PAGE method would not accurately calculate the intensity above the spatial Nyquist frequency, but that was not always the case. There were times that the PAGE calculation was not accurate above the spatial Nyquist frequency, as can be observed by the discrepancy in sound intensity levels between the PAGE calculation and the benchmark in Figure 2.4 and Figure 2.5 for spatial Nyquist frequencies of 1715 Hz and 1143.3 Hz, respectively (see Table 2.1). However, the PAGE method often did accurately calculate the intensity above the spatial Nyquist frequency, and sometimes well above the spatial Nyquist frequency. One such example can be seen in Figure 2.6, where it can be observed that the PAGE calculation overlays the benchmark intensity level with sufficient accuracy for a sine wave at 1700 Hz. Notice that this sine wave is more than 500 Hz above the spatial Nyquist frequency for this microphone spacing of 15 cm (see Table 2.1). The intensity magnitude and direction compared to the traditional calculation can be seen in Figure 2.7 and Figure 2.8, respectively, and it is seen that the

traditional method at this frequency is both more than 5 dB too low and 180° off the correct direction. It is suspected that the PAGE method calculated the intensity correctly at this frequency due to some noise that was broadband in nature from the data acquisition system getting into the tube and traveling down the tube, creating a linear phase relationship with enough information to unwrap and therefore get the correct answer at high frequencies. This can be seen in the phase of the transfer function for this microphone pair in Figure 2.9. This idea is explored further in Chapter 4, including experiments where broadband noise is intentionally added at a relatively low level in an attempt to aid unwrapping.

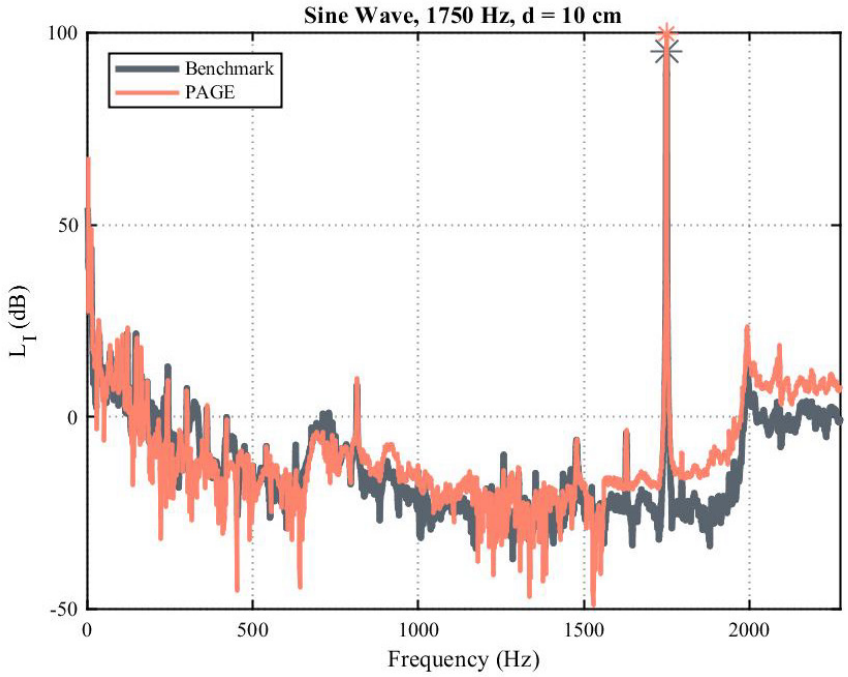

Figure 2.4: For a 1750 Hz sine wave in the plane wave tube, a benchmark of $\boldsymbol{I} = \frac{p_{rms}^2}{\rho_0 c}$ *is compared to the PAGE calculation of active intensity. Markers on each curve are at the frequency of the sine wave.*

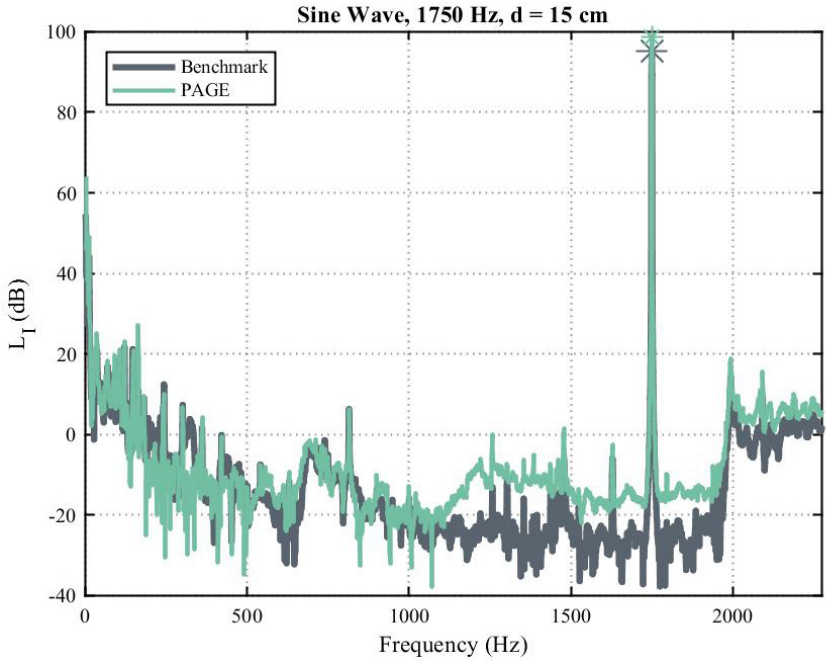

Figure 2.5: For a 1750 Hz sine wave in the plane wave tube, a benchmark of $\boldsymbol{I} = \frac{p_{rms}^2}{\rho_0 c}$ *is compared to the PAGE calculation of active intensity. Markers on each curve are at the frequency of the sine wave.*

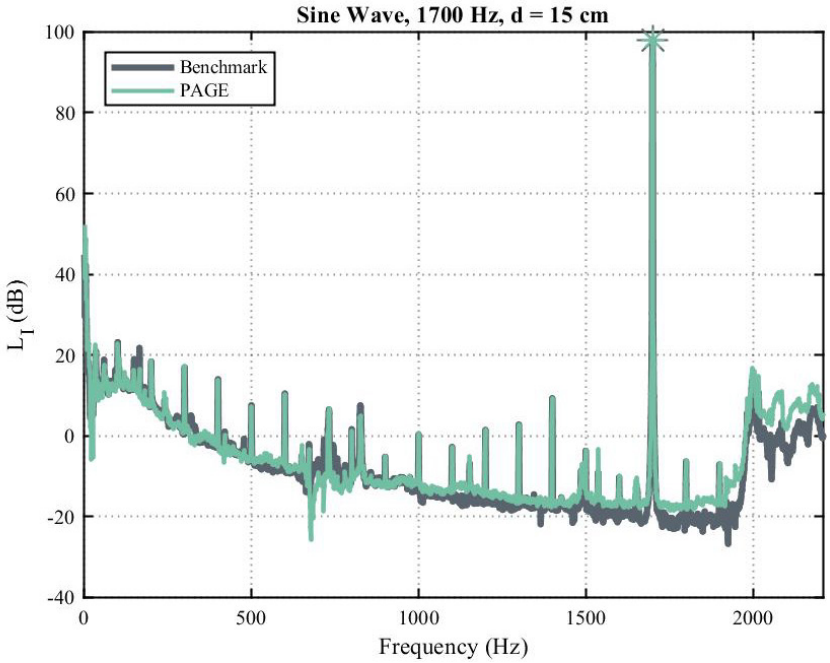

Figure 2.6: For a 1700 Hz sine wave in the plane wave tube, a benchmark of $\boldsymbol{I} = \frac{p_{rms}^2}{\rho_0 c}$ *is compared to the PAGE calculation of active intensity. Markers on each curve are at the frequency of the sine wave.*

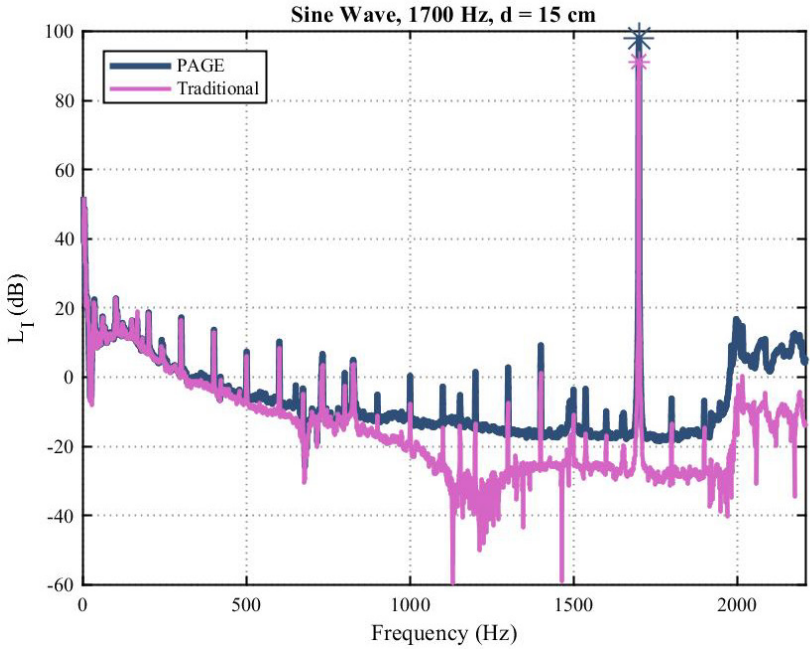

Figure 2.7: For a 1700 Hz sine wave in the plane wave tube, the active intensity calculated using the PAGE method is compared to the active intensity calculated using the traditional method. Markers on each curve are at the frequency of the sine wave.

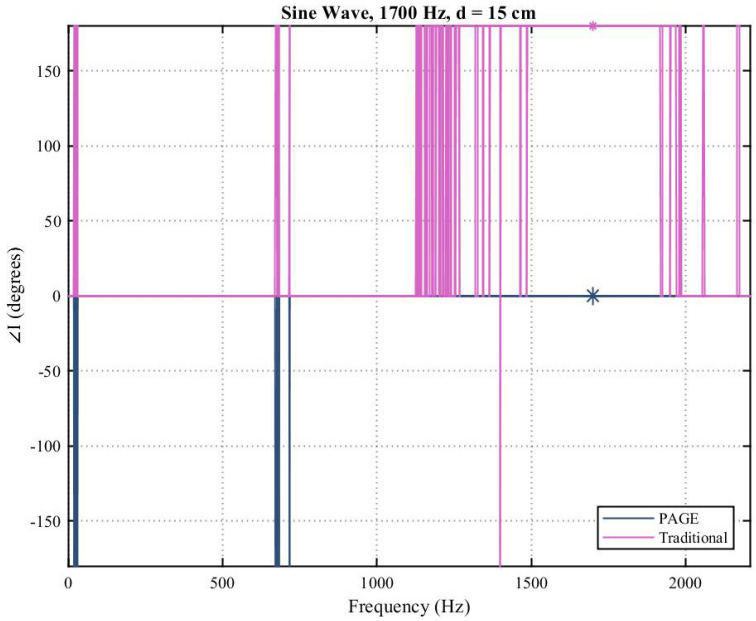

Figure 2.8: For a 1700 Hz sine wave in the plane wave tube, the intensity direction calculated using the PAGE method is compared to the intensity direction calculated using the traditional method. Markers on each curve are at the frequency of the sine wave.

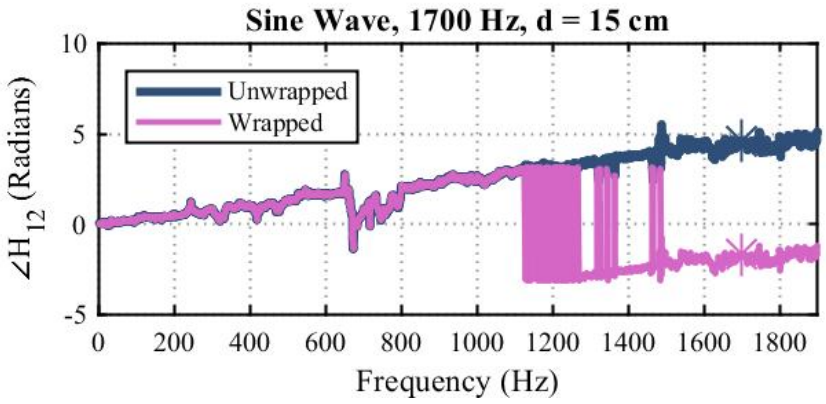

Figure 2.9: For a 1700 Hz sine wave in the plane wave tube, the wrapped and unwrapped phase of the transfer function are compared for d = 15 cm. Markers on each curve are at the frequency of the sine wave.

2.3 Sawtooth waves

Experiments with sawtooth waves were conducted as a way to test a narrowband source which contains several separate tones. As was expected, any peaks of the sawtooth wave below the spatial Nyquist frequency were calculated correctly by the PAGE method. However, harmonics above the spatial Nyquist frequency were not calculated correctly using the normal PAGE calculation. These results can be observed in Figure 2.10. Only the peak at 500 Hz is below the spatial Nyquist frequency of 686 Hz, and at this peak the PAGE calculation can be seen to match the benchmark curve well. However, above the spatial Nyquist frequency, the intensity magnitude calculated using the PAGE method begins to be erroneous at each of the peaks. This is due to the fact that there is only accurate phase information at the frequencies corresponding to the fundamental and harmonics of the sawtooth wave, and that is not enough frequencies with correct phase information for the phase unwrapping algorithm to correctly unwrap the phase.

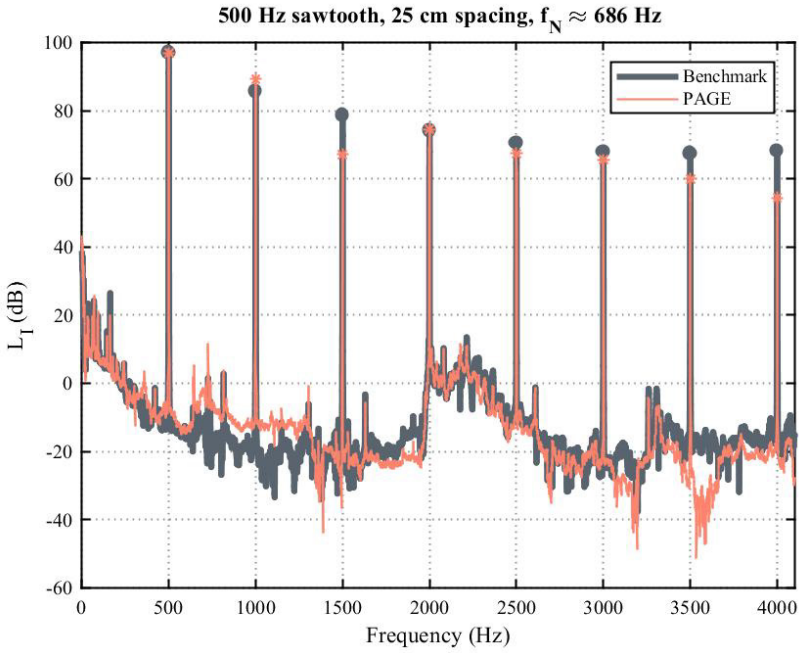

Figure 2.10: For a 500 Hz sawtooth wave in the plane wave tube, a benchmark of $\boldsymbol{I} = \frac{p_{rms}^2}{\rho_0 c}$ *is compared to the PAGE calculation of active intensity. Markers on each curve are at the frequencies which correspond to the peaks of the sawtooth.*

In a plane wave tube, known information about the field and signal can aid in obtaining intensity above the spatial Nyquist frequency. The field is known to be primarily propagating, and it is also known that the transfer function phase should start at 0°. If one peak of the sawtooth is below the spatial Nyquist frequency, it has been shown that the phase would be correct at that frequency. Since the field is primarily propagating, the phase relationship should be linear. A line can be drawn using the two known accurate phases—at 0 Hz and at the frequency of the first peak—and extrapolated to higher frequencies, as illustrated in Figure 2.11 for a 500 Hz sawtooth. This line can then be used as the unwrapped phase. Using this "extrapolated PAGE" method, the active intensity of peaks of the sawtooth far above the spatial Nyquist frequency can be correctly calculated, as shown in Figure 2.12. The intensity direction is also correct, as can be seen in Figure 2.14. By comparing Figure 2.10 and Figure 2.12, it can be seen that the extrapolated PAGE calculation improves on the results of the PAGE method alone.

As would be expected, the traditional method underestimates the intensity magnitude at all of the peaks of the sawtooth, as is shown in Figure 2.13. This figure shows the difference between the successful calculation obtained from the extrapolated PAGE method and what would be calculated using the traditional method.

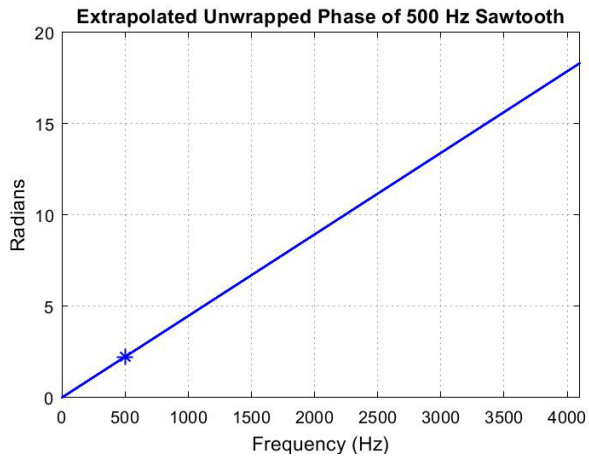

Figure 2.11: Extrapolated phase using knowledge that the phase should be linear since the field is propagating and the known phases at 0 and 500 Hz (marked on plot).

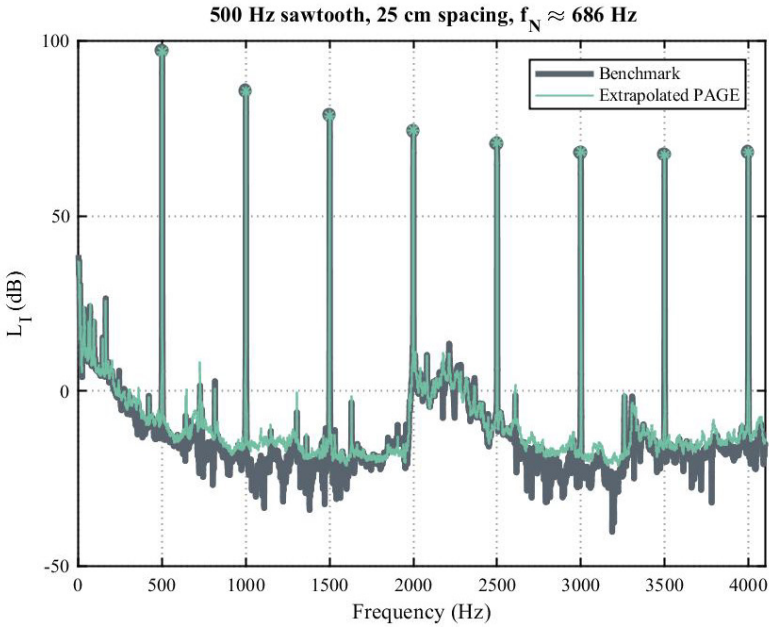

Figure 2.12: For a 500 Hz sawtooth wave in the plane wave tube, a benchmark of $\boldsymbol{I} = \frac{p_{rms}^2}{\rho_0 c}$ *is compared to the new, extrapolated PAGE calculation of active intensity. Markers on each curve are at the frequencies which correspond to the peaks of the sawtooth.*

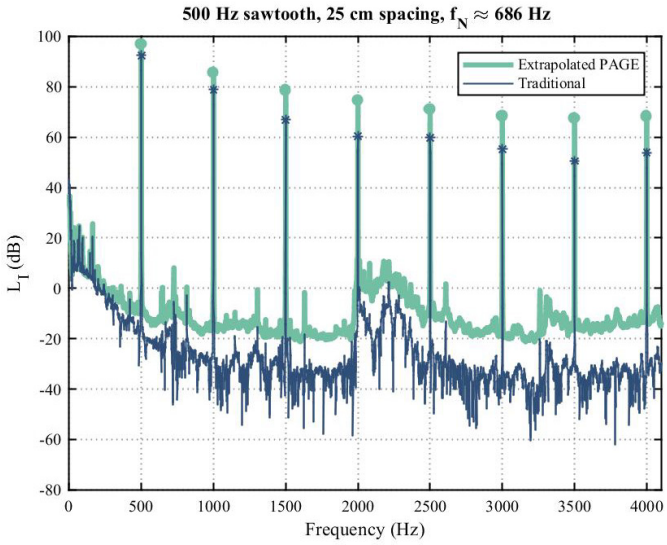

Figure 2.13: For a 500 Hz sawtooth wave in the plane wave tube, the active intensity obtained from the new, extrapolated PAGE method is compared to that obtained by the traditional method. Markers on each curve are at the frequencies which correspond to the peaks of the sawtooth.

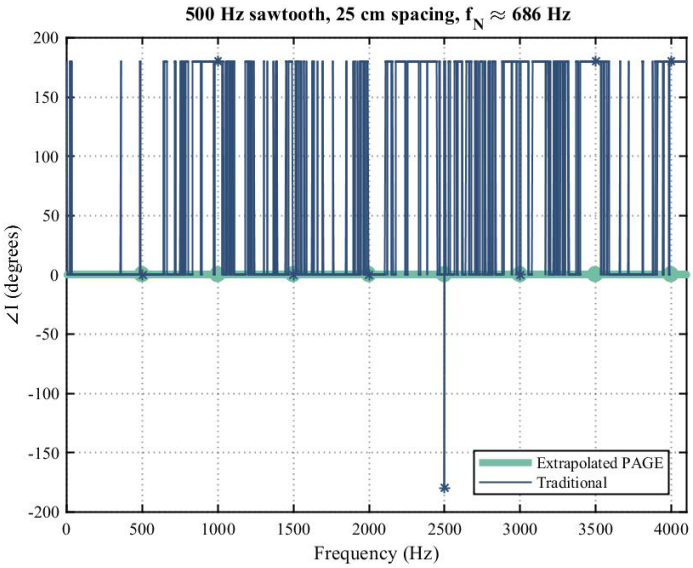

Figure 2.14: For a 500 Hz sawtooth wave in the plane wave tube, the intensity direction obtained from the new, extrapolated PAGE method is compared to that obtained by the traditional method. Markers on each curve are at the frequencies which correspond to the peaks of the sawtooth.

The extrapolated PAGE method is successfully used here for sawtooth waves, but its success is limited to only cases where it is known that the field is a propagating field and at least one peak is below the spatial Nyquist frequency. However, when it can be done, it works very well.

2.4 Bandlimited white noise

As a hybrid case between broadband noise and narrowband noise, the test of bandlimited white noise explores the limits of where unwrapping stops working. The microphone spacings used for this case can be seen in Table 2.2. Three different noise cases, as defined in Table 2.3, were tested to determine the effect that signal-to-noise ratio (SNR) would have on the effectiveness of the unwrapping. The additive noise was obtained by driving a speaker with white noise outside of the plane wave tube. It should again be noted that the stated bandwidths are defined by the cutoff frequencies for the filters used on the white noise, and therefore do not represent the entire bandwidth over which there will be good coherence. The filters being used are third-order Butterworth filters, meaning they have an 18 dB/octave roll off. As stated in the experimental setup section of this chapter, agreement between the intensity level obtained using the PAGE method and the benchmark curve based on $\boldsymbol{I} = \frac{p_{rms}^2}{\rho_0 c}$ are considered to match well when there is 0.25 dB or less discrepancy at the frequencies of interest.

Table 2.2: Spatial Nyquist frequencies for the spacings used for bandlimited white noise testing in plane wave tube

d: Microphone Spacing (cm)	f_N: Spatial Nyquist Frequency (Hz)
5	3430
30	571.7
90	190.6

Table 2.3: Approximate signal-to-noise ratio (SNR) by frequency range and case

Case	700-800 Hz (avg) (dB)	1200-1300 Hz (avg) (dB)
Highest SNR (no added noise)	52.4 – 69.3 (62.4)	65.7-73.1 (70.6)
Lower SNR	46.3-50.0 (48.4)	58.7-60.1 (59.6)
Lowest SNR	24.9-30.9 (28.7)	38.3-39.3 (38.8)

It should also be noted that since the experimental setup is the same as that in the sine wave case, extraneous broadband noise from the equipment in the experimental setup might propagate down the tube for the case with no additive noise, which could potentially aid in unwrapping. Also, the additive noise at certain levels could potentially aid in unwrapping as well.

As would be expected based on the previous two tests, the PAGE method worked below the spatial Nyquist frequency regardless of bandwidth and noise level. Specifically, the intensity level obtained by the PAGE method was within 0.25 dB of the benchmark intensity level for all cases, including with additive random noise. These results for magnitude can be seen in Figure 2.15 and for direction can be seen in Figure 2.17. In Figure 2.16 and Figure 2.17 it is shown that the PAGE method does not demonstrate significant improvement over the traditional method in this frequency range, since it is well below the spatial Nyquist frequency for this spacing of 3430 Hz (see Table 2.2). However, this case illustrates that the additive noise did not inhibit the PAGE method's ability to accurately estimate the sound intensity level below the spatial Nyquist frequency at the frequencies where there is signal.

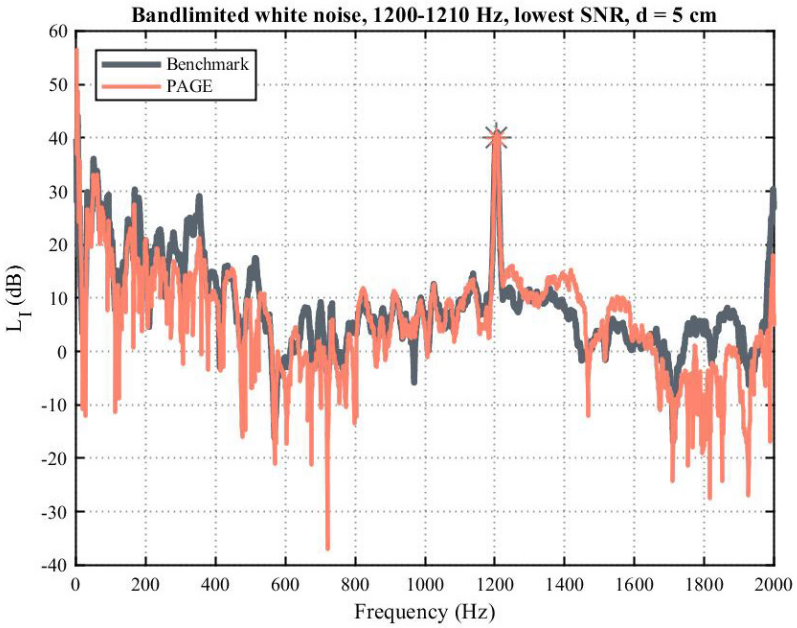

Figure 2.15: For filtered white noise from 1200-1210 Hz in the plane wave tube and additive noise resulting in the lowest tested SNR, a benchmark of $\boldsymbol{I} = \frac{p_{rms}^2}{\rho_0 c}$ *is compared to active intensity calculated using the PAGE method. A marker on each curve is at the center of the bandwidth, in this case at 1205 Hz.*

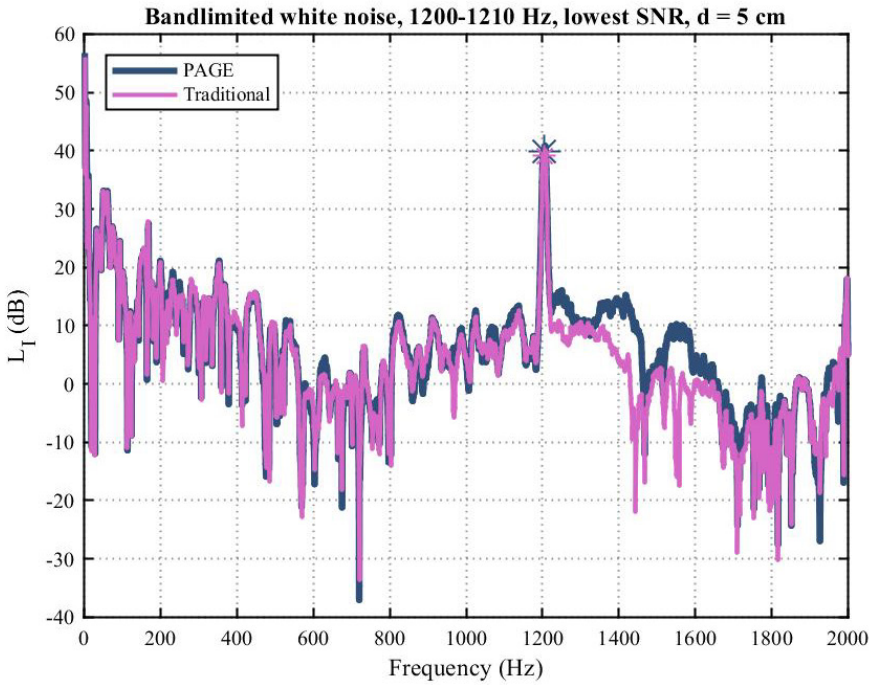

Figure 2.16: For filtered white noise from 1200-1210 Hz in the plane wave tube and additive noise resulting in the lowest tested SNR, active intensity calculated using the PAGE method is compared to active intensity calculated using the traditional method. A marker on each curve is at the center of the bandwidth, in this case at 1205 Hz.

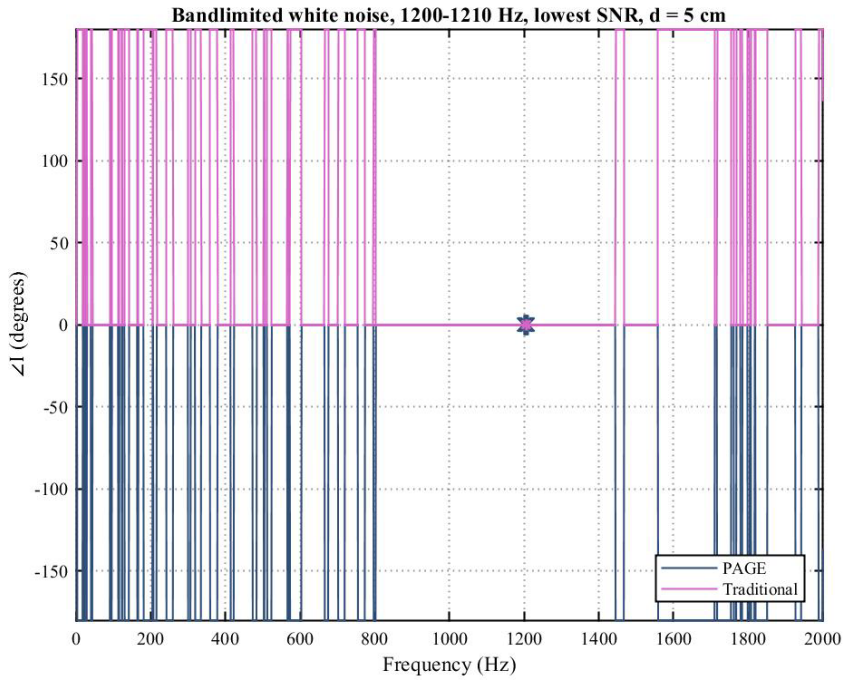

Figure 2.17: For filtered white noise from 1200-1210 Hz in the plane wave tube and additive noise resulting in the lowest tested SNR, intensity direction calculated using the PAGE method is compared to intensity direction calculated using the traditional method. Markers on each curve are over the entire bandwidth, in this case from 1200-1210 Hz.

It was shown that phase unwrapping can be achieved with only a limited band of white noise. The case where the phase unwrapping extended the bandwidth most impressively was using a 90 cm microphone spacing from 1200-1210 Hz with the best SNR. From Table 2.2, it is seen that for this spacing, the spatial Nyquist frequency is 191.6 Hz. The results of this case can be seen in Figure 2.18, where over the region of signal the intensity level obtained using the PAGE method overlays the benchmark intensity level well, and in Figure 2.20, where the correct direction of 0° is obtained. The improvement over the traditional method can be seen in Figure 2.19 for magnitude and Figure 2.20 for direction. This shows that even a small bandwidth of noise can be sufficient for unwrapping under the right conditions. However, as previously noted, some of the background noise from the setup could have potentially aided in achieving the correct phase unwrapping to achieve this result.

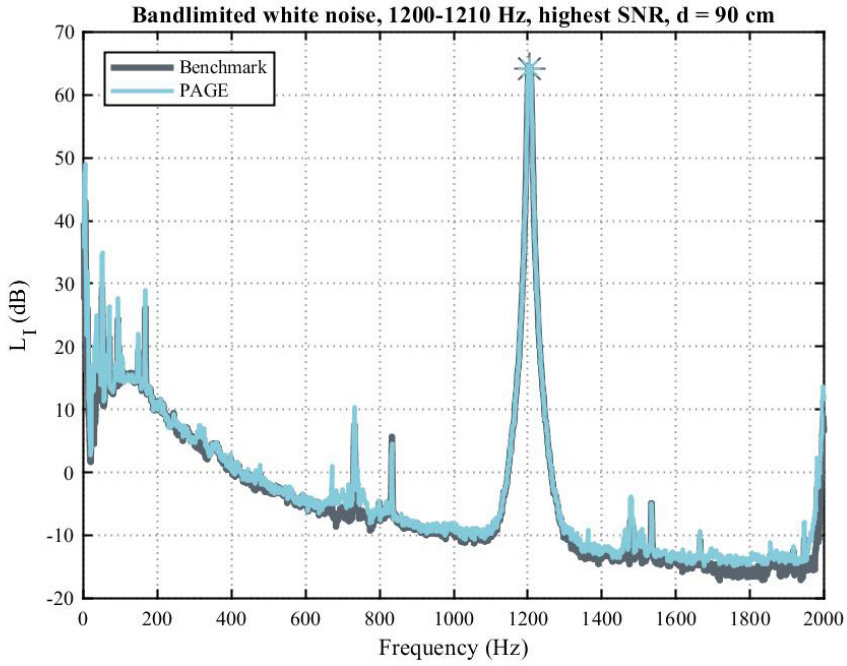

Figure 2.18: For filtered white noise from 1200-1210 Hz in the plane wave tube and no additive noise and therefore the highest tested SNR, a benchmark of $\boldsymbol{I} = \frac{p_{rms}^2}{\rho_0 c}$ *is compared to active intensity calculated using the PAGE method. A marker on each curve is at the center of the bandwidth, in this case at 1205 Hz.*

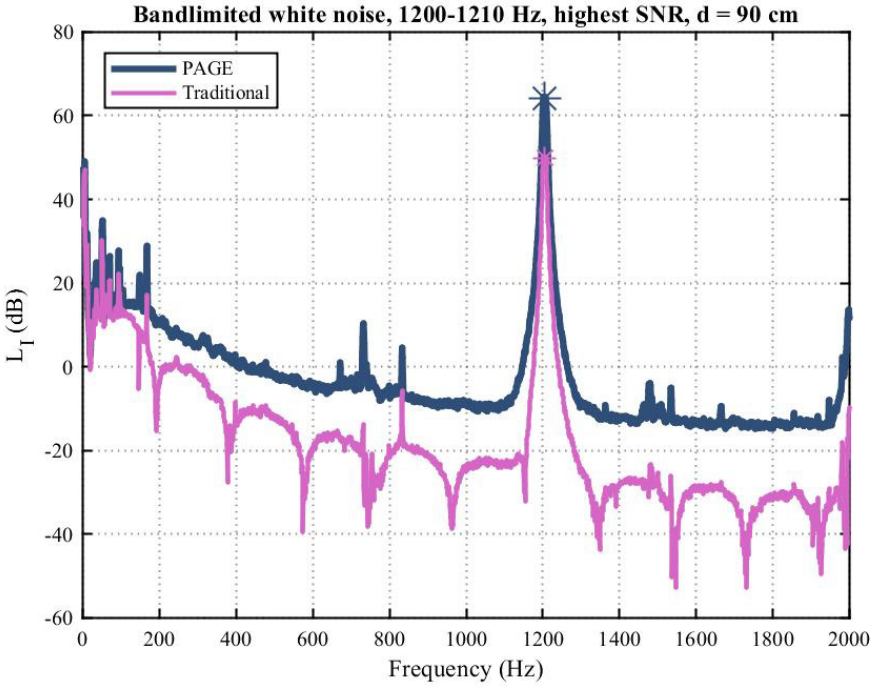

Figure 2.19: For filtered white noise from 1200-1210 Hz in the plane wave tube and no additive noise and therefore the highest tested SNR, active intensity calculated using the PAGE method is compared to active intensity calculated using the traditional method. A marker on each curve is at the center of the bandwidth, in this case at 1205 Hz.

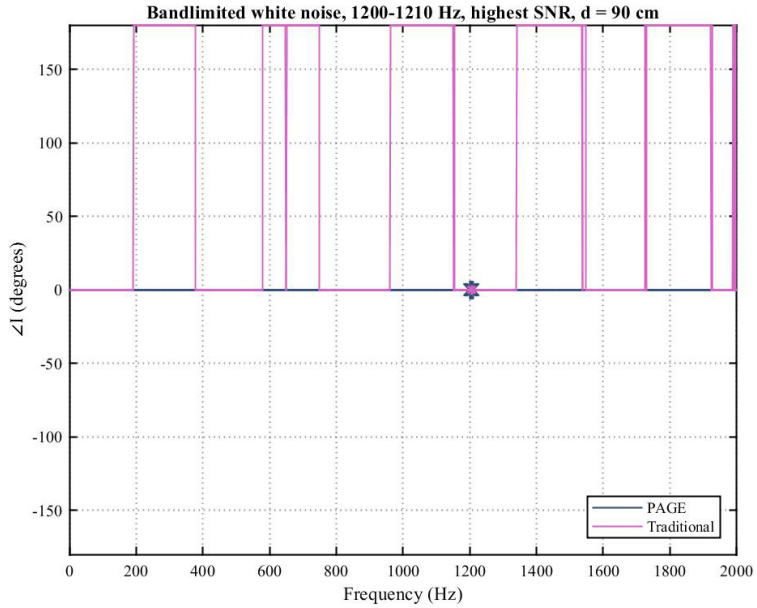

Figure 2.20: For filtered white noise from 1200-1210 Hz in the plane wave tube and no additive noise and therefore the highest tested SNR, intensity direction calculated using the PAGE method is compared to intensity direction calculated using the traditional method. Markers on each curve are over the entire bandwidth, in this case from 1200-1210 Hz.

Although the PAGE method can utilize phase unwrapping for small bandwidths with a high SNR, a lower SNR can provide less reliable results. In cases with additive noise, it is not certain whether phase unwrapping will work properly or not. A lower SNR decreases the chances of the PAGE method producing the correct result. For example, for a 1200-1230 Hz signal with the lower SNR noise case (see Table 2.3), the PAGE method accurately calculates the intensity level (see Figure 2.21) and the intensity direction (see Figure 2.23) even though this frequency range is well above the spatial Nyquist frequency of 571.7 Hz (see Table 2.2). These represent an improvement over the traditional method, as can be seen in Figure 2.22 and Figure 2.23. However, for the lowest SNR noise case (see Table 2.3), the PAGE method does not accurately calculate the intensity level for the same frequency range and microphone spacing (see Figure 2.24), even though it happens to accurately calculate the direction (see Figure 2.25). This demonstrates how a worse SNR can cause the unwrapping algorithm to no longer work, even for the same frequency range and spacing.

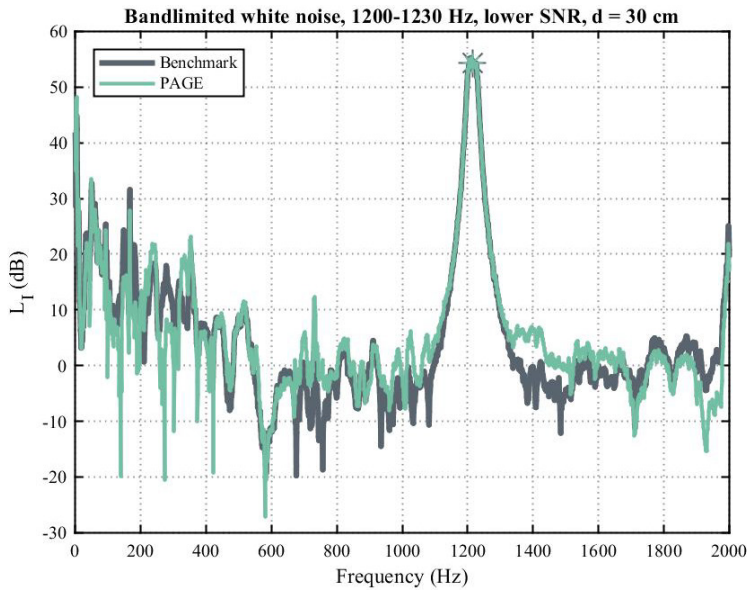

Figure 2.21: For filtered white noise from 1200-1230 Hz in the plane wave tube and some additive noise and therefore a lower SNR than the highest tested, a benchmark of $\boldsymbol{I} = \frac{p_{rms}^2}{\rho_0 c}$ *is compared to active intensity calculated using the PAGE method. A marker on each curve is at the center of the bandwidth, in this case at 1215 Hz.*

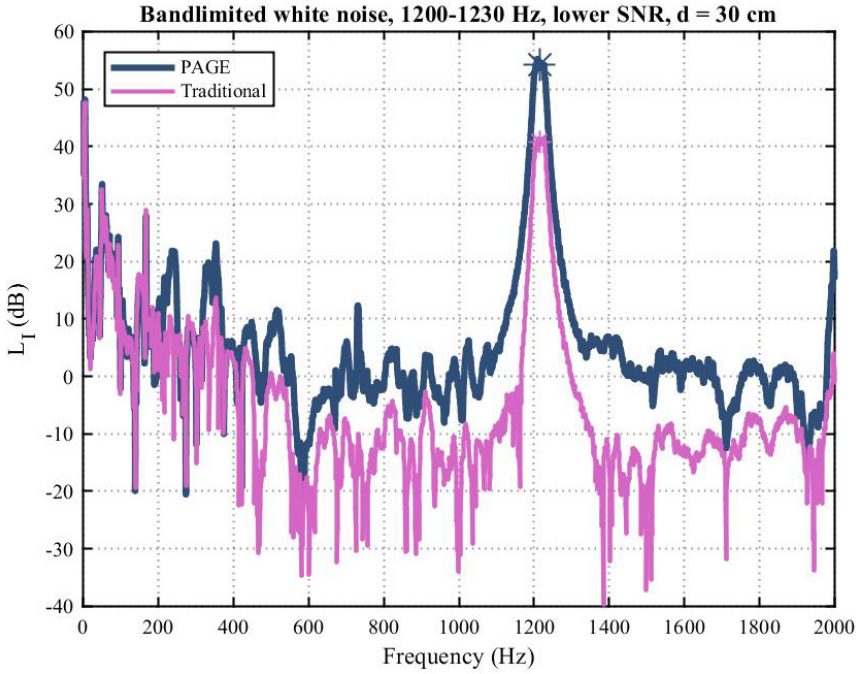

Figure 2.22: For filtered white noise from 1200-1230 Hz in the plane wave tube and some additive noise and therefore a lower SNR than the highest tested, active intensity calculated using the PAGE method is compared to active intensity calculated using the traditional method. A marker on each curve is at the center of the bandwidth, in this case at 1215 Hz.

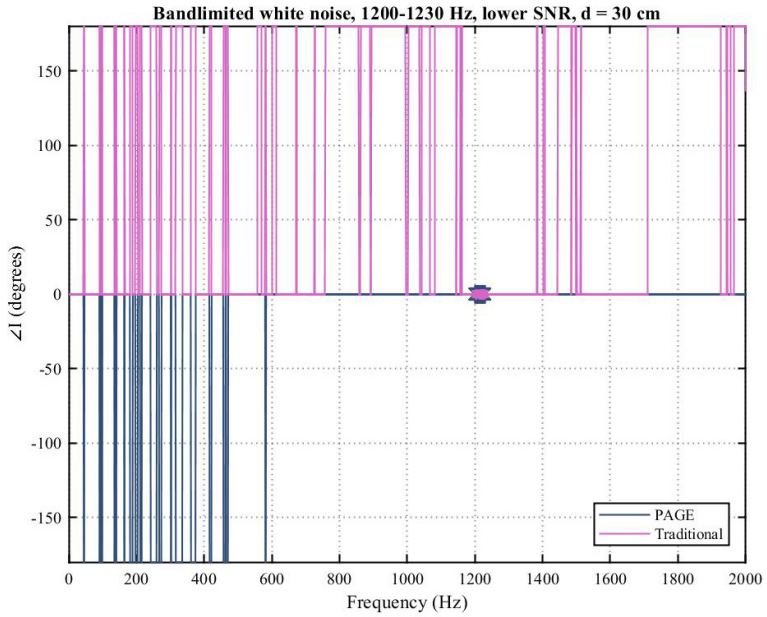

Figure 2.23: For filtered white noise from 1200-1230 Hz in the plane wave tube and some additive noise and therefore a lower SNR than the highest tested, intensity direction calculated using the PAGE method is compared to intensity direction calculated using the traditional method. Markers on each curve are over the entire bandwidth, in this case from 1200-1230 Hz.

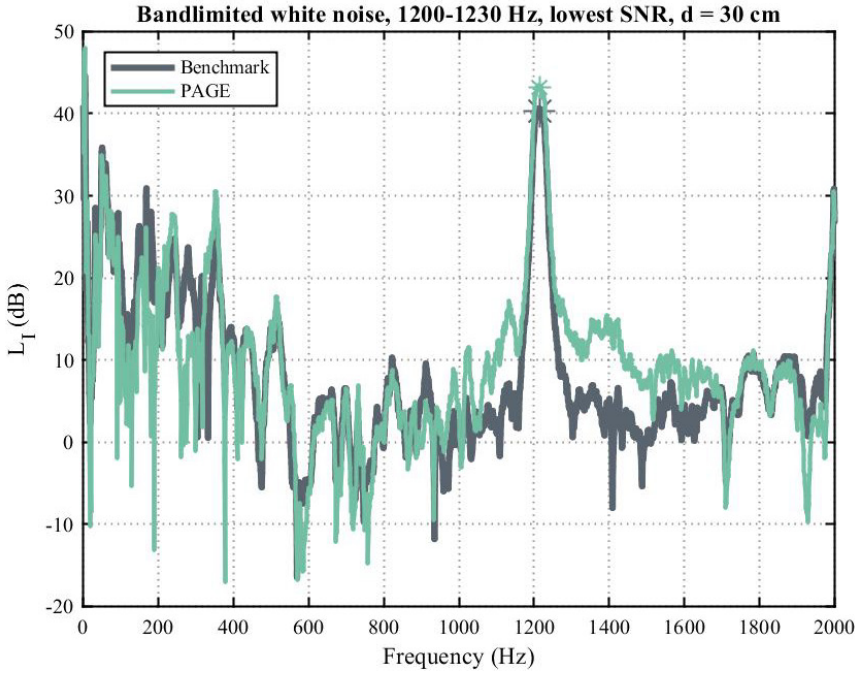

Figure 2.24: For filtered white noise from 1200-1230 Hz in the plane wave tube and additive noise resulting in the lowest tested SNR, a benchmark of $\boldsymbol{I} = \frac{p_{1ms}^2}{\rho_0 c}$ *is compared to active intensity calculated using the PAGE method. A marker on each curve is at the center of the bandwidth, in this case at 1215 Hz.*

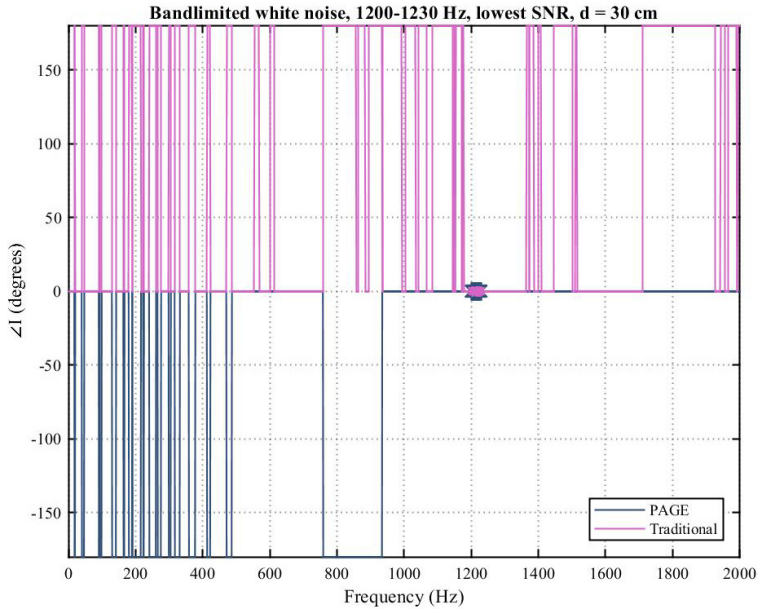

Figure 2.25: For filtered white noise from 1200-1230 Hz in the plane wave tube and additive noise resulting in the lowest tested SNR, intensity direction calculated using the PAGE method is compared to intensity direction calculated using the traditional method. Markers on each curve are over the entire bandwidth, in this case from 1200-1230 Hz.

Results involving unwrapping are more likely to be accurate if the frequency range of the narrowband signal is closer to the spatial Nyquist frequency. When the frequency band is closer to the spatial Nyquist frequency, there are not as many frequencies where there could be inaccurate phase information to cause erroneous phase unwrapping. As previously discussed and as can be seen in Figure 2.24, the PAGE method was not successful in calculating the sound intensity level for a bandwidth of 1200-1230 Hz, with the lowest tested SNR (see Table 2.3) and a microphone spacing of 30 cm and therefore a spatial Nyquist frequency of 571.7 Hz (see Table 2.2). Using the same spacing, SNR, and bandwidth, a frequency range closer to the spatial Nyquist frequency of 700-730 Hz was tested. As can be seen from Figure 2.26 for magnitude and Figure 2.28 for direction, the PAGE method now can successfully match the benchmark with sufficient accuracy. The PAGE calculations are also an improvement in both magnitude and direction over the traditional method, as seen in Figure 2.27 and Figure 2.28. From this example,

it is shown that bandlimited white noise at lower frequencies (relative to the spatial Nyquist frequency) has a better chance of unwrapping properly.

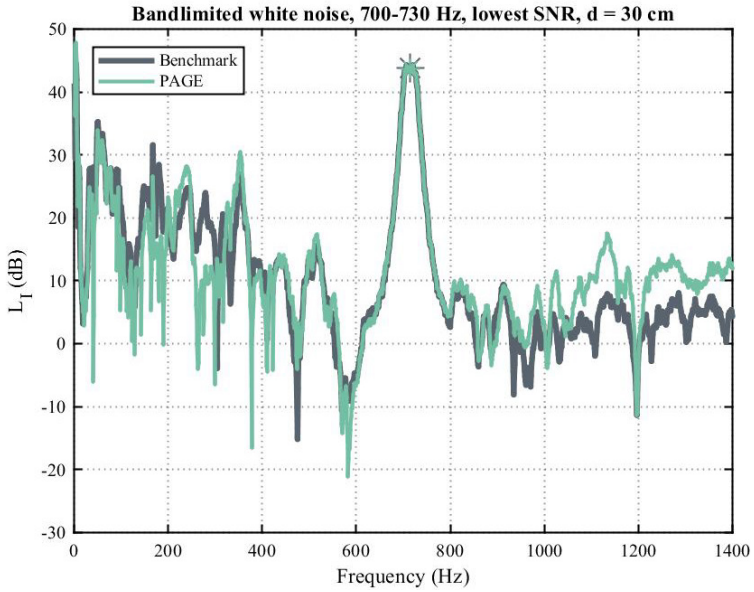

Figure 2.26: For filtered white noise from 700-730 Hz in the plane wave tube and additive noise resulting in the lowest tested SNR, a benchmark of $\boldsymbol{I} = \frac{p_{rms}^2}{\rho_0 c}$ *is compared to active intensity calculated using the PAGE method. A marker on each curve is at the center of the bandwidth, in this case at 715 Hz.*

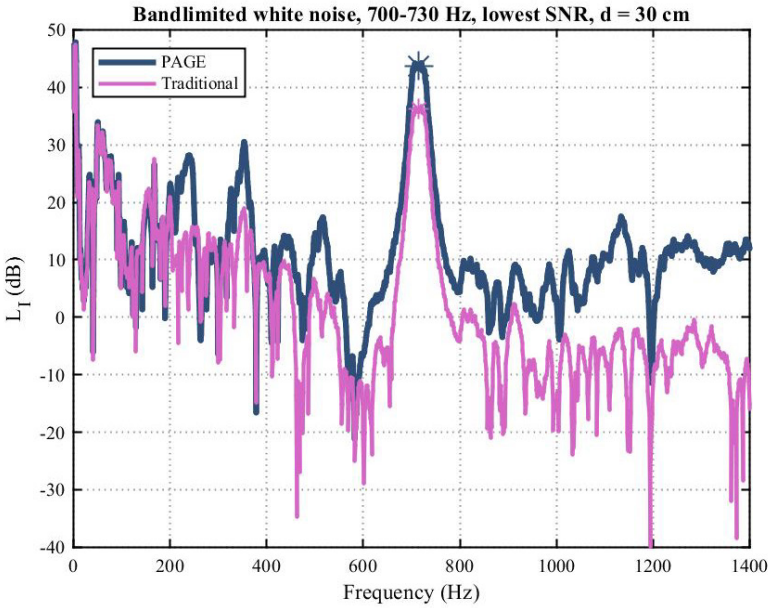

Figure 2.27: For filtered white noise from 700-730 Hz in the plane wave tube and additive noise resulting in the lowest tested SNR, active intensity calculated using the PAGE method is compared to active intensity calculated using the traditional method. A marker on each curve is at the center of the bandwidth, in this case at 715 Hz.

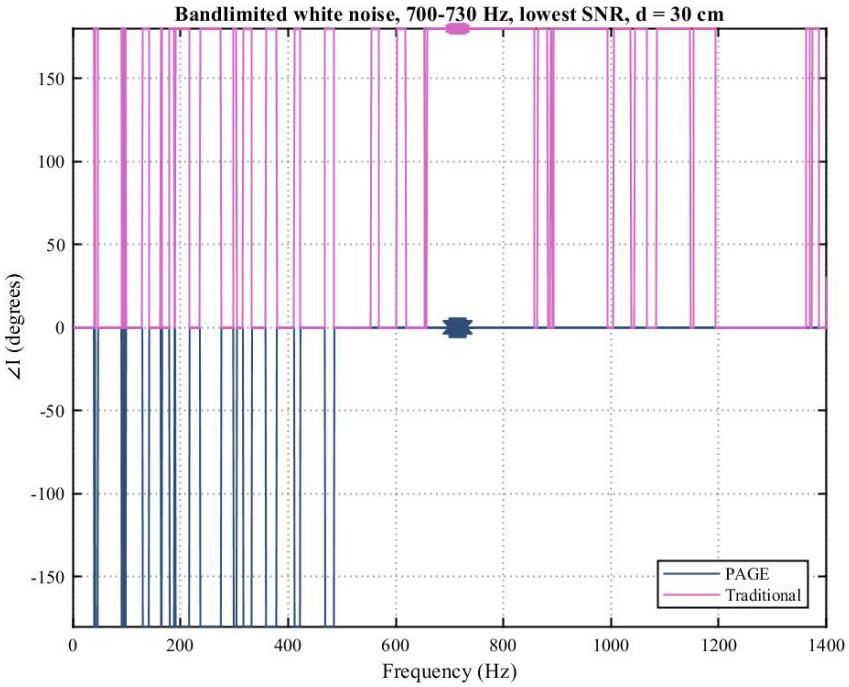

Figure 2.28: For filtered white noise from 700-730 Hz in the plane wave tube and additive noise resulting in the lowest tested SNR, intensity direction calculated using the PAGE method is compared to intensity direction calculated using the traditional method. Markers on each curve are at each frequency of the bandwidth, in this case from 700-730 Hz.

The bandwidth of noise affects the likelihood that unwrapping will or will not work. As previously discussed and can be seen in Figure 2.21, the PAGE method was successful in calculating the sound intensity level for a bandwidth of 1200-1230 Hz, at the lower SNR case (see Table 2.3) and with a microphone spacing of 30 cm and therefore a spatial Nyquist frequency of 571.7 Hz (see Table 2.2). To demonstrate the effect of bandwidth, a case with the same SNR and microphone spacing but a smaller bandwidth of only 1200-1210 Hz was tested. The results of this test can be seen in Figure 2.29 for level and Figure 2.30 for direction. It can be seen that the PAGE method no longer has phase information at enough frequencies to properly unwrap, as seen by the poor agreement between the PAGE calculation and the benchmark curve. This shows that greater bandwidth of the noise increases the chances of properly unwrapping phase.

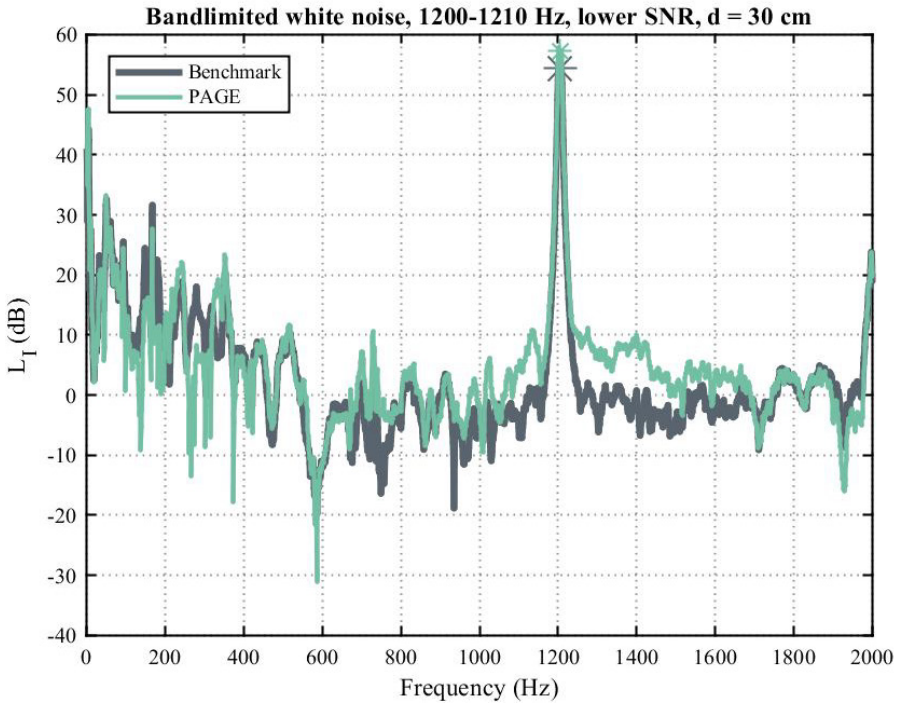

Figure 2.29: For filtered white noise from 1200-1210 Hz in the plane wave tube and some additive noise and therefore a lower SNR than the highest tested, a benchmark of $\boldsymbol{I} = \frac{p_{rms}^2}{\rho_0 c}$ *is compared to active intensity calculated using the PAGE method. A marker on each curve is at the center of the bandwidth, in this case at 1205 Hz.*

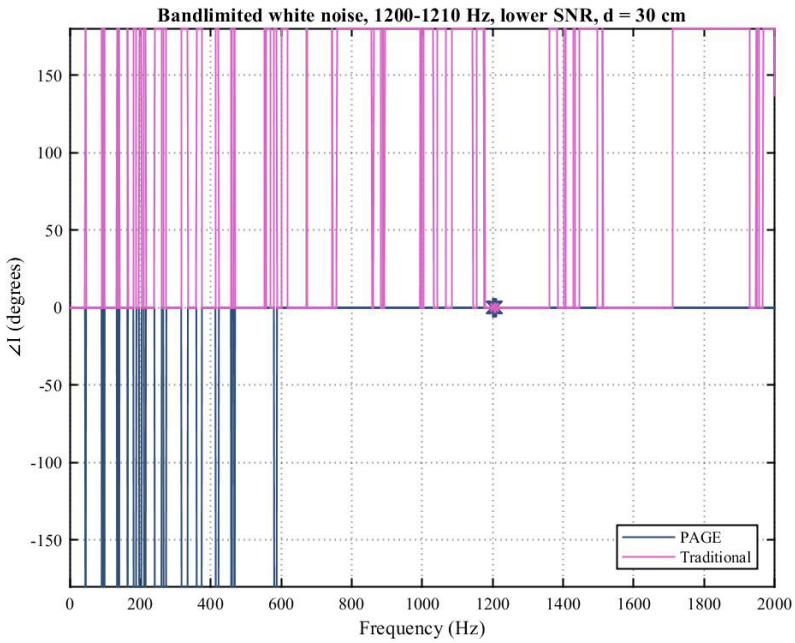

Figure 2.30: For filtered white noise from 1200-1210 Hz in the plane wave tube and some additive noise and therefore a lower SNR than the highest tested, intensity direction calculated using the PAGE method is compared to intensity direction calculated using the traditional method. Markers on each curve are at each frequency of the bandwidth, in this case from 1200-1210 Hz.

2.5 Conclusions

For all cases, it was shown that the PAGE method always works below the spatial Nyquist frequency, regardless of other conditions. For the sine wave case, it was shown that a small amount of broadband noise can aid in unwrapping when it is propagating down the tube and across the microphones in the same direction as the sine wave. This concept will be explored more in Chapter 4. For sawtooth waves, an extrapolated PAGE method assumed a propagating field and utilized the correct phase of the fundamental of the sawtooth wave that was below the spatial Nyquist frequency to create an unwrapped phase. Using this unwrapped phase, the intensity of the sawtooth wave was accurately calculated for several of the harmonics above the spatial Nyquist frequency. For the bandlimited white noise, it was shown that phase unwrapping can occur properly with only a limited band of noise above the spatial Nyquist frequency, but it is less likely to work with smaller bandwidths, a lower SNR, and at higher frequencies. Although it is possible that the unwrapping of bandwidths entirely above the spatial Nyquist frequency was aided by the extraneous broadband noise from the setup, the same guidelines outlined here for increasing likelihood of successful phase unwrapping hold true.

Chapter 3

Multi-dimensional narrowband signals

3.1 Introduction

In Chapter 2, sine waves, sawtooth waves, and bandlimited white noise were used to determine limits of the PAGE method in a plane wave tube. In this chapter, experiments for these signals and a few other test cases are conducted in an anechoic chamber to further determine the limits of the PAGE method.

A two-dimensional, five-microphone probe with five GRAS phase-matched microphones was used for all experiments. The probe was composed of two orthogonal pairs with one microphone in the middle, as can be observed in Figure 3.1. The probe diameter was 4 inches and therefore had an approximate spatial Nyquist frequency of $f_N \approx 1688$ Hz. In all cases in this chapter, the microphone probe was on a turntable, allowing for different angles of incidence from the speaker to the probe. The rotation angle of the probe was considered to be 0° when the source was on the same line as microphones 1, 2, and 3, and microphone 2 was the closest to the source (see Figure 3.2). Also, where possible the source or sources were kept at approximately the same height as the top of the microphones, and all sources were at least 2 meters away so that the sound field would behave locally like a plane wave at the probe, where applicable.

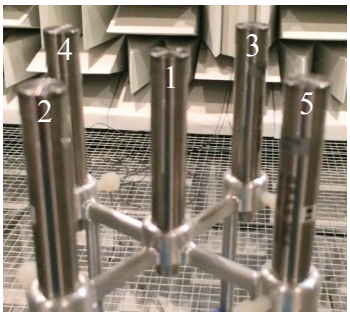

Figure 3.1: The multi-microphone probe used for the measurements in Chapters 3 and 4, labeled with microphone number labels. The rotation angle was 0° when the speaker was on the same line as microphones 1, 2, and 3, and microphone 2 was the closest to the speaker.

3.2 Sine waves and effective spatial Nyquist frequency investigation

3.2.1 Experiment

The main purpose of this experiment is to verify in the multi-dimensional case that the PAGE method successfully estimates sine waves at frequencies up to the spatial Nyquist frequency and to observe if the spatial Nyquist frequency changes based on the rotation angle of the probe relative to the source.

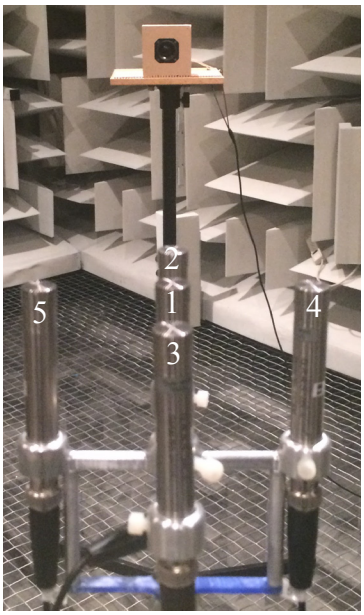

Figure 3.2: The configuration used for all experiments which only required one speaker in an anechoic chamber. The configuration shown corresponds to a rotation angle of 0°.

For this experiment, only one speaker was used. The speaker was placed on a stand approximately 2 meters away and with the center of the speaker cone at about the same height as the top of the microphones in the probe. This setup can be seen in Figure 3.2. It should be noted that the pictured setup is what was considered a rotation angle of 0°.

With the speaker at different angles of incidence to the probe, the microphone spacing across which the plane wave is moving is expected to change, resulting in a different spatial Nyquist frequency. For example, if the probe is at 45°, as shown in Figure 3.1, the microphone spacing would be effectively smaller as seen by the wave. It was expected that the effective spatial Nyquist frequency would increase as

$$f_{N,\text{eff},23} = \left|\frac{f_{N,0^\circ}}{\cos(\theta_{\text{rotation}})}\right| \tag{5}$$

and

$$f_{N,\text{eff},45} = \left|\frac{f_{N,0^\circ}}{\sin(\theta_{\text{rotation}})}\right|, \tag{6}$$

where $f_{N,\text{eff},23}$ is the effective spatial Nyquist frequency for microphones 2 and 3, $f_{N,\text{eff},45}$ is the effective spatial Nyquist frequency for microphones 4 and 5, $f_{N,0^\circ}$ is the spatial Nyquist frequency for a 0° angle of rotation, and θ_{rotation} is the angle of rotation. Due to the combination of the two orthogonal pairs on the same probe, the overall effective spatial Nyquist frequency of the probe, or $f_{N,\text{eff}}$, is the lower frequency of $f_{N,\text{eff},23}$ and $f_{N,\text{eff},45}$. This results in the highest possible effective spatial Nyquist frequency occurring at $\theta_{\text{rotation}} = 45°$, where there would be an effective microphone spacing of $2\sqrt{2}$ inches. The resulting spatial Nyquist frequency for the whole probe would be $f_{N,\text{eff}} \approx 2387$ Hz, which would be a significant improvement over the $f_{N,0^\circ}$ of about 1688 Hz.

3.2.2 Results and analysis

As expected, the PAGE method calculates the intensity magnitude and direction correctly below the spatial Nyquist frequency. One such example is at 1600 Hz, which is below the spatial Nyquist frequency of $f_{N,0^\circ} \approx 1688$ Hz. The results can be seen for magnitude in Figure 3.3 and for direction in Figure 3.5. The intensity direction error in degrees is calculated using

$$I_{\text{dir error}} = \frac{180}{\pi} \cos^{-1}\left(\frac{\boldsymbol{I}_{\text{calc}} \cdot \boldsymbol{I}_{\text{bench}}}{||\boldsymbol{I}_{\text{calc}}||\,||\boldsymbol{I}_{\text{bench}}||}\right) \tag{7}$$

over each of the rotation angles, where $\boldsymbol{I}_{\text{calc}}$ is the calculated two-dimensional vector and $\boldsymbol{I}_{\text{bench}}$ is the vector two-dimensional benchmark intensity obtained based on the rotation angle and a magnitude of $\frac{p_{rms}^2}{\rho_0 c}$ from the pressure at the center microphone. The improvement of the PAGE calculation over the traditional calculation can be seen in Figure 3.4 for intensity magnitude at a rotation angle of 0° and for intensity direction error over all of the rotation angles in Figure 3.5. This is consistent with our findings in Chapter 2.

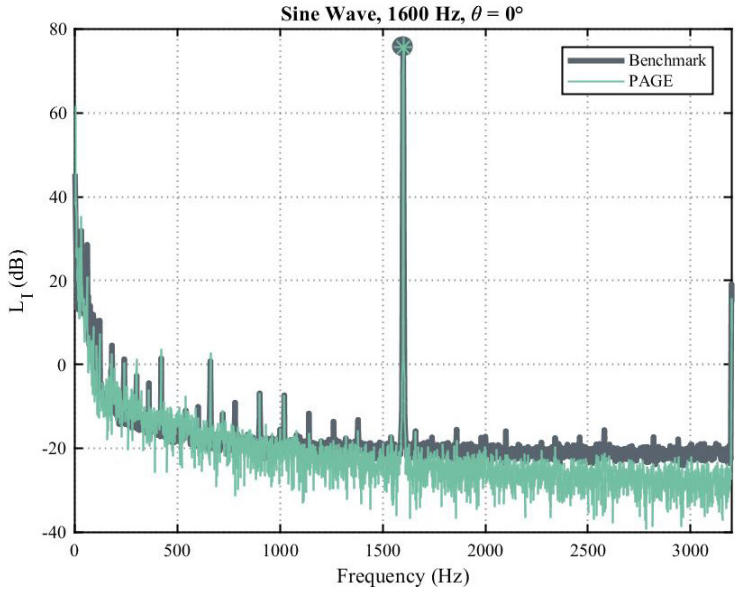

Figure 3.3: For a 1600 Hz sine wave in an anechoic chamber, a benchmark of $\boldsymbol{I} = \frac{p_{rms}^2}{\rho_0 c}$ *is compared to the PAGE calculation of active intensity for a probe with a 0° angle of rotation. Markers on each curve are at the frequency of the sine wave.*

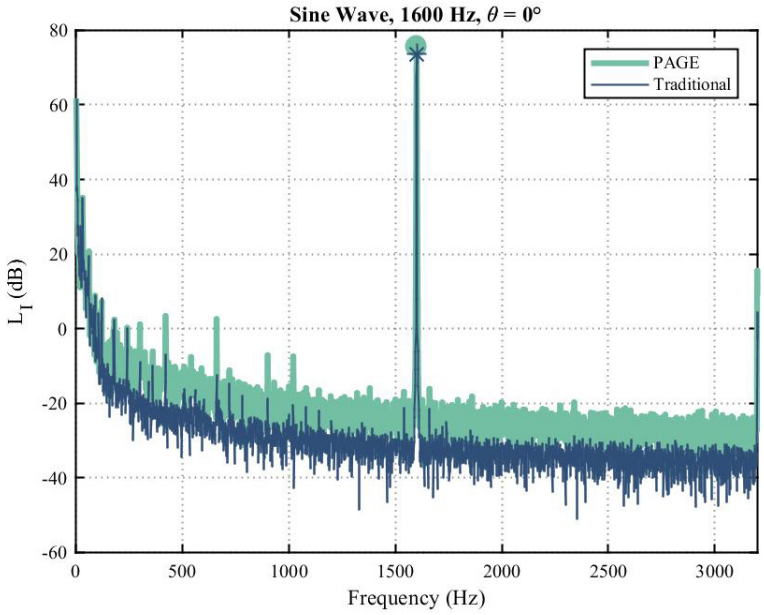

Figure 3.4: For a 1600 Hz sine wave in an anechoic chamber, the active intensity calculated using the PAGE method is compared to the active intensity calculated using the traditional method for a probe with a 0° angle of rotation. Markers on each curve are at the frequency of the sine wave.

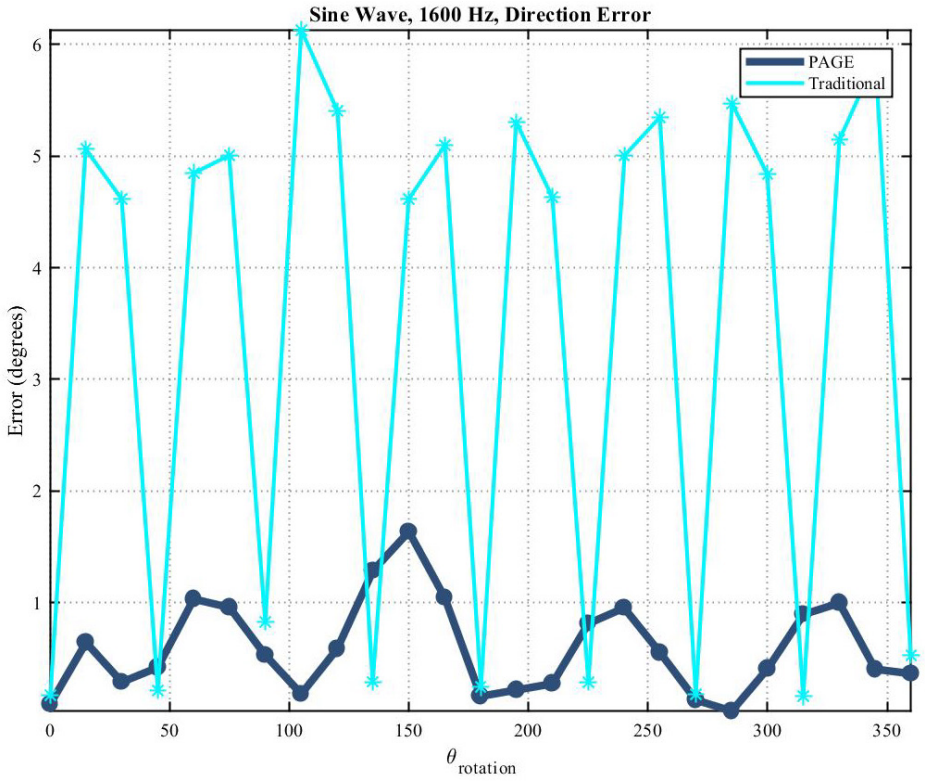

Figure 3.5: For a 1600 Hz sine wave in an anechoic chamber, the intensity direction error for the PAGE method is compared to the intensity direction error for the traditional method over all rotation angles.

The effective spatial Nyquist frequency was found to increase for the cases where Eq. (5) and Eq. (6) predicts it would. For example, at a rotation angle of 30°, $f_{N,\text{eff}} \approx$ 1949 Hz, which shows an improvement over $f_{N,0°}$, which is about 1688 Hz. The results for $\theta_{\text{rotation}} = 30°$ for a 1900 Hz sine wave can be seen in Figure 3.6, where it can be observed that the PAGE calculation matches the benchmark at this angle. However, for a 0° rotation angle, the PAGE method cannot correctly calculate the intensity because 1900 Hz is above $f_{N,0°}$ (see Figure 3.7). This represents a small improvement over the traditional method at 30°, as is seen in Figure 3.8 and Figure 3.9. In Figure 3.9, the direction error is seen at all rotation angles, but the error at 30°, 60°, 120°, etc. can be observed to be small.

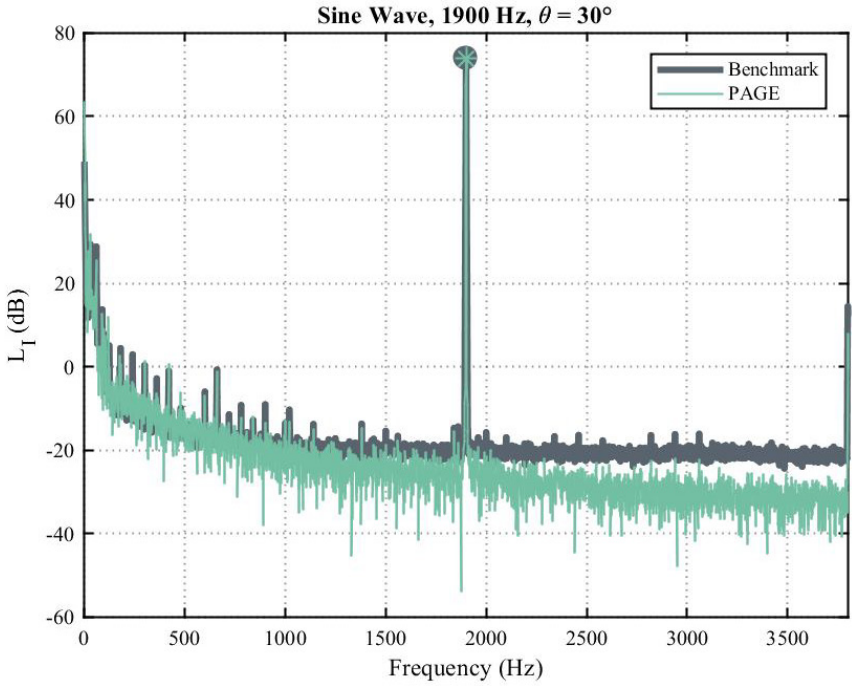

Figure 3.6: For a 1900 Hz sine wave in an anechoic chamber, a benchmark of $\boldsymbol{I} = \frac{p_{rms}^2}{\rho_0 c}$ *is compared to the PAGE calculation of active intensity for a probe with a 30° angle of rotation. Markers on each curve are at the frequency of the sine wave.*

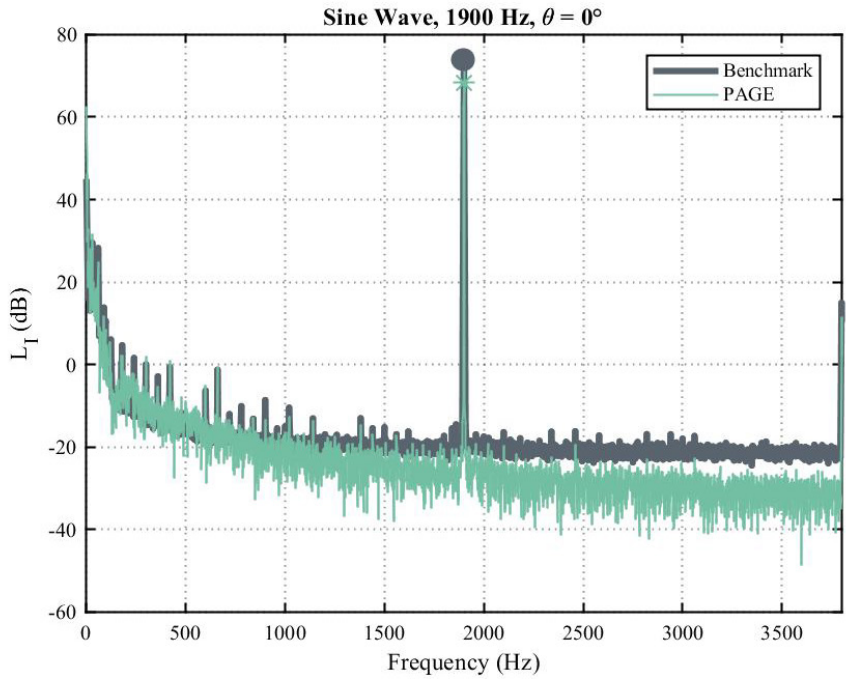

Figure 3.7: For a 1900 Hz sine wave in an anechoic chamber, a benchmark of $\boldsymbol{I} = \frac{p_{rms}^2}{\rho_0 c}$ *is compared to the PAGE calculation of active intensity for a probe with a 0° angle of rotation. Markers on each curve are at the frequency of the sine wave.*

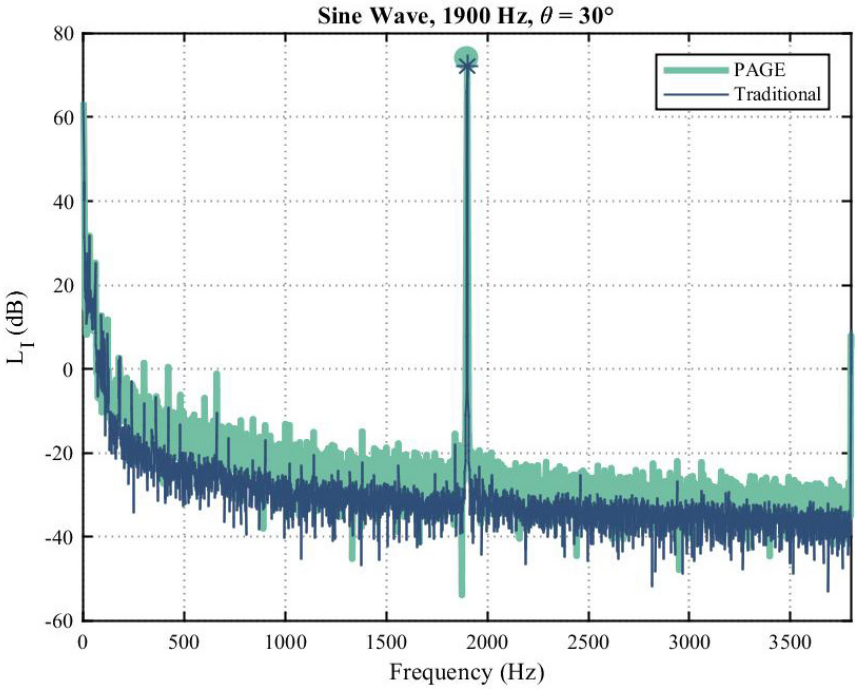

Figure 3.8: For a 1900 Hz sine wave in an anechoic chamber, the active intensity calculated using the PAGE method is compared to the active intensity calculated using the traditional method for a probe with a 30° angle of rotation. Markers on each curve are at the frequency of the sine wave.

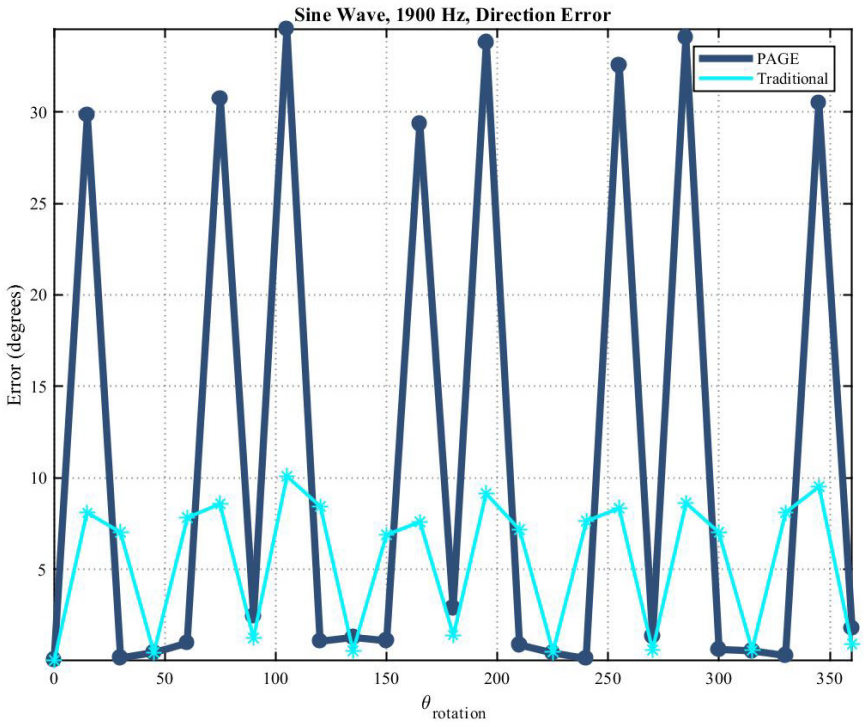

Figure 3.9: For a 1900 Hz sine wave in an anechoic chamber, the intensity direction error for the PAGE method is compared to the intensity direction error for the traditional method over all rotation angles.

The upper limit of the effective spatial Nyquist frequency was tested by seeing how high in frequency sine wave magnitude and direction could be correctly calculated using the PAGE method. The theoretical maximum possible $f_{N,\text{eff}}$ is about 2387 Hz based on a rotation angle of 45° in Eq. (5) and Eq. (6). Based on this limit, a sine wave at 2300 Hz was tested. As can be seen in Figure 3.10, the PAGE method underestimates the intensity level at 2300 Hz for a rotation angle of 45°. Due to this, a lower frequency of 2100 Hz was tested for the same angle of rotation. The results of this test are in Figure 3.11, and it can be seen that the PAGE method accurately calculates the intensity level for this frequency. The comparison with the traditional method is observable in Figure 3.12 and Figure 3.13. The improvement for magnitude in Figure 3.12 is not as significant as may be expected because the effective microphone spacing is also smaller for the traditional method. In Figure 3.13, it is shown that some of the smallest errors at 2100 Hz are

at 45°, 135°, etc., as expected. It is important to note that the maximum measured $f_{N,\text{eff}}$ is 2100 Hz, with the possibility of it being between 2100 Hz and 2300 Hz.

Possible reasons for the experimental result to not quite reach the theoretical maximum could be directional alignment errors in the original setup, possible separation of the microphones from the centerline of propagation, or a sound speed different from the nominal 343 m/s used in calculations. Directional alignment errors in the setup were always kept to less than 3°, but a 3° error could decrease the theoretical maximum down to about $f_{N,\text{eff}} \approx 2271$ Hz. In this orientation, microphones 2 and 5 are the closest to the source (see Figure 3.1 and Figure 3.2), but would be a maximum of an approximate 1° angle from the source. This 1° difference could make a difference of no more than 41 Hz on the spatial Nyquist frequency depending on the angle of rotation. If this error is combined with a 3° alignment error, the spatial Nyquist frequency maximum drops to approximately 2237 Hz. Differences in sound speed would only make a difference of about 7 Hz to the spatial Nyquist frequency per 1 m/s. The explanations presented are only possible reasons and one or all of them could be contributing factors to the experimental results not matching the theoretical maximum.

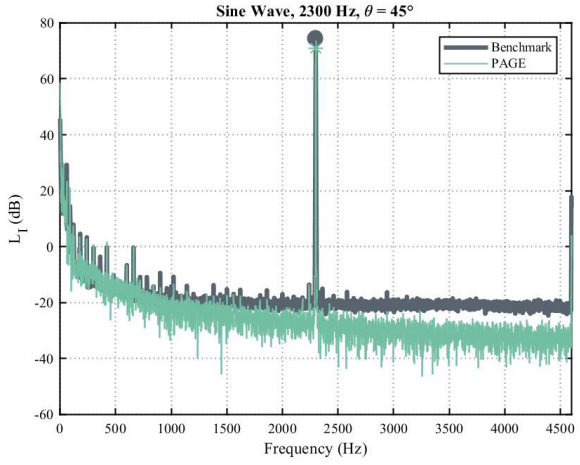

Figure 3.10: For a 2300 Hz sine wave in an anechoic chamber, a benchmark of $\boldsymbol{I} = \frac{p_{rms}^2}{\rho_0 c}$ *is compared to the PAGE calculation of active intensity for a probe with a 45° angle of rotation. Markers on each curve are at the frequency of the sine wave.*

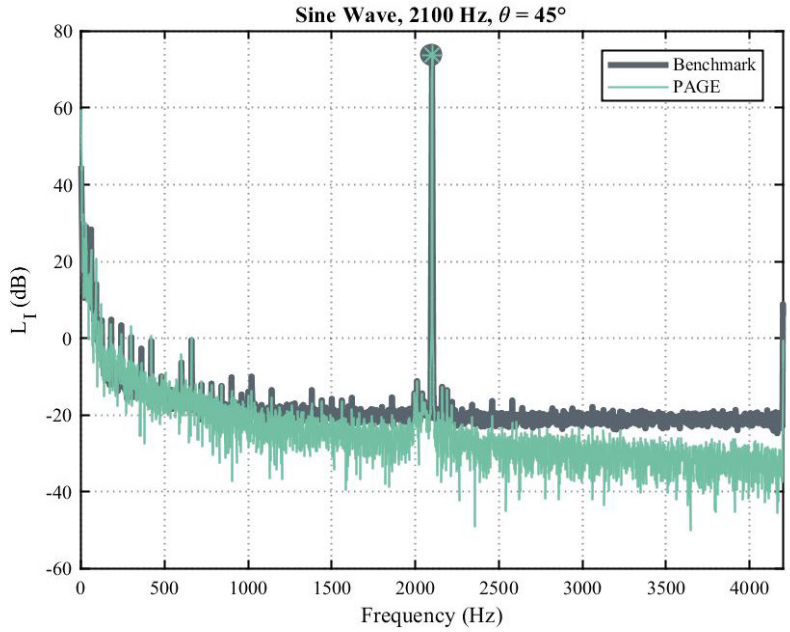

Figure 3.11: For a 2100 Hz sine wave in an anechoic chamber, a benchmark of $\boldsymbol{I} = \frac{p_{rms}^2}{\rho_0 c}$ *is compared to the PAGE calculation of active intensity for a probe with a 45° angle of rotation. Markers on each curve are at the frequency of the sine wave.*

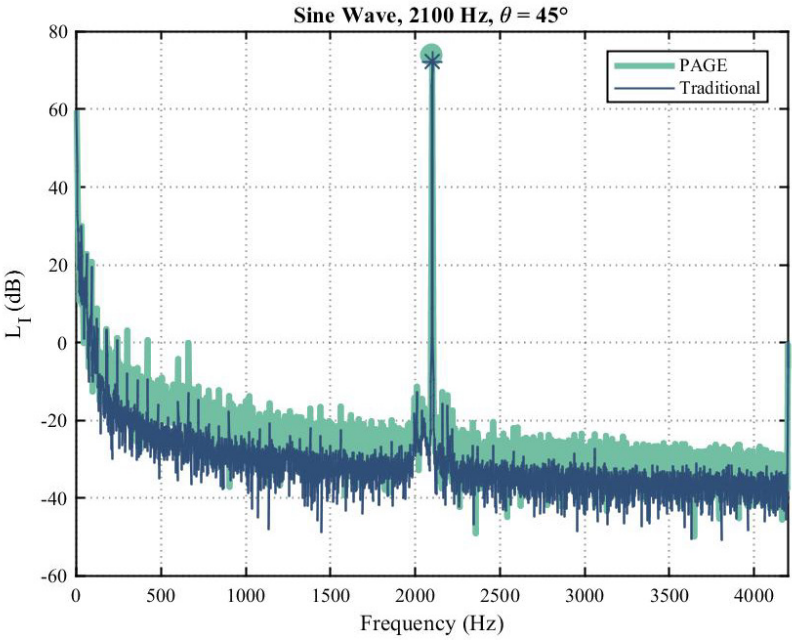

Figure 3.12: For a 2100 Hz sine wave in an anechoic chamber, the active intensity calculated using the PAGE method is compared to the active intensity calculated using the traditional method for a probe with a 45° angle of rotation. Markers on each curve are at the frequency of the sine wave.

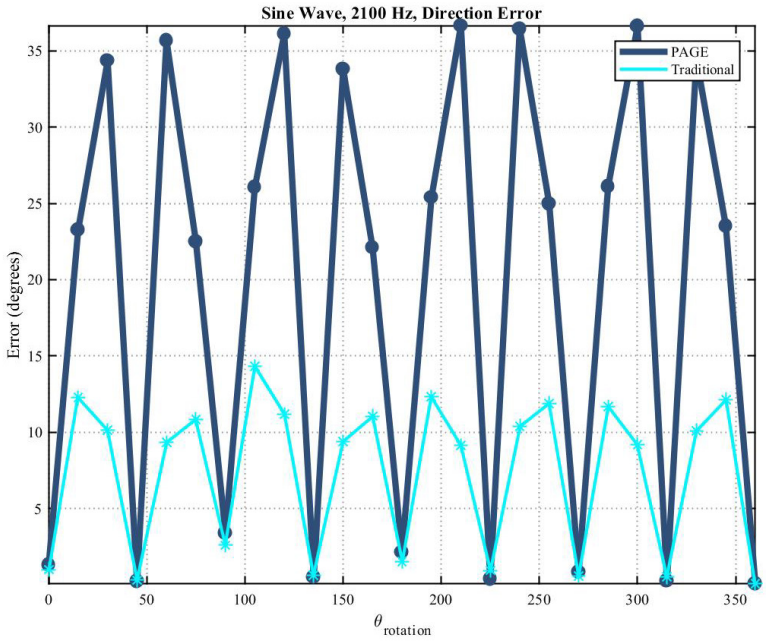

Figure 3.13: For a 2100 Hz sine wave in an anechoic chamber, the intensity direction error for the PAGE method is compared to the intensity direction error for the traditional method over all rotation angles.

In both Figure 3.9 and Figure 3.13, the smallest intensity direction errors occur at 0° and 45° and their counterparts (90°, 135°, etc.) for any frequency above $f_{N,0^\circ}$. The relatively low errors at 0°, 90°, etc. despite their lower spatial Nyquist frequencies is due to the fact that the phase difference across one pair of microphones at that angle is very close to zero, which makes it easy for the direction to be calculated correctly even when the magnitude is not. It is also worth noting from both Figure 3.9 and Figure 3.13 that at angles where the frequency is only a few hundred Hz above the effective spatial Nyquist frequency for that rotation angle, the traditional method has a noticeably smaller direction error than the PAGE method does.

It is important to note that all of the calculations for the sine wave case were done without unwrapping. If unwrapping was attempted, significant errors occurred. In our processing, it was hardcoded that no unwrapping could occur until close to $f_{N,0^\circ}$ to prevent erroneous unwrapping before it made sense for it to occur. For this microphone spacing, this means that based on only the fact that the probe had a maximum spacing of 4 inches, $f_{N,0^\circ} \approx$

1688 Hz was calculated and no unwrapping was allowed until 90% of this f_N , which turns out to be about 1519 Hz. However, since sine waves only have coherent phase information at the frequency of the sine wave, erroneous unwrapping was occurring in the frequency band between where it was no longer hardcoded not to unwrap (1519 Hz) and the actual frequency of the sine wave. These errors were especially egregious at rotation angles where the effective spatial Nyquist frequency was increasing, because where it was being allowed to unwrap (1519 Hz) could not be adjusted for angle of incidence, so there was a greater frequency band over which errors could occur. An example of this case can be observed in the phase of the transfer functions in Figure 3.14. Also, notice that this case is at a rotation angle of 45°, so 1800 Hz is well below the effective spatial Nyquist frequency, so the phase should still be between $-\pi$ and π. Notice that the scale for phase is in radians, so the error is significant. The phase of the transfer function is used to calculate the particle velocity and therefore the intensity, and the resulting error in intensity magnitude can be seen in Figure 3.15. This was only a problem when the sine wave being tested was above the frequency at which unwrapping was allowed to occur in the code and below the effective spatial Nyquist frequency, but this was a significant range for these tests since one goal was to observe the change in effective spatial Nyquist frequency with angle of incidence. Other unwrapping algorithms, such as coherence-based unwrapping,[55] may be able to overcome some of these difficulties. However, as previously stated, the chosen solution to this problem was turning unwrapping off for all frequencies.

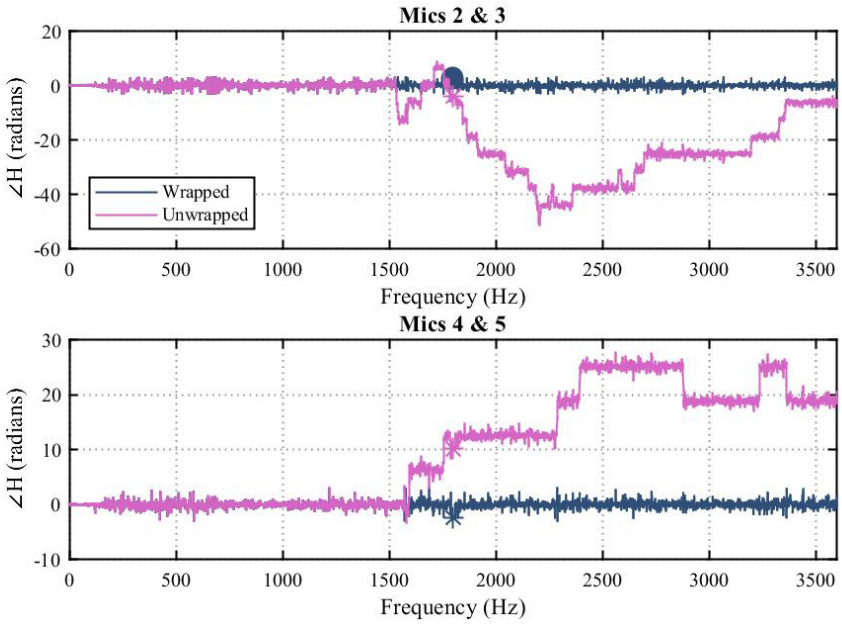

Figure 3.14: For an 1800 Hz sine wave in an anechoic chamber, the phase of the wrapped vs unwrapped phase of the PAGE method is shown for a probe at a rotation angle of 45°.

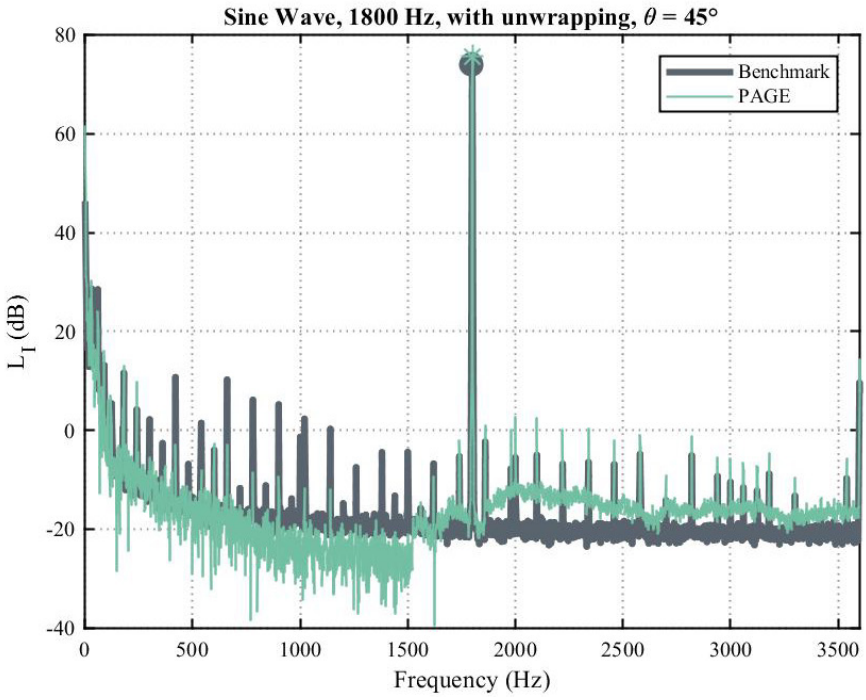

Figure 3.15: For a 1800 Hz sine wave in an anechoic chamber, a benchmark of $\boldsymbol{I} = \frac{p_{rms}^2}{\rho_0 c}$ *is compared to the PAGE calculation of active intensity for a probe with a 45° angle of rotation. In this case, unwrapping is turned on for the PAGE calculation. Markers on each curve are at the frequency of the sine wave.*

3.3 Sawtooth waves

3.3.1 Experiment

Experiments with sawtooth waves were conducted to verify the results from our one-dimensional sawtooth wave experiments for a multi-dimensional field and verify the conclusions in Section 3.2.2. These conclusions were that the PAGE method works up to the effective spatial Nyquist frequency, and that for a sawtooth wave an extrapolated PAGE method can be used to obtain correct intensity magnitude and direction above the spatial Nyquist frequency. It was expected that these conclusions would all hold for these experiments. The experimental setup was the same as was used for sine waves, and can be seen in Figure 3.2. For reasons similar to those cited in the sine wave case, unwrapping was turned off for the normal PAGE processing.

3.3.2 Results and analysis

As expected, the intensity of any peaks below the spatial Nyquist frequency was calculated correctly using the PAGE method. A 250 Hz sawtooth wave case demonstrates this effectively because it shows many peaks both above and below the spatial Nyquist frequency. The plot for the 250 Hz sawtooth wave intensity level for the PAGE method at a rotation angle of 45° can be seen in Figure 3.16. Notice that for this rotation angle, the PAGE method matches the benchmark well up through the peak at 2000 Hz. After that, the PAGE method starts to underestimate the benchmark. This further confirms our findings in the previous sections and narrows the upper range of the effective spatial Nyquist frequency for this spacing to be between 2100 Hz and 2250 Hz.

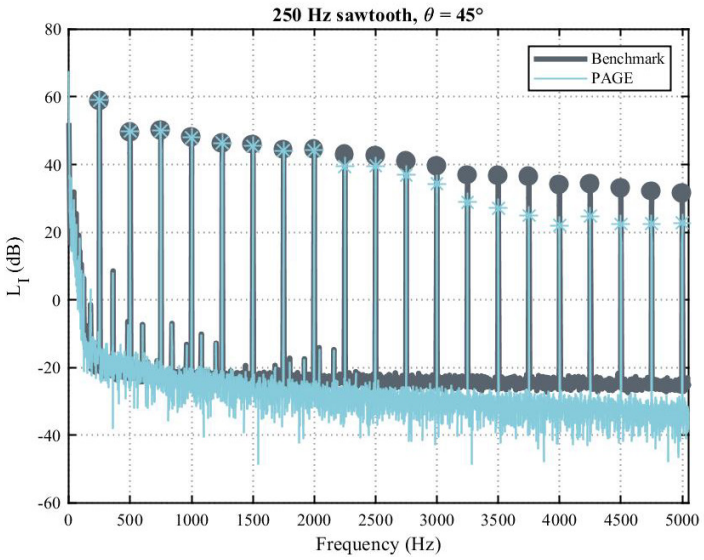

Figure 3.16: For a 250 Hz sawtooth wave in an anechoic chamber, a benchmark of $\boldsymbol{I} = \frac{p_{rms}^2}{\rho_0 c}$ *is compared to the PAGE calculation of active intensity for a probe with a 45° angle of rotation. Markers on each curve are at the frequencies which correspond to the peaks of the sawtooth.*

The extrapolated PAGE method, as described in Section 2.3, was applied to the multi-dimensional case. As previously stated in Section 2.3, the method requires a propagating field and for at least one peak of the sawtooth to be below the effective spatial Nyquist frequency. For the two-dimensional probe, the method of extrapolating the phase based on the phase of the first peak was done for each microphone pair. Due to the symmetry of the probe, the only pairs that end up contributing to the answer are microphones 2 and 3 and microphones 4 and 5 (see Figure 3.1). The phase extrapolation for a 1000 Hz sawtooth wave at a rotation angle of 45° can be seen in Figure 3.17. The markers are at each frequency of the sawtooth, but the extrapolation is based only on the fundamental frequency. The intensity magnitude results of the PAGE method without extrapolation and with extrapolation (for the same case as Figure 3.17) are shown in Figure 3.18 and Figure 3.19, respectively. Note that the frequency range of these plots up to 20 kHz. The regular PAGE method in Figure 3.18 only matches the benchmark for the peaks at 1 kHz and 2 kHz, as would be expected for a 45° rotation angle. Also notice in Figure 3.19 that

despite the sawtooth wave not being an ideal sawtooth due to the imperfections of the speaker, the extrapolated PAGE matches the benchmark up to 20 kHz. Figure 3.20 shows the improvement of the extrapolated PAGE method over the traditional method for intensity magnitude. The comparison of the direction error that is calculated from Eq. (7) for the extrapolated PAGE method, the PAGE method, and the traditional method are compared as a function of rotation angle at 2 kHz in Figure 3.21 and at 20 kHz in Figure 3.22. For the comparison at 2 kHz in Figure 3.21, the PAGE and traditional methods predictably have their lowest error at rotation angles where 2 kHz is below the effective spatial Nyquist frequency, and the extrapolated PAGE method always has an error of less than 2°. For the comparison at 20 kHz in Figure 3.22, the extrapolated PAGE method still always has less than 2° of error but the other two methods have very large errors at all angles of rotation. Based on some uncertainty in our setup, within about 3° was considered an acceptable tolerance for direction; the extrapolated PAGE method was always within this tolerance. The extrapolated PAGE method successfully was able to calculate intensity magnitude and direction at frequencies far above the spatial Nyquist frequency.

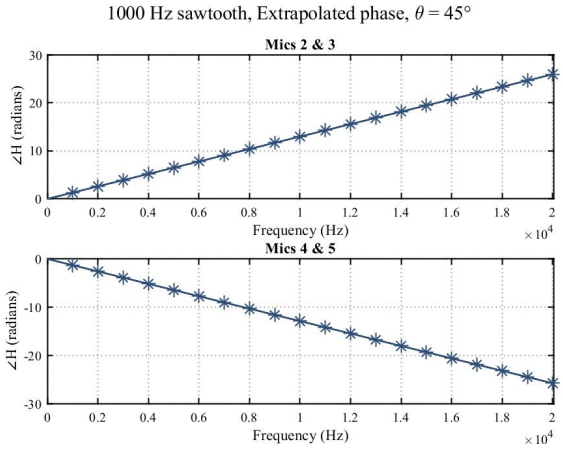

Figure 3.17: For a 1000 Hz sawtooth wave in an anechoic chamber, the extrapolated phase is shown for a probe at a rotation angle of 45°. Markers on each curve are at the frequencies which correspond to the peaks of the sawtooth. The extrapolated phase is based on the phase of the fundamental frequency.

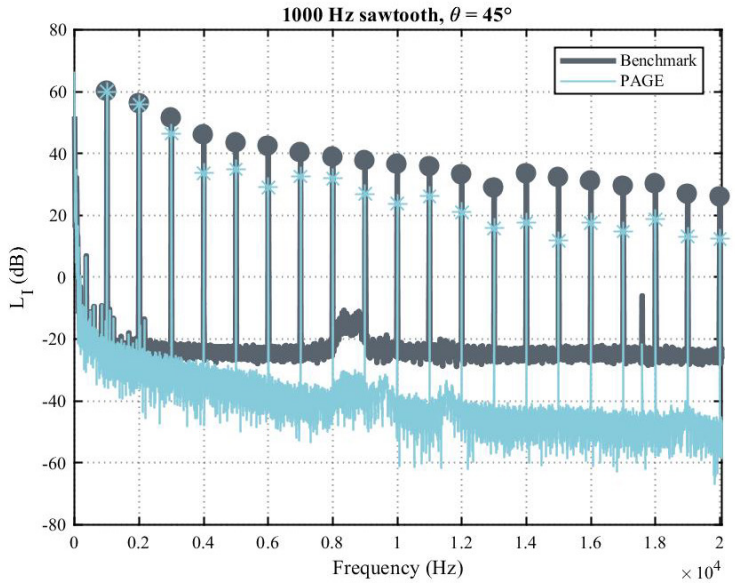

Figure 3.18: For a 1000 Hz sawtooth wave in an anechoic chamber, a benchmark of $\boldsymbol{I} = \frac{p_{rms}^2}{\rho_0 c}$ *is compared to the PAGE calculation of active intensity for a probe with a 45° angle of rotation. Markers on each curve are at the frequencies which correspond to the peaks of the sawtooth.*

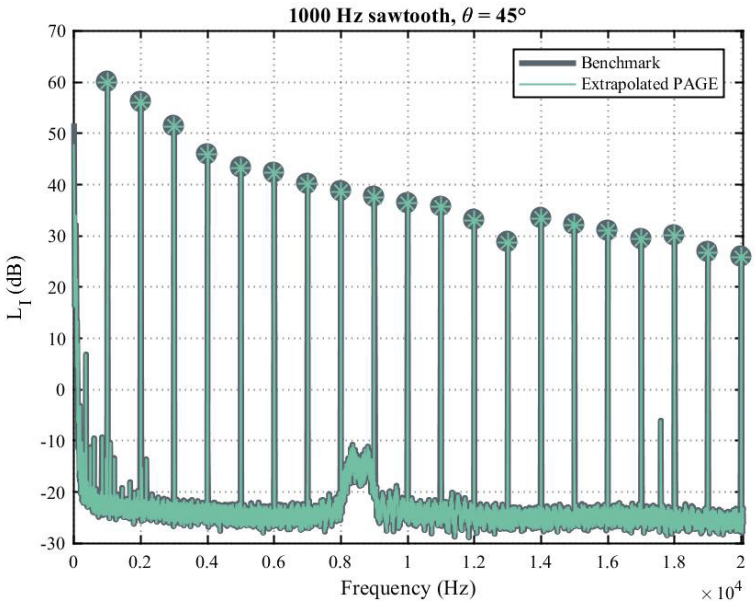

Figure 3.19: For a 1000 Hz sawtooth wave in an anechoic chamber, a benchmark of $\boldsymbol{I} = \frac{p_{rms}^2}{\rho_0 c}$ *is compared to the extrapolated PAGE calculation of active intensity for a probe with a 45° angle of rotation. Markers on each curve are at the frequencies which correspond to the peaks of the sawtooth.*

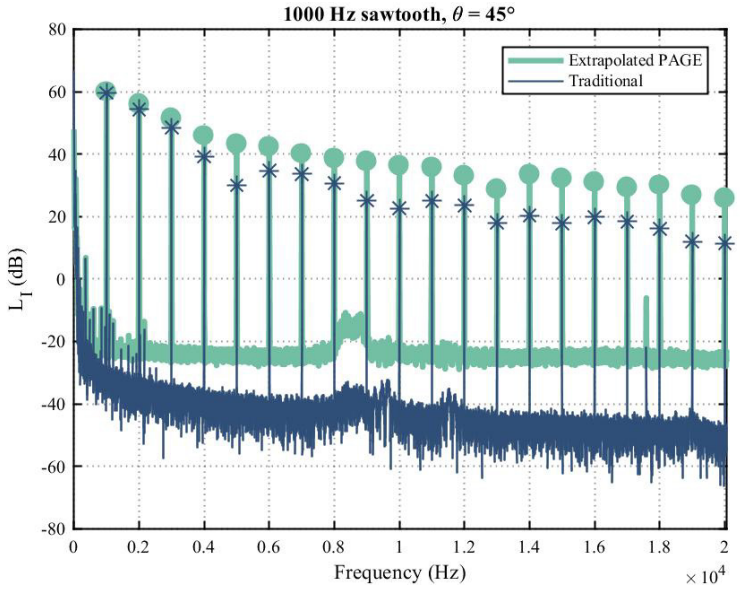

Figure 3.20: For a 1000 Hz sawtooth wave in an anechoic chamber, the active intensity calculated using the extrapolated PAGE method is compared to the active intensity calculated using the traditional method for a probe with a 45° angle of rotation. Markers on each curve are at the frequencies which correspond to the peaks of the sawtooth.

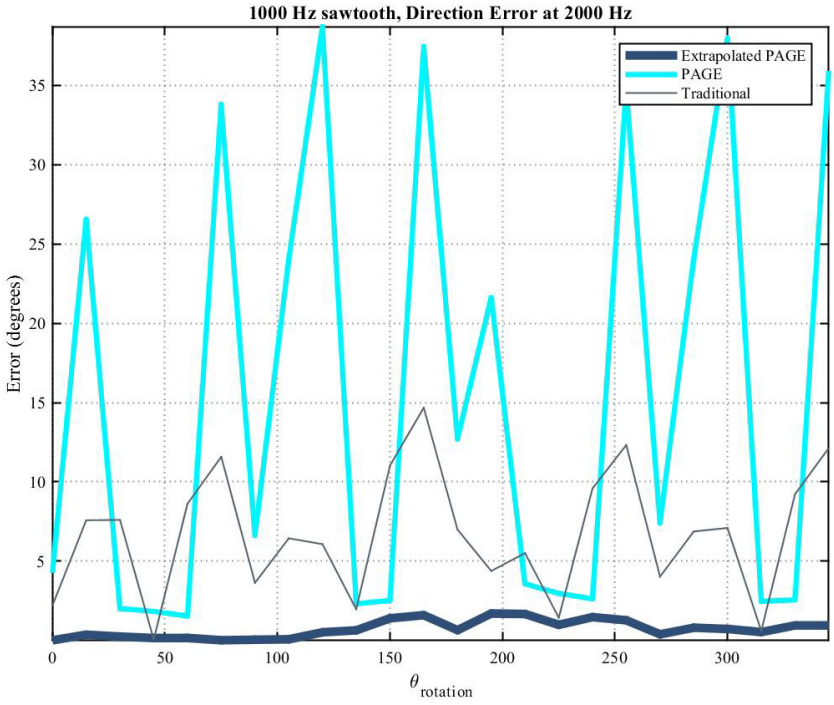

Figure 3.21: For a 1000 Hz sine wave in an anechoic chamber, the intensity direction error for the extrapolated PAGE method is compared to the intensity direction error for the PAGE method and the traditional method at 2000 Hz over all rotation angles.

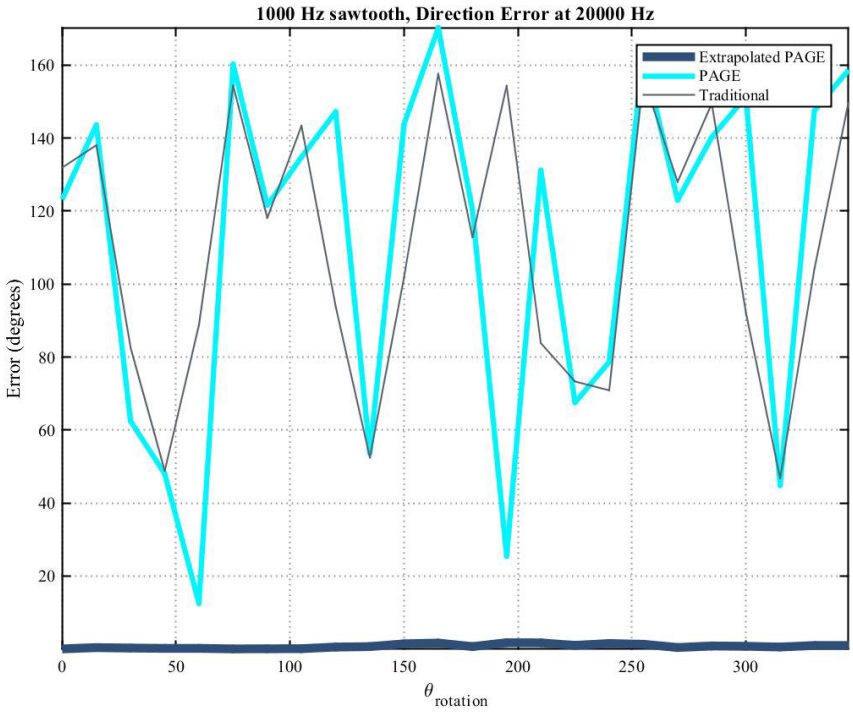

Figure 3.22: For a 1000 Hz sine wave in an anechoic chamber, the intensity direction error for the extrapolated PAGE method is compared to the intensity direction error for the PAGE method and the traditional method at 2000 Hz over all rotation angles.

3.4 Tones from multiple sources

3.4.1 Experiment

The purpose of this experiment was to see if the extrapolated PAGE method used for sawtooth waves could also be applied when the tone below the spatial Nyquist frequency came from a different source and potentially at a different angle than the tone above the spatial Nyquist frequency.

The setup for this experiment used two separate speakers. One speaker was on an arm connected to the turntable and therefore rotated with the probe, meaning it always had a 0° rotation angle. The other speaker was on a stand, slightly higher than the speaker on the arm to allow them to both be at a 0° rotation angle at the same time. This setup can be seen in Figure 3.23. The speaker on the arm, which is the lower one in Figure 3.23, was raised up on a piece of

wood to decrease the effects of scattering off the arm. The blue piece of foam on the arm is also for the purpose of decreasing scattering. Both speakers are approximately 2 meters away from the center of the probe in the horizontal direction.

Figure 3.23: One variation of the two-speaker setup in an anechoic chamber. The speaker on the arm rotates, and the angle of rotation then becomes the same as the angle of separation between the speakers.

One speaker broadcasted a sine wave at 1000 Hz and the other broadcasted a different, higher-frequency sine wave. The higher-frequency sine wave from the second speaker was chosen to be above the spatial Nyquist frequency for all rotation angles, and the 1000 Hz sine wave from the first speaker was always below the spatial Nyquist frequency. For reasons similar to those cited in the sine wave case, unwrapping was turned off for the normal PAGE processing.

3.4.2 Results and analysis

From normal PAGE processing, as expected, it was found that the normal PAGE method underestimates the intensity level for the higher frequency from the second speaker because it is above the spatial Nyquist frequency (see Figure 3.24).

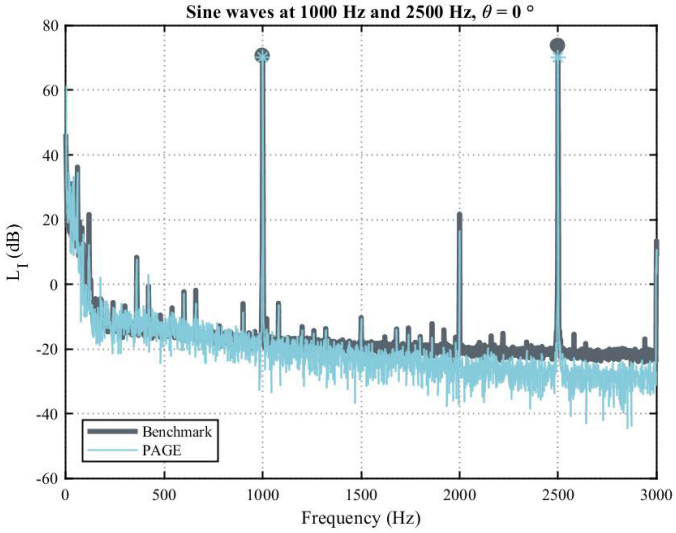

Figure 3.24: For a 1000 Hz sine wave from one speaker and a 2500 Hz sine wave from another speaker in an anechoic chamber, a benchmark of $\boldsymbol{I} = \frac{p_{rms}^2}{\rho_0 c}$ *is compared to the PAGE calculation of active intensity for a probe with a 0° angle of rotation. Markers on each curve are at the frequency of each sine wave.*

Similar to Sections 2.3 and 3.3, the extrapolated PAGE method was used in an effort to improve on the PAGE method. However, in this case the 1000 Hz tone from one speaker was used to extrapolate the phase of the transfer function in hopes of being able to correctly calculate the intensity for the tone above the spatial Nyquist frequency from the other speaker. The resulting extrapolated phase at a 0° rotation angle can be seen in Figure 3.25. For this rotation angle, it was expected that the extrapolated PAGE would work very well for both direction and angle because both sources are propagating from the same direction. From Figure 3.26, it can be seen that the extrapolated PAGE method was successful in matching the benchmark intensity magnitude even for the 2500 Hz tone that is above the spatial Nyquist frequency and from a

different source. The improvement over the traditional method can be seen in Figure 3.27. The comparison of the error in direction for the extrapolated PAGE method, the PAGE method, and the traditional method at the 2500 Hz is in Figure 3.28, as calculated from Eq. (7). This graph will be discussed more in subsequent paragraphs, but at 0° it can be observed that the extrapolated PAGE method has no direction error.

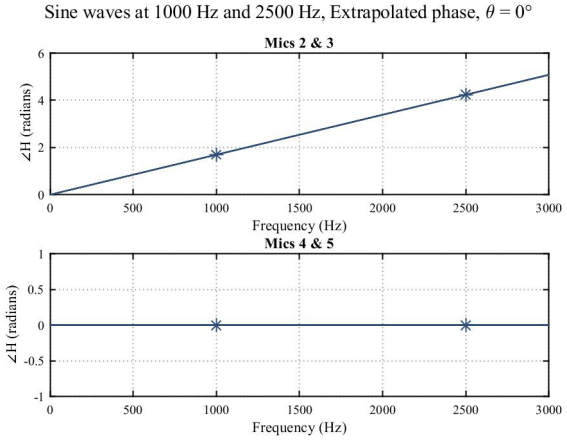

Figure 3.25: For a 1000 Hz sine wave from one speaker and a 2500 Hz sine wave from another speaker in an anechoic chamber, the extrapolated phase is shown for a probe at a rotation angle of 0°. Markers on each curve are at the frequency of each sine wave. The extrapolated phase is based on the phase of the 1000 Hz tone.

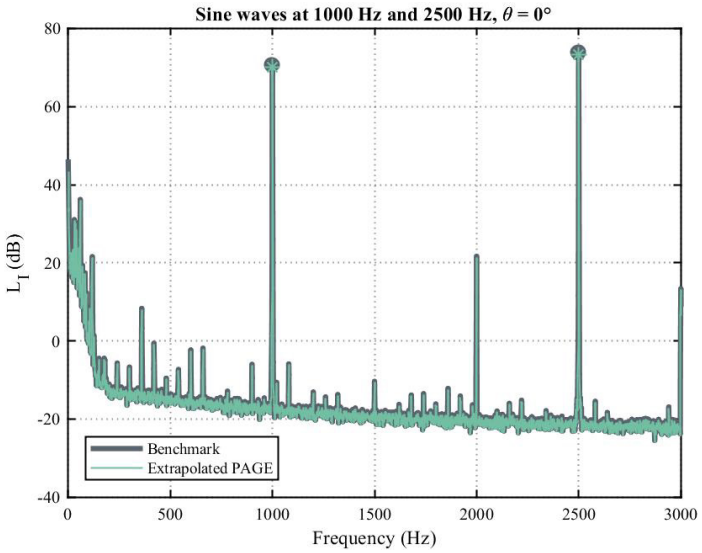

Figure 3.26: For a 1000 Hz sine wave from one speaker and a 2500 Hz sine wave from another speaker in an anechoic chamber, a benchmark of $\boldsymbol{I} = \frac{p_{rms}^2}{\rho_0 c}$ *is compared to the extrapolated PAGE calculation of active intensity for a probe with a 0° angle of rotation. Markers on each curve are at the frequency of each sine wave.*

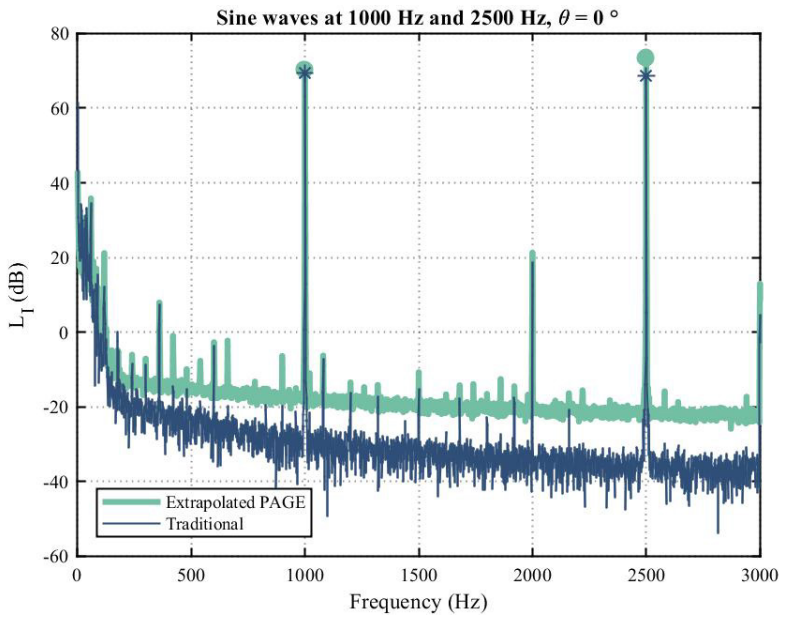

Figure 3.27: For a 1000 Hz sine wave from one speaker and a 2500 Hz sine wave from another speaker in an anechoic chamber, the active intensity calculated using the extrapolated PAGE method is compared to the active intensity calculated using the traditional method for a probe with a 0° angle of rotation. Markers on each curve are at the frequency of each sine wave.

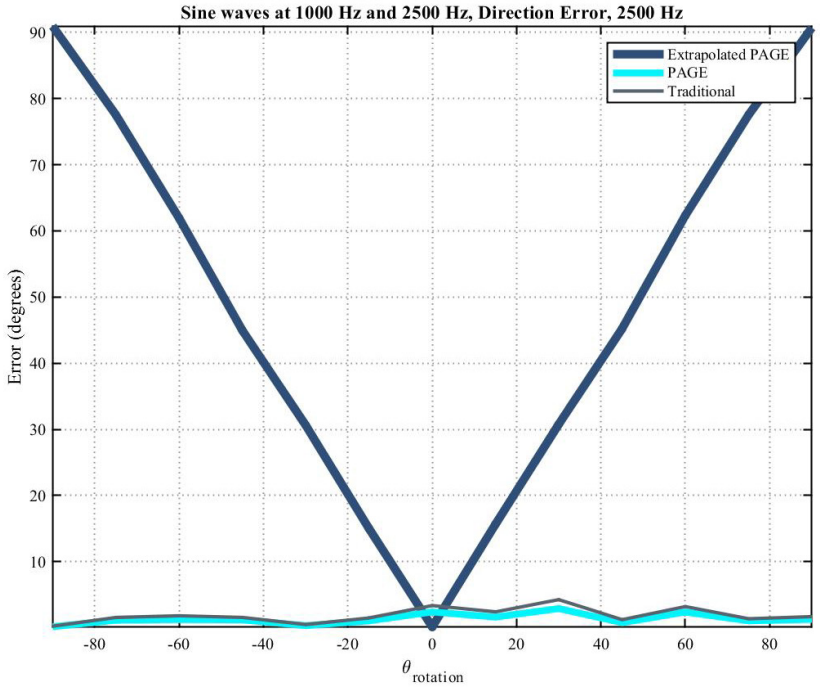

Figure 3.28: For a 1000 Hz sine wave from one speaker and a 2500 Hz sine wave from another speaker in an anechoic chamber, the intensity direction error for the extrapolated PAGE method is compared to the intensity direction error for the PAGE method and the traditional method at 2500 Hz over all rotation angles.

As seen in Figure 3.28, the direction error for the extrapolated PAGE method is essentially the same as the rotation angle. In retrospect, this makes sense since the 1000 Hz tone is always at a rotation angle of 0°, and the phase of the 1000 Hz tone is what is used to extrapolate the phase of the 2500 Hz tone. Thus, the 2500 Hz tone always gets a direction from the extrapolated PAGE method of 0°. However, at every tested angle the extrapolated PAGE method did calculate the intensity level correctly for all higher frequencies tested. For a frequency from the second speaker of 2500 Hz, the intensity level results can be seen for extrapolated PAGE at 45° and 90° in Figure 3.29 and Figure 3.30, respectively. These figures show that the magnitude is correctly calculated using the extrapolated PAGE method even though the error in direction is 45° and 90°, respectively. The improvement over the traditional method for the 90° rotation angle can be seen in Figure 3.31.

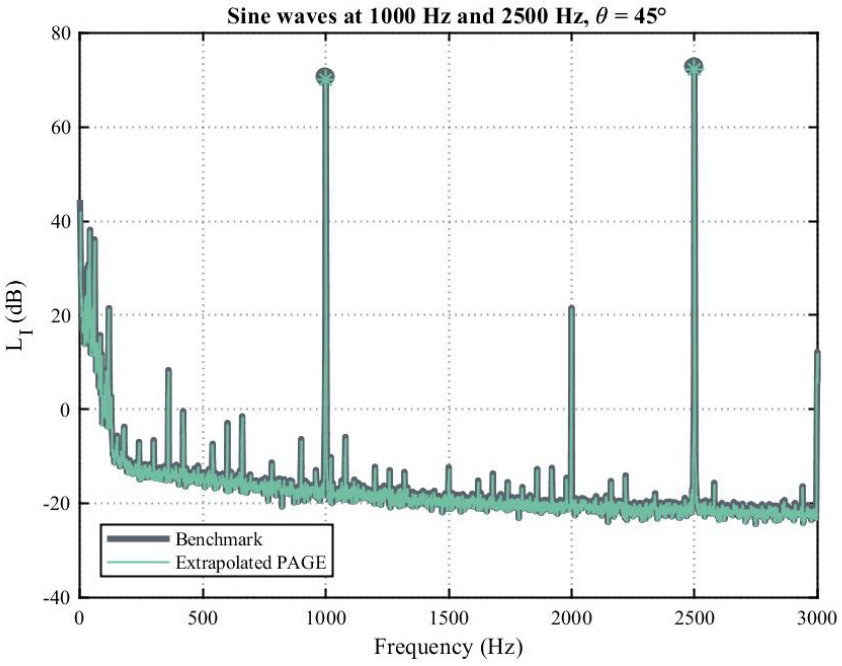

Figure 3.29: For a 1000 Hz sine wave from one speaker and a 2500 Hz sine wave from another speaker in an anechoic chamber, a benchmark of $\boldsymbol{I} = \frac{p_{rms}^2}{\rho_0 c}$ *is compared to the extrapolated PAGE calculation of active intensity for a probe with a 45° angle of rotation. Markers on each curve are at the frequency of each sine wave.*

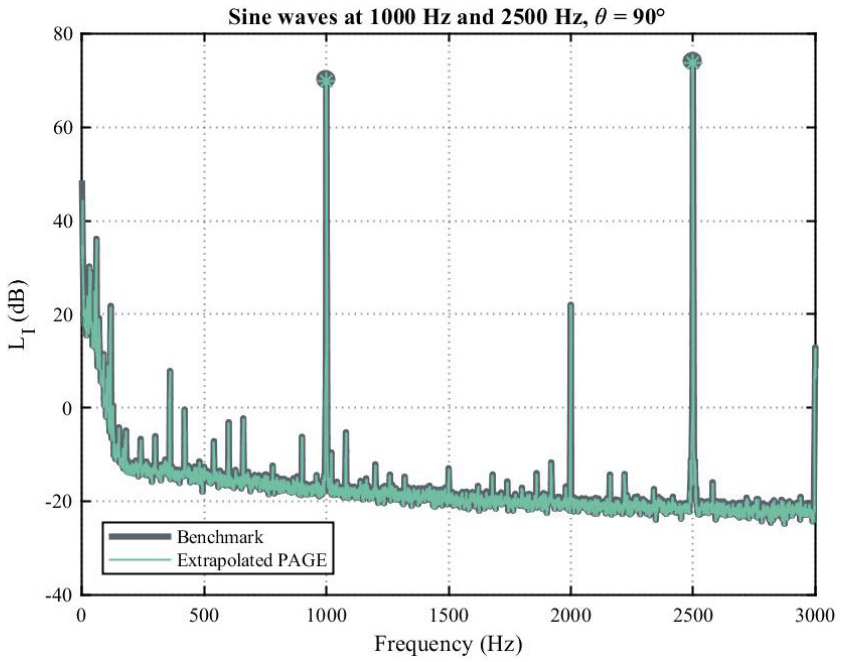

Figure 3.30: For a 1000 Hz sine wave from one speaker and a 2500 Hz sine wave from another speaker in an anechoic chamber, a benchmark of $\frac{p^2}{\rho_0 c}$ is compared to the extrapolated PAGE calculation of active intensity for a probe with a 90° angle of rotation. Markers on each curve are at the frequency of each sine wave.

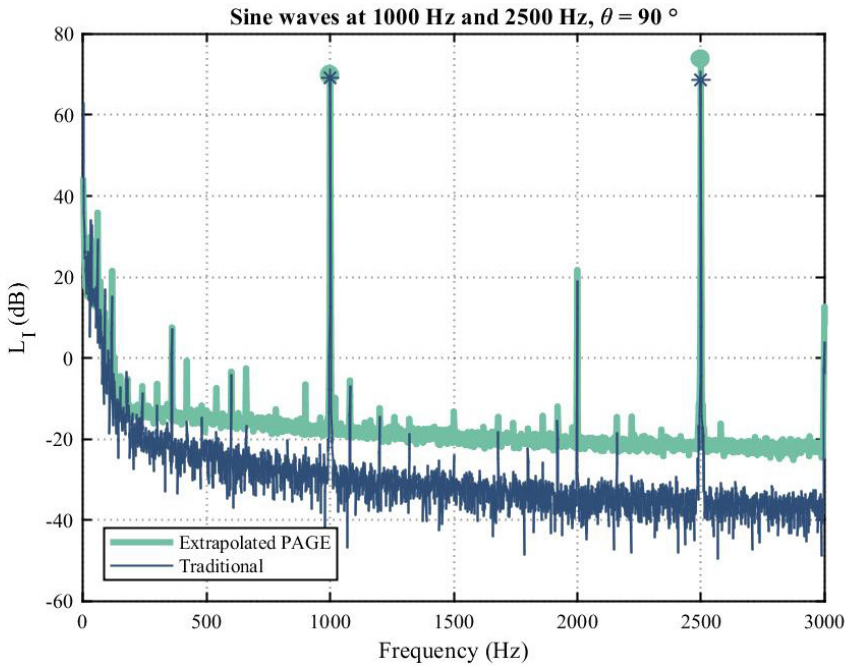

Figure 3.31: For a 1000 Hz sine wave from one speaker and a 2500 Hz sine wave from another speaker in an anechoic chamber, the active intensity calculated using the extrapolated PAGE method is compared to the active intensity calculated using the traditional method for a probe with a 90° angle of rotation. Markers on each curve are at the frequency of each sine wave.

From the results in this section, it is found that the extrapolated PAGE method for the two-speaker case explored here is only valuable when the angle of rotation is within the allowable direction error for a given measurement. Within this range, the intensity magnitude and direction are both calculated correctly by the extrapolated PAGE method, even if one tone is above the spatial Nyquist frequency. However, at greater angular differences, it may be just as valuable to just use one microphone to get the magnitude without frequency limitations because the direction obtained from this method is so inaccurate.

3.5 Same tone from multiple speakers

3.5.1 Experiment

The main goal of this experiment was to explore an interesting case of two speakers at various separation angles to each other, teed off from the same sine wave signal below the spatial Nyquist frequency, and see if we were able to match analytical results using the PAGE method.

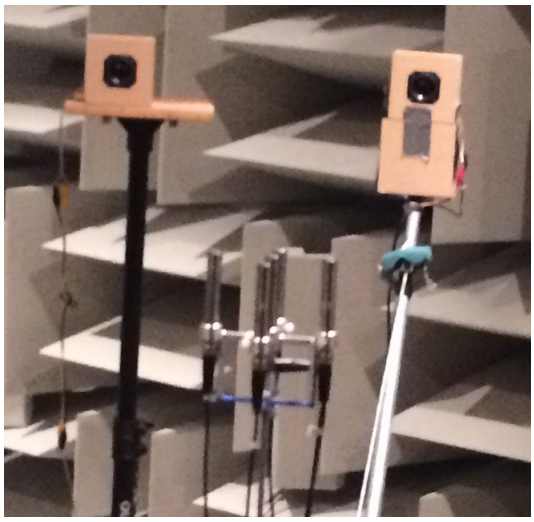

Figure 3.32: The setup for two speakers playing exactly the same signal. The path length to the center of the probe is approximately equal from each speaker.

Although similar to the setup used in Figure 3.23, the setup for this experiment was slightly different because it was important to have the same path length from each speaker to the

center of the probe, or as close as possible. For this reason, the speakers were put at approximately the same height and approximately the same distance from the probe. The setup is seen in Figure 3.32, where it can also be observed that the probe is always at 0° rotation from the speaker on the arm because they move together.

For this experiment, it was expected that the magnitude calculated by the PAGE method would match analytical values, and that the direction would be close to the middle of the two rotation angles. This was predicted based on the idea that the two waves would be in phase and therefore add coherently at the probe, creating an intensity magnitude that would represent a vector addition of the two signals and with a direction exactly halfway between the two rotation angles. It was expected that this would break down to some extent at separation angles approaching 180°, because there would be standing wave effects where the waves met at the probe due to the wavelengths being the same and in completely opposite directions.

3.5.2 Results and analysis

First, the accuracy of the intensity magnitude using the PAGE and traditional method were compared to a numerical simulation of the experiment. The results for the intensity magnitude are in Figure 3.33 for a sine wave signal at 700 Hz. The numerical cases go to negative infinity because the numerical intensity at a rotation angle of 180° is 0, so the intensity level is infinite. It can be observed in Figure 3.33 that the traditional method slightly underestimates the PAGE calculation in both the numerical and experimental cases. For both the PAGE method and the traditional method, the experimental results follow the same general trends as the numerical results.

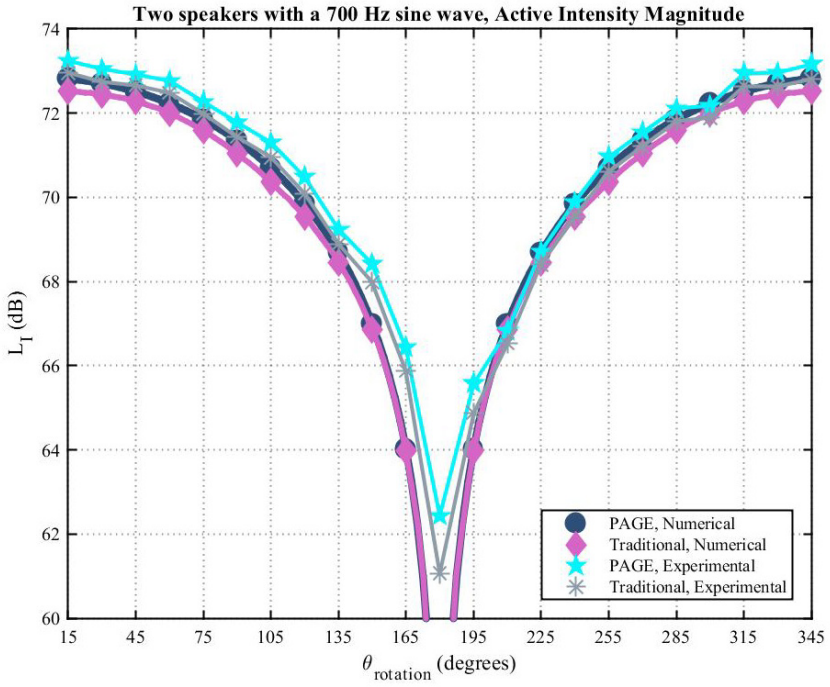

Figure 3.33: For two speakers teed off the same 700 Hz sine wave signal, the active intensity magnitude is compared between an ideal numerical case and experimental results using both the PAGE method and the traditional method over all rotation angles. Markers are at each angle of rotation in the actual experiment.

For intensity direction, the PAGE and traditional method were compared to the same numerical simulation of the experiment. The results of this comparison are in Figure 3.34 for a sine wave signal at 700 Hz. As expected, the ideal numerical result corresponds to an angle which is half of the angle of separation between the speakers. It can be observed that the results for both the PAGE method and the traditional method begin to underestimate the expected result, especially between rotation angles of 90° and 270°. Results similar to the experimental results were able to be obtained in the numerical simulation by adding a fixed phase of up to a 0.16-radian difference across the microphone pair comprised of microphones 2 and 3. The result of this phase difference, compared to the results from Figure 3.34, is shown in Figure 3.35. Although the results are not identical, they are similar. The results of applying this phase error to the intensity magnitude numerical simulation and a comparison with the experimental results is shown in Figure 3.36 for a 700 Hz sine wave signal. It can be observed that adding a phase offset

increases agreement with the experimental results for both intensity magnitude and intensity direction.

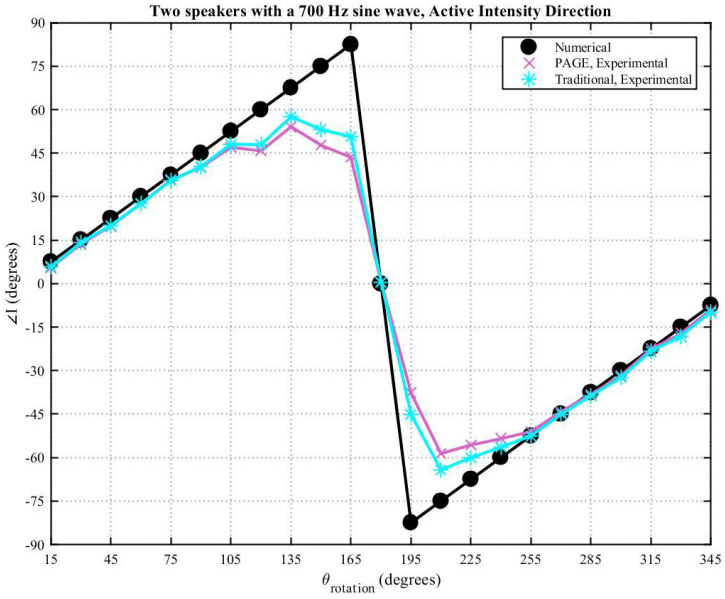

Figure 3.34: For two speakers teed off the same 700 Hz sine wave signal, the active intensity direction is compared between an ideal numerical case and experimental results using both the PAGE method and the traditional method at 700 Hz over all rotation angles. Markers are at each angle of rotation in the actual experiment.

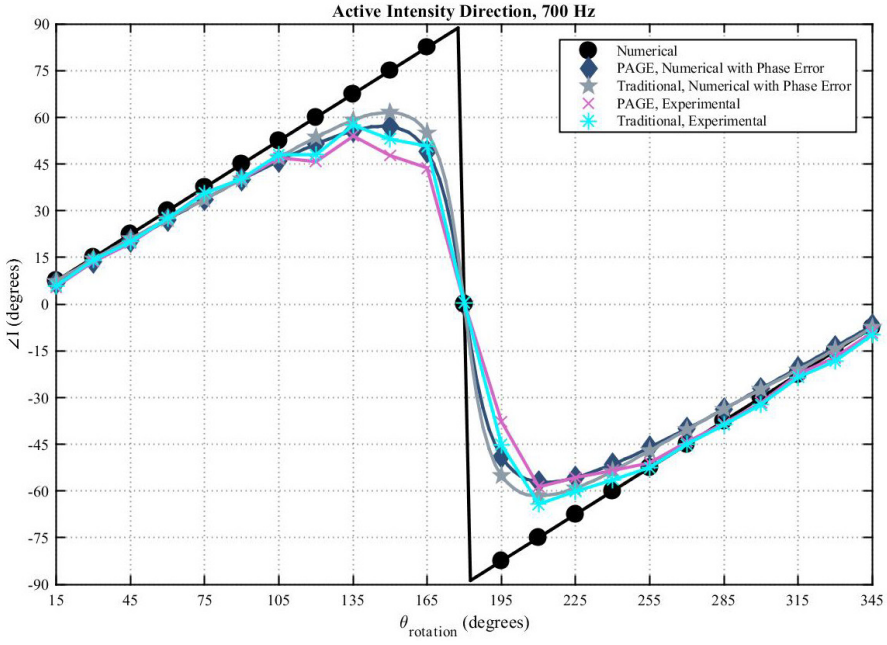

Figure 3.35: For two speakers teed off the same 700 Hz sine wave signal, the active intensity direction is compared between an ideal numerical case, the numerical case with added phase error, and experimental results using both the PAGE method and the traditional method at 700 Hz over all rotation angles. Markers are at each angle of rotation in the actual experiment.

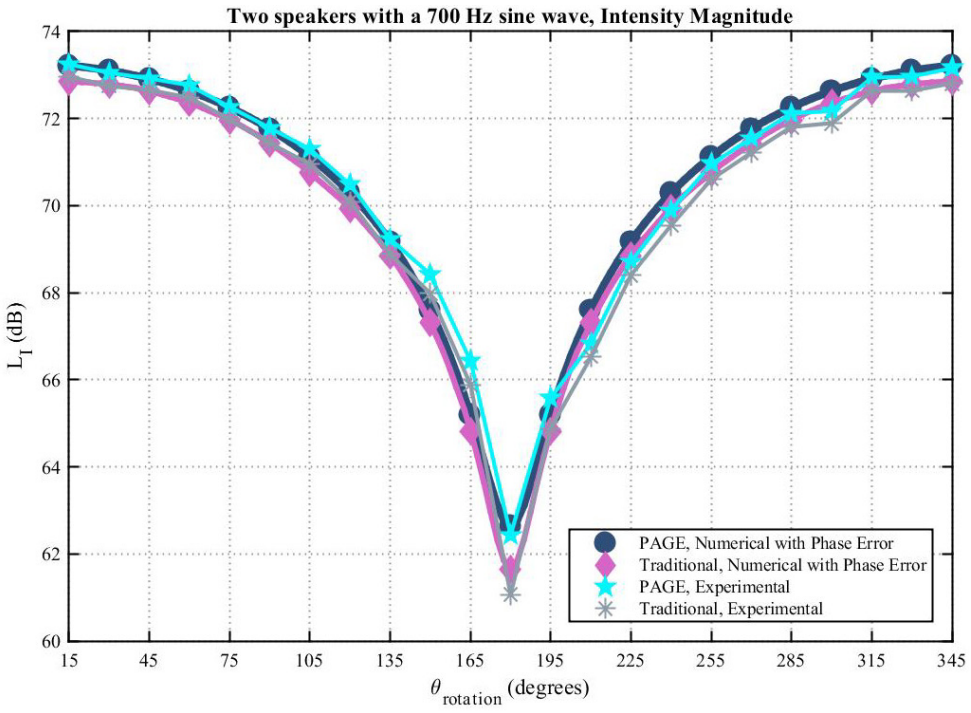

Figure 3.36: For two speakers teed off the same 700 Hz sine wave signal, the active intensity magnitude is compared between an ideal numerical case, the numerical case with added phase error, and experimental results using both the PAGE method and the traditional method at 700 Hz over all rotation angles. Markers are at each angle of rotation in the actual experiment.

A possible explanation for a fixed phase difference across microphones 2 and 3 would be that the path length from each speaker to the microphone is not equal or the volume of the sine waves is not equal. Specifically, the speaker on the arm is always propagating along the line of microphones 2 and 3, so a higher volume from that speaker or a shorter path length between that speaker and the microphone probe could account for the positive phase offset across microphones 2 and 3.

At higher frequencies still below the spatial Nyquist frequency, additional phenomena can be observed in the results. For example, the intensity magnitude calculated using the PAGE method, the traditional method, and the numerical simulation with phase error can be observed in Figure 3.37 for a sine wave signal at 1500 Hz. It can be observed that between rotation angles of 135° and 225°, the intensity magnitude calculated using the PAGE method no longer follows the

expected trends. The same problem over the same frequencies is observed for the intensity direction in Figure 3.38 for a sine wave signal at 1500 Hz. The problem can be observed at lower frequencies as well, as can be seen for intensity magnitude in Figure 3.39 and for intensity direction in Figure 3.40 for a sine wave signal at 1200 Hz. These problematic angles for the PAGE method results increase in severity with increasing frequency.

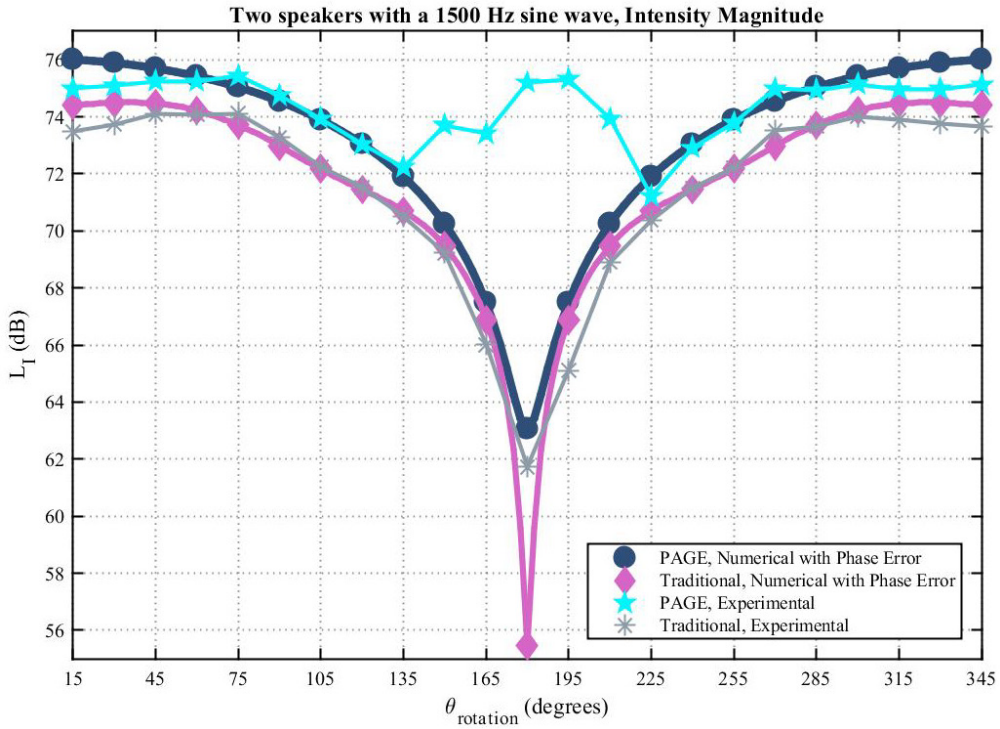

Figure 3.37: For two speakers teed off the same 1500 Hz sine wave signal, the active intensity magnitude is compared between an ideal numerical case, the numerical case with added phase error, and experimental results using both the PAGE method and the traditional method at 1500 Hz over all rotation angles. Markers are at each angle of rotation in the actual experiment.

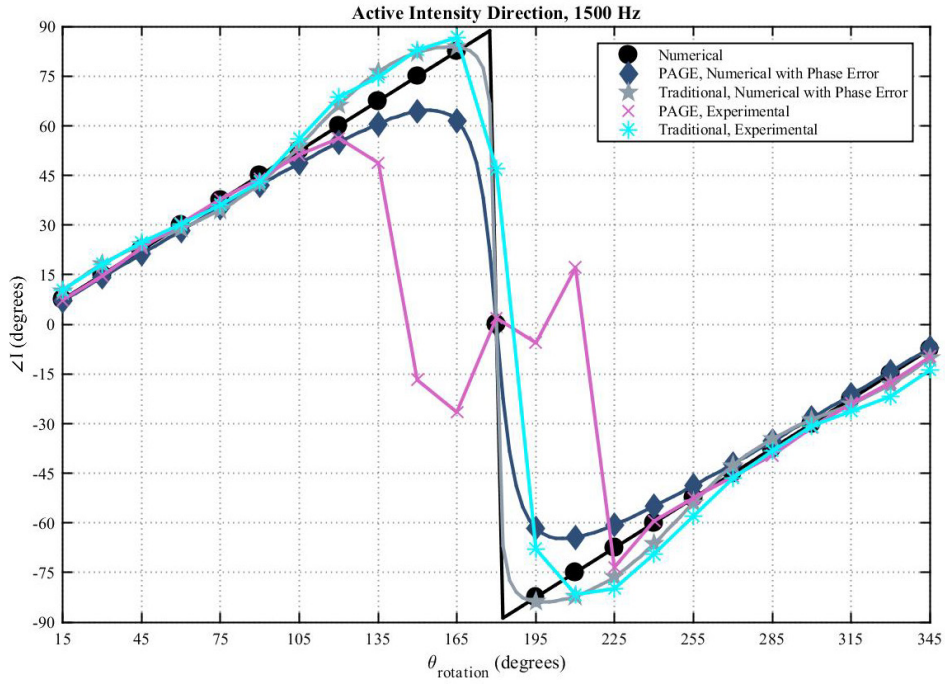

Figure 3.38: For two speakers teed off the same 1500 Hz sine wave signal, the active intensity direction is compared between an ideal numerical case, the numerical case with added phase error, and experimental results using both the PAGE method and the traditional method at 1500 Hz over all rotation angles. Markers are at each angle of rotation in the actual experiment.

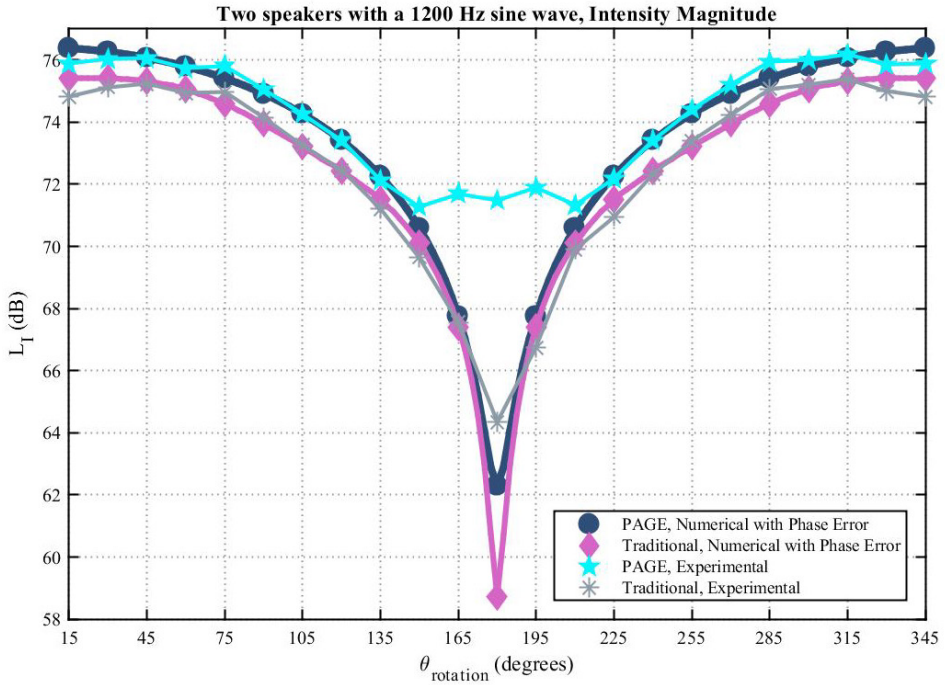

Figure 3.39: For two speakers teed off the same 1200 Hz sine wave signal, the active intensity magnitude is compared between an ideal numerical case, the numerical case with added phase error, and experimental results using both the PAGE method and the traditional method at 1200 Hz over all rotation angles. Markers are at each angle of rotation in the actual experiment.

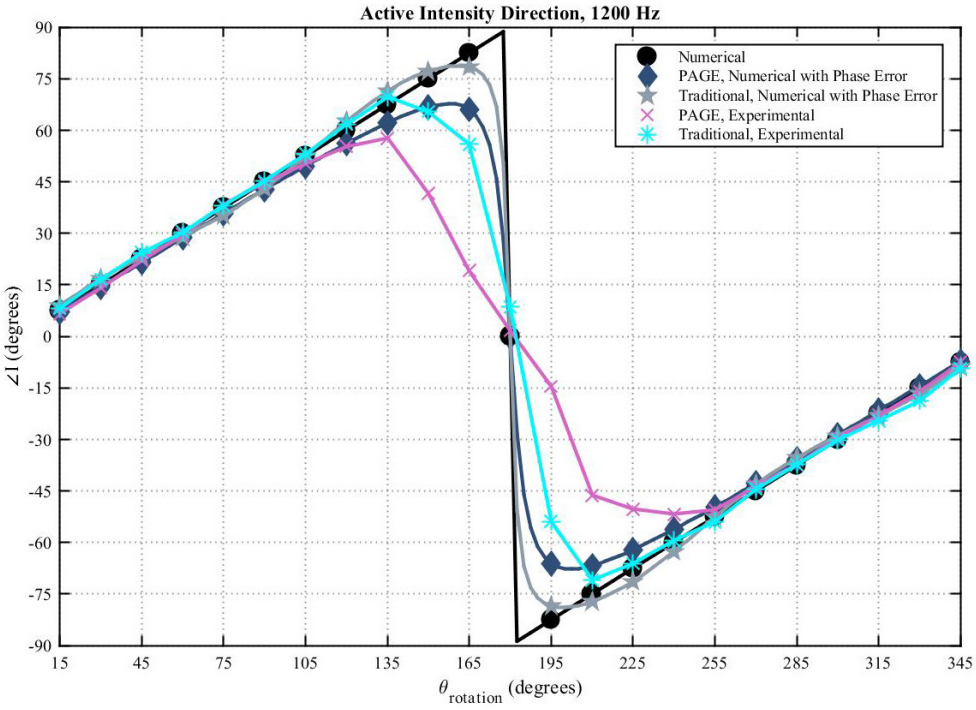

Figure 3.40: For two speakers teed off the same 1200 Hz sine wave signal, the active intensity direction is compared between an ideal numerical case, the numerical case with added phase error, and experimental results using both the PAGE method and the traditional method at 1200 Hz over all rotation angles. Markers are at each angle of rotation in the actual experiment.

One possible reason for these increased errors would be the presence of standing wave effects at these angles, resulting in a mixed sound field as opposed to a propagating field. These effects are present to some extent at these angles, as can be seen by the numerical reactive intensity magnitude at these angles in Figure 3.41 for a sine wave signal at 1500 Hz. The relative level of the active and reactive intensity components stays approximately consistent with frequency though, so the errors at these angles do not occur simply due to the relative level of the components. However, at higher frequencies, there will be a greater spatial variation in the standing wave field due to the smaller wavelengths, so a null near or between the microphones of the probe is more likely to occur. Evidence of the effect of the spatially varying sound field at these angles of rotation can be observed by comparison of pressure waveforms at different frequencies. When comparing a 700 Hz sine wave signal and a 1500 Hz sine wave signal at a

150° angle of rotation, as seen in Figure 3.42 and Figure 3.43, respectively, it can be observed that there are significant differences in pressure amplitude and time alignment between the signals of each microphone. The most distinctive differences are observed for microphone 2. The magnitude of microphone 2 is shown to be significantly smaller than for the 1500 Hz case (Figure 3.43) than for the 700 Hz case (Figure 3.42). The 1500 Hz case also has a time shift in microphone 2 from the other microphones that is more significant than in the 700 Hz case. These differences could potentially be attributed to a mixed propagating and standing wave field which varies more spatially at higher frequencies due to decreased wavelength, resulting in a greater variation between microphones. It is also possible that other effects in the sound field contribute to the errors at these frequencies and angles of rotation.

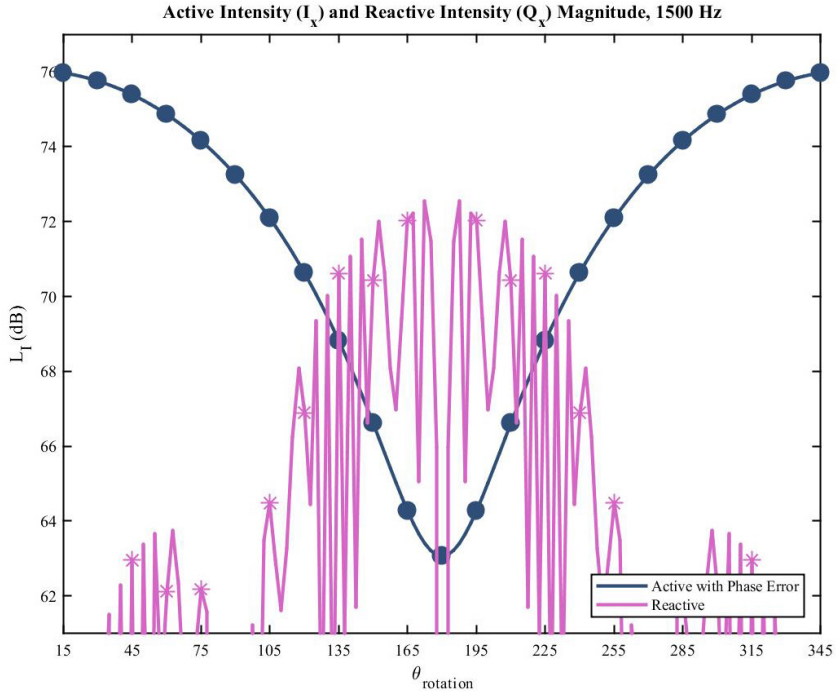

Figure 3.41: For two speakers teed off the same 1500 Hz sine wave signal, the intensity magnitude is compared between an active intensity numerical case with added phase error and analytical reactive intensity results at 1500 Hz over all rotation angles. Markers are at each angle of rotation in the actual experiment.

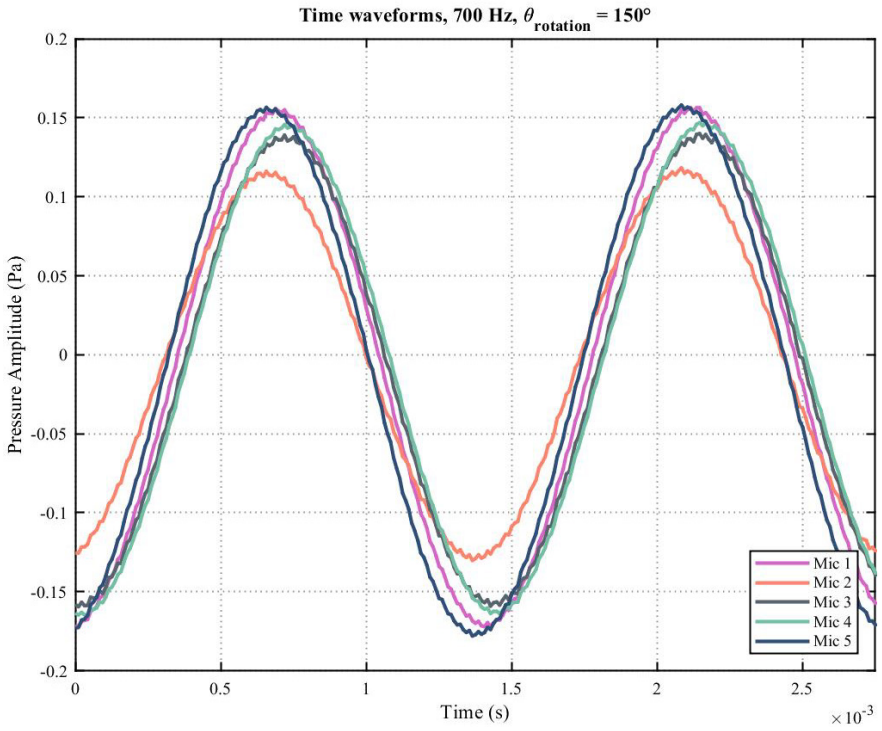

Figure 3.42: For two speakers teed off the same 700 Hz sine wave signal, the pressure waveform in time is compared for each microphone.

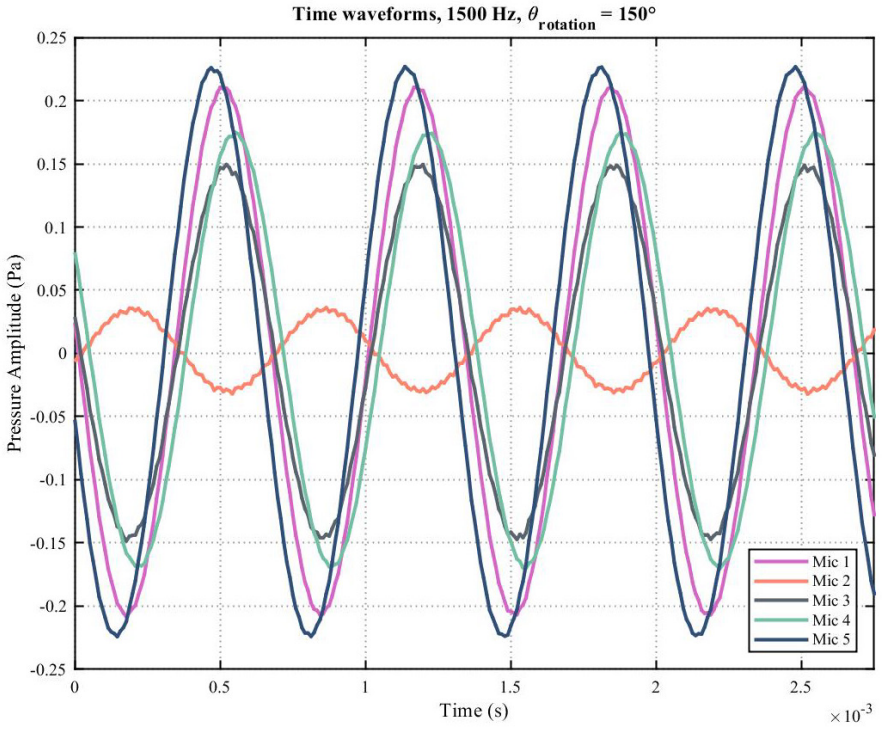

Figure 3.43: For two speakers teed off the same 1500 Hz sine wave signal, the pressure waveform in time is compared for each microphone.

3.6 Bandlimited white noise

3.6.1 Experiment

Similar to Section 2.4, the purpose of these experiments was to discover if unwrapping could occur with bands of noise that are entirely above the spatial Nyquist frequency. As with the plane wave experiments, the bandlimited white noise was obtained by applying low-pass and high-pass filters to broadband noise. The cutoffs of the filters are the frequencies used to specify the bands, which are denoted by Δf, and the filters being used are third-order Butterworth filters, meaning they have an 18 dB/octave roll off. It was expected that with sufficient bandwidth, even bands of noise at very high frequencies could be accurately unwrapped. It was also expected that larger bands would be required for proper unwrapping at higher frequencies. The experimental setup had the probe on the turntable and just one speaker on a stand about 2 meters away and at approximately the same height, as seen in Figure 3.2.

3.6.2 Results and analysis

As with most experiments involving broadband noise, the amount of averaging in the processing makes a significant difference on the random error. The time data used for this experiment was 15 seconds long, collected at a 96 kHz sampling frequency. The averaging was done with a 50% overlap of blocks and a block size of 9600, resulting in about 300 averages. This helped overcome some problematic extraneous noise in the setup, such as the electrical noise of the turntable.

As was found in the one-dimensional case in Section 2.4, the higher the frequency band was above the spatial Nyquist frequency ($f_N \approx 1688$ Hz), the higher Δf had to be for unwrapping to occur properly. A graph of the increasing amount of bandwidth needed for unwrapping to work properly as the center frequency of the band increased can be seen in Figure 3.44. Only

bands of noise completely above the spatial Nyquist frequency were tested, but some of the coherent bandwidth could potentially extend below the spatial Nyquist frequency. Each case was only considered to "work" if phase unwrapping worked for all rotation angles. For the highest frequency band tested, a center frequency, or f_c,of 18 kHz required a Δf of 12 kHz for unwrapping to occur properly. The smallest band had a f_c of 1800 Hz and only required a Δf of 100 Hz.

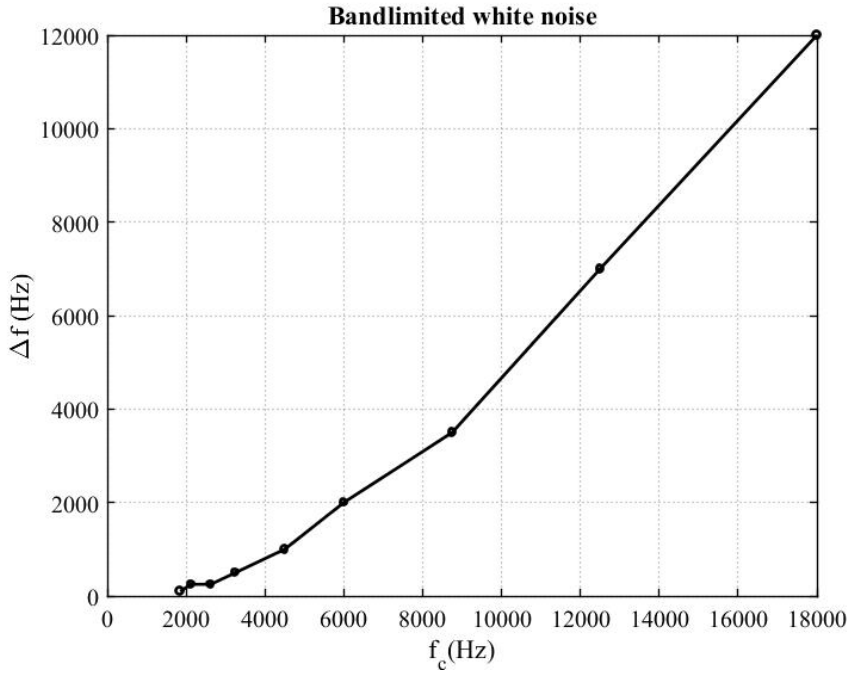

Figure 3.44: For bandlimited white noise, the center frequency of each band (f_c) is compared to the amount of bandwidth needed for unwrapping to work properly (Δf).

Regardless of the other parameters, all cases worked if the coherence for both microphone pairs was above 0.1 from the entire band from 1500-1800 Hz ($f_N \approx 1688$ Hz). Some cases still worked with a lower coherence than 0.1 for that bandwidth, but less consistently. This suggests that only rarely can bands of noise which have an entire coherent bandwidth far above the spatial Nyquist frequency use phase unwrapping accurately. However, a coherence of 0.1 is still relatively low, and other methods such as coherence-based unwrapping[55] could be used to improve the results.

One example of a working case is with a f_c = 6000 Hz and a Δf = 2000 Hz. The comparison between the benchmark and the PAGE and traditional methods for intensity magnitude are shown in Figure 3.45, with the accompanying phase and coherence results in Figure 3.46. These results are for a 0° angle of rotation. Notice the slight increase in coherence around 1500 Hz in Figure 3.46, resulting in a coherence above 0.1 above 1500 Hz. The improvement over the traditional method is in Figure 3.47 for direction across all angles of rotation. The noisy intensity level and phase below the spatial Nyquist frequency can be attributed to the very low coherence there. The results for all other cases were very similar, with the improvement over the traditional method growing even more impressive with increasing center frequency.

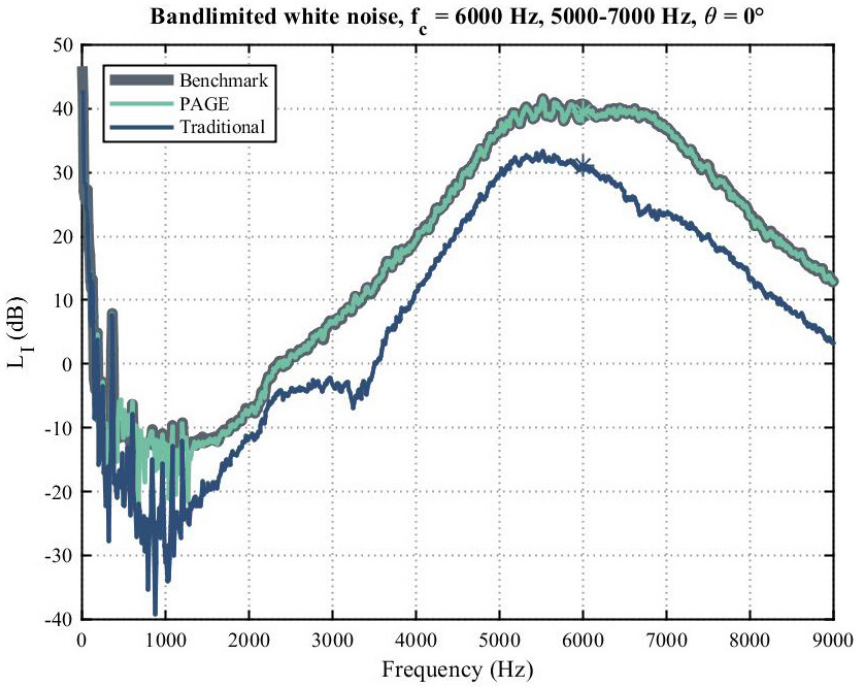

Figure 3.45: For filtered white noise from 5000-7000 Hz in an anechoic chamber, a benchmark of $\boldsymbol{I} = \frac{p_{rms}^2}{\rho_0 c}$ *is compared to active intensity calculated using the PAGE method and the traditional method for a probe at a 0° angle of rotation. A marker on each curve is at* f_c.

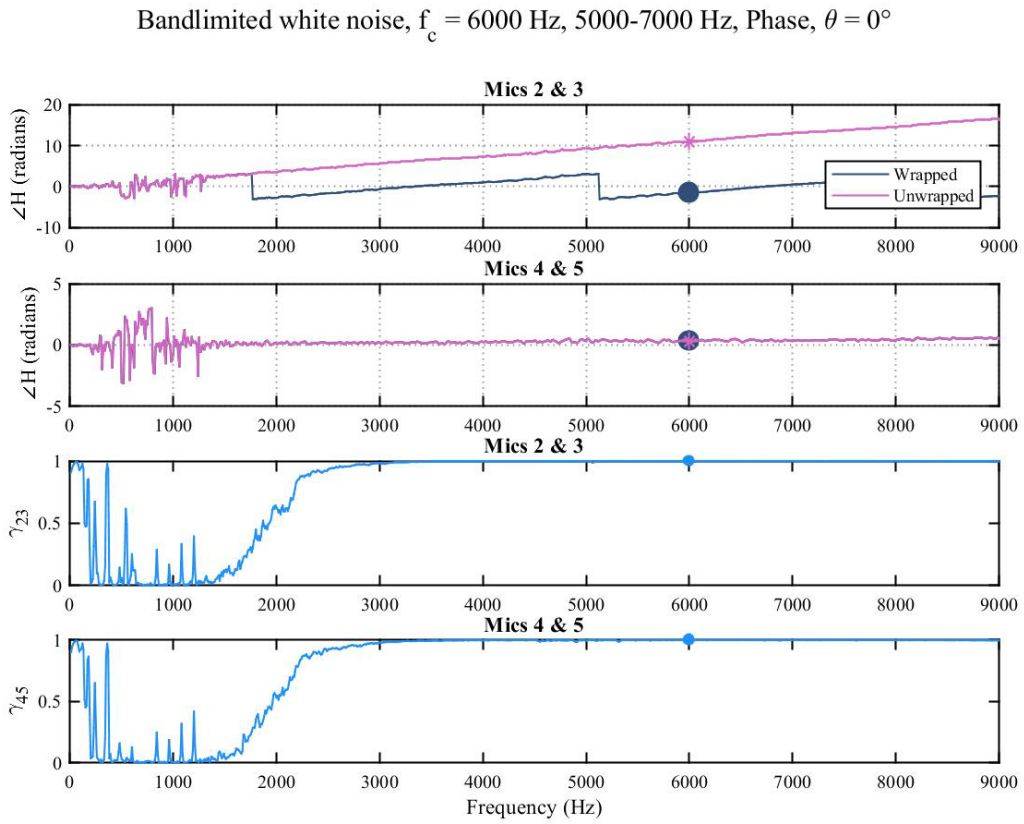

Figure 3.46: For filtered white noise from 5000-7000 Hz in an anechoic chamber, the wrapped and unwrapped phase of the transfer function as well as the coherence for each microphone pair are compared for a probe at a 0° angle of rotation. A marker on each curve is at f_c.

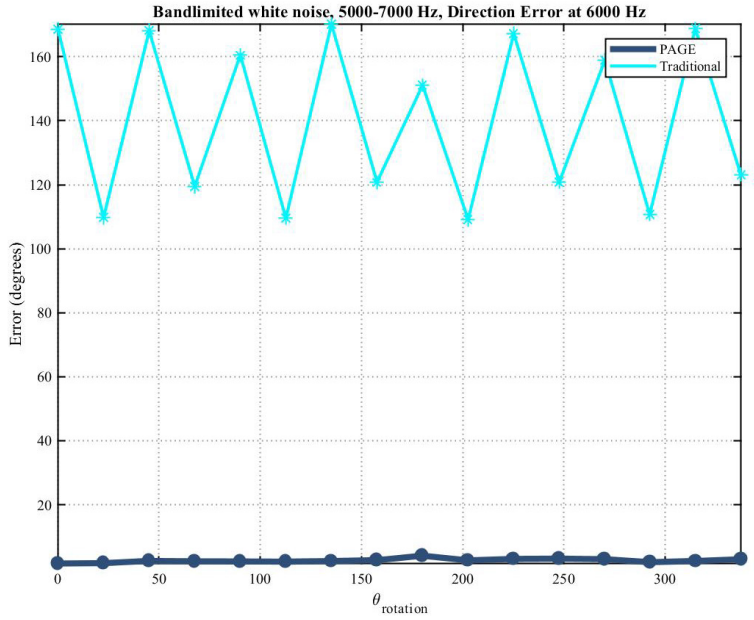

Figure 3.47: For filtered white noise from 5000-7000 Hz in an anechoic chamber, the intensity direction error for the PAGE method is compared to the intensity direction error for the traditional method at f_c = 6000 Hz over all rotation angles.

3.7 Conclusions

In an anechoic chamber, experiments using the same three signals which were tested in the plane wave tube were conducted and a few more tests were added that could not be done in a plane wave tube. For all cases, a probe with a spatial Nyquist frequency of about 1688 Hz for normal incidence was used.

In the first experiment, it was confirmed that the intensity magnitude and direction of sine waves were calculated correctly using the PAGE method up to the spatial Nyquist frequency. As part of this testing, it was found that an effective spatial Nyquist frequency could be obtained from the effective microphone spacing at a rotation angle. This effective spatial Nyquist frequency is higher than the spatial Nyquist frequency based only on the maximum spacing of the microphones, or the microphone spacing for a 0° angle of rotation. It was found that the actual effective spatial Nyquist frequency was at least 2100 Hz but less than 2250 Hz, despite a theoretical value of 2387 Hz. Possible reasons for this error are discussed, including possible alignment errors in the experimental setup. All successful PAGE calculations were improvements over the traditional method.

The sawtooth wave results were as expected. First, they confirmed the effective spatial Nyquist frequency findings from the sawtooth experiments. Then, the same extrapolated PAGE method from Section 2.3 was used to accurately predict the magnitude and phase of the sawtooth wave up to 20 kHz. This is the entire range of human hearing and represents a bandwidth extension of over 10 times. This represents a significant improvement over both the normal PAGE method and the traditional method.

The extrapolated PAGE method was then applied to sound from two speakers, each playing different sine waves: one was playing a tone above the spatial Nyquist frequency and

one was playing a tone below the spatial Nyquist frequency. When the two speakers were broadcasting in the same direction, this method worked very well. However, due to how the method is implemented, the intensity direction always stayed the same as the tone below the spatial Nyquist frequency, meaning the error in degrees was essentially equal to the angle of separation between the speakers. The intensity magnitude was always correct using the extrapolated PAGE method. For intensity magnitude, the extrapolated PAGE method represents an improvement over the normal PAGE method and the traditional method. However, for intensity direction the extrapolated PAGE only does as well as the normal PAGE method and the traditional method for very small angles of separation between the speakers.

The case of two speakers broadcasting the same input signal from approximately the same distance was explored. At lower frequencies and small angles of separation, the experimental results matched the numerical results fairly well. However, for increasing angles of separation a phase error was introduced across microphones 2 and 3 to the numerical results in order to continue matching the experimental data. This phase error could be due to one speaker being louder in amplitude than the other and/or having a shorter path length between the speaker and the probe than the other. At higher frequencies, additional deviations from expected results occurred at high angles of separation. This could be due to high levels of reactive intensity at these angles of separation, combined with the microphone spacing being larger relative to a wavelength for those frequencies.

In an anechoic chamber, it was explored if the magnitude and direction of bandlimited white noise completely above the spatial Nyquist frequency could be calculated accurately using the phase unwrapping in the PAGE method. Similar to the results in the plane wave tube, it was found that phase unwrapping can work properly for a bandwidth of noise at least mainly above

the spatial Nyquist frequency, but it requires a greater bandwidth at higher frequencies. However, for phase unwrapping to work consistently, a coherence of at least 0.1 in the frequency range from 1500-1800 Hz ($f_N \approx 1688$ Hz) was required. The results obtained represent a significant improvement over the traditional method.

Chapter 4

Low-level broadband noise with tones

4.1 Introduction

In Section 2.2, it was discovered that some broadband noise from the experimental equipment had entered into the plane wave tube and was propagating down the tube, causing the magnitude and direction of intensity of a sine wave to be calculated correctly by the PAGE method above the spatial Nyquist frequency. This result led to the design of these experiments, with the purpose of finding if adding a low level of broadband noise would consistently provide enough phase information for correct intensity magnitude and direction for a narrowband source above the spatial Nyquist frequency.

In pursuit of further understanding, theoretical expressions were developed by Mylan Cook, another BYU graduate student working in this area. The most pertinent to these experiments are the expressions for the argument of the transfer function when there is one narrowband plane wave and one broadband plane wave measured with the 5-microphone planar probe being used for these experiments (see Figure 3.1). The expressions are:

$$\arg\{H_{23}\} = \arg\left\{e^{-2jk_p d\cos\theta_s} + N_p^2 e^{-2jkd\cos\theta_n}\right\} \qquad (8)$$

and

$$\arg\{H_{45}\} = \arg\left\{e^{-2jk_p d\sin\theta_s} + N_p^2 e^{-2jkd\sin\theta_n}\right\}, \qquad (9)$$

where d is the spacing between the center microphone and the outer microphones, H_{23} is the transfer function between microphones 2 and 3 (see Figure 3.1), H_{45} is the transfer function

between microphones 4 and 5, k is the acoustic wavenumber, k_p is the acoustic wavenumber at the frequencies of the narrowband source (e.g., corresponding to the peaks of a sawtooth wave) and is zero at any other frequency, θ_s is the rotation angle of the source with the sine or sawtooth wave relative to the 0° rotation angle of the probe (see Figure 3.2), θ_n is the rotation angle of the source with the noise relative to the 0° rotation angle of the probe, and N_p is the plane wave amplitude of the broadband noise. Some interesting things about these expressions are that for the wavenumbers that correspond to the frequencies of the sine or sawtooth wave, the first term dominates and the phase suddenly jumps to the phase for just the sine or sawtooth at that frequency. For all other frequencies, the noise term dominates.

4.2 Additive broadband noise experiments

4.2.1 Experiment

The purpose of these experiments was to verify the theoretical results and ultimately discover if the addition of low-level broadband noise to a narrowband signal would lead to accurate intensity magnitude and direction calculations above the spatial Nyquist frequency using the PAGE method.

This experimental setup was the same as the two-speaker setup in Figure 3.23, with one speaker on a stand and another on the arm that is attached to the turntable. In all cases, the broadband noise was played through the speaker on the stand, and the speaker on the arm was playing the sine or sawtooth wave depending on the experiment. This means that the θ_s from Eq. (8) and Eq. (9) is always 0°. The probe used was the same one that was used in Chapter 3, which is shown in Figure 3.1. Experiments were performed with the second speaker at angles (θ_n) ranging from -90° to 90°.

It was expected that for many cases, both intensity magnitude and intensity direction of the sine and sawtooth waves would be accurately calculated using the PAGE method. The PAGE method would be expected to work above a certain threshold of broadband noise level where the noise is sufficiently high to provide coherent information at enough frequencies for unwrapping to occur properly. If the noise level is too low, the noise will not be coherent enough to provide accurate points for phase unwrapping. The PAGE method would also be expected to work if the noise has unwrapped the correct number of times to be close enough to jump to the correct answer for the sine or sawtooth wave at the corresponding frequency, since the jumps will not span more than 2π. For example, for the pair of microphones 4 and 5, the narrowband signal always has a phase difference of 0 across those microphones because the speaker playing the narrowband signal is on the arm that rotates with the probe. Therefore, only for ranges of angles and frequencies at which the broadband noise is not yet unwrapped across microphones 4 and 5 will the phase be able to jump back to the accurate phase for the sine/sawtooth wave of 0 for that pair.

For all cases in this section, an intensity direction of 0° is considered correct because it is the direction the sine or sawtooth wave is propagating and our goal is to get that correct.

4.2.2 Sine waves

With only a low level of added noise, the correct intensity magnitude was obtained for a 4000 Hz sine wave using the PAGE method up to a separation angle of 30°. This result can be seen in Figure 4.1. For this case, the improvement over the traditional method is noticeable in Figure 4.2. This range is actually slightly better than the range for which intensity direction is correctly calculated using the PAGE method, as seen in Figure 4.3.

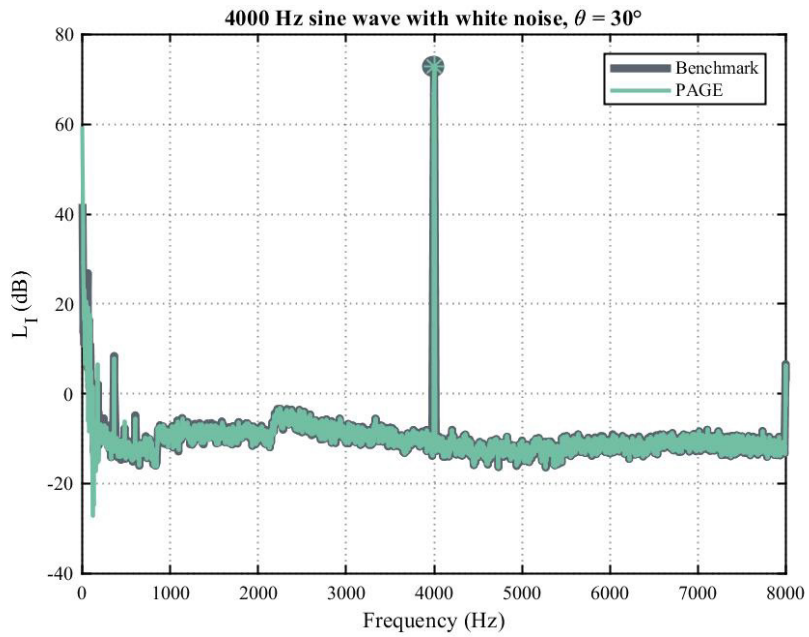

Figure 4.1: For a speaker broadcasting a 4000 Hz sine wave (θ_s = 0°) and another speaker broadcasting white noise (θ_n = 30°), a benchmark of $\boldsymbol{I} = \frac{p_{rms}^2}{\rho_0 c}$ is compared to active intensity calculated using the PAGE method. Markers on each curve are at the frequency of the sine wave.

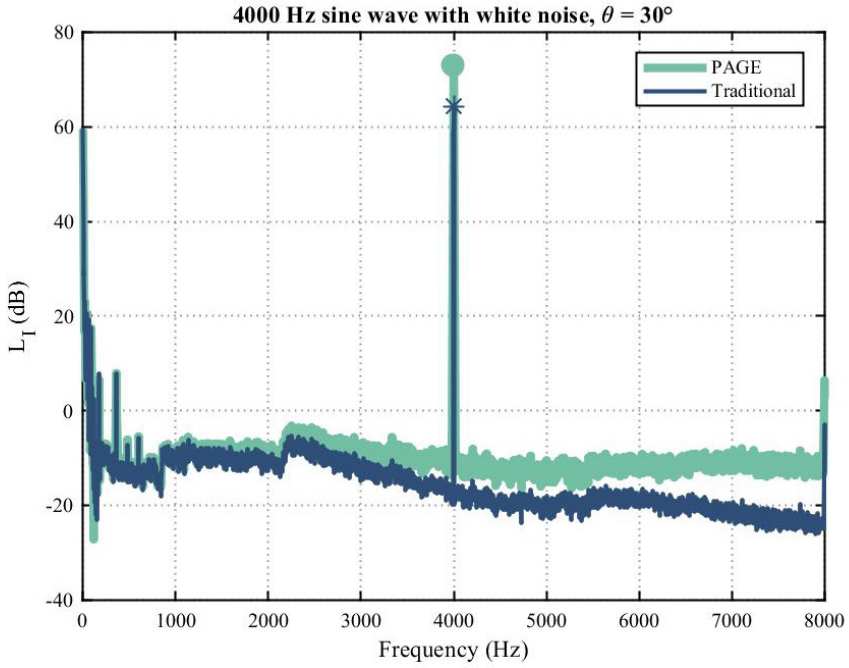

Figure 4.2: For a speaker broadcasting a 4000 Hz sine wave (θ_s = 0°) and another speaker broadcasting white noise (θ_n = 30°), the active intensity calculated using the PAGE method is compared to the active intensity calculated using the traditional method. Markers on each curve are at the frequency of the sine wave.

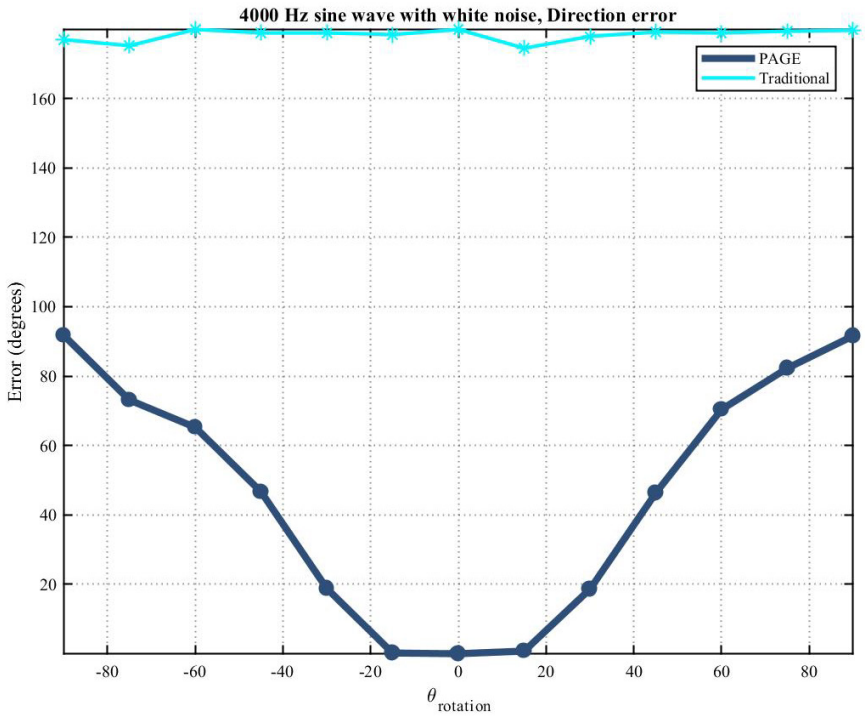

Figure 4.3: For a speaker broadcasting a 4000 Hz sine wave (θ_s = 0°) and another speaker broadcasting white noise ($\theta_n = \theta_{rotation}$), the intensity direction error for the PAGE method is shown across all rotation angles. Markers are at each tested angle of rotation.

4.2.3 Sawtooth waves

The main sawtooth waves tested were a 250 Hz sawtooth for resolution purposes and a 1000 Hz sawtooth. The broadband source for these experiments was brown noise because it would roll off at nominally the same rate as the sawtooth waves, giving each harmonic of the sawtooth an approximately equal SNR. There are two main noise cases discussed in this section, which we will refer to as noise case 1 and noise case 2, which are shown in Table 4.1 with the approximate SNR they correspond to.

Table 4.1: Approximate signal-to-noise ratio (SNR) for each brown noise case at each peak

Case	250 Hz sawtooth SNR (dB)	1000 Hz sawtooth SNR (dB)
Noise case 1	34	46
Noise case 2	50	63

The effect of the additive noise on the intensity magnitude of the peaks of the sawtooth wave was minimal. This was tested by observing the change in the magnitude of the tones for varying additive noise levels. Even for a change in additive noise level of over 50 dB, the magnitude of the tones varied over a range of less than 0.5 dB. Some of this variation also could have occurred due to inconsistency of the speaker over time. These results are very encouraging for the efficacy of the method, as it suggests that a sufficient amount of noise to help in phase unwrapping can be added without significantly affecting the intensity magnitude measurement.

The main reason for intensity error in these experiments were errors in unwrapping of the transfer function phase. As was mentioned in the expected results section in Section 4.2.1, one instance of this error is when phase unwrapping occurs for the phase between microphones 4 and 5 due to the broadband noise. This will cause an error in the intensity calculation using the PAGE method because the sawtooth will always have a zero phase for those microphone pairs, and when phase unwrapping occurs due to the broadband noise, the phase will no longer jump to the correct value of 0 for the sawtooth wave (see Figure 4.4). In Figure 4.4, the jumps back to 0 for microphones 4 and 5 can be observed at the frequencies of the 1000 Hz sawtooth up to 4000 Hz, which has brown noise levels corresponding to noise case 2 (see Table 4.1). For frequencies above but still close to the spatial Nyquist frequency, a much wider range of rotation angles still lead to a correct intensity magnitude because the unwrapping will not occur until the effective spatial Nyquist frequency for microphones 4 and 5. So for each angle, any frequency above the spatial Nyquist frequency for the probe at 0° but below the effective spatial Nyquist frequency for microphones 4 and 5 described in Eq. (6) should have a correct phase and therefore a correct intensity magnitude and direction. This also means that the lower the angle of separation between the speakers, the higher in frequency intensity can be calculated accurately. Another

possible reason for unwrapping error is that the noise is so low that unwrapping of the noise is not occurring properly, as can be seen around approximately 9000 Hz in Figure 4.5. Figure 4.5 is a 250 Hz sawtooth with brown noise levels corresponding to noise case 1 (see Table 4.1). For the brown noise case, this leads to more accurate calculations at lower frequencies better because the noise gets lower with increasing frequency.

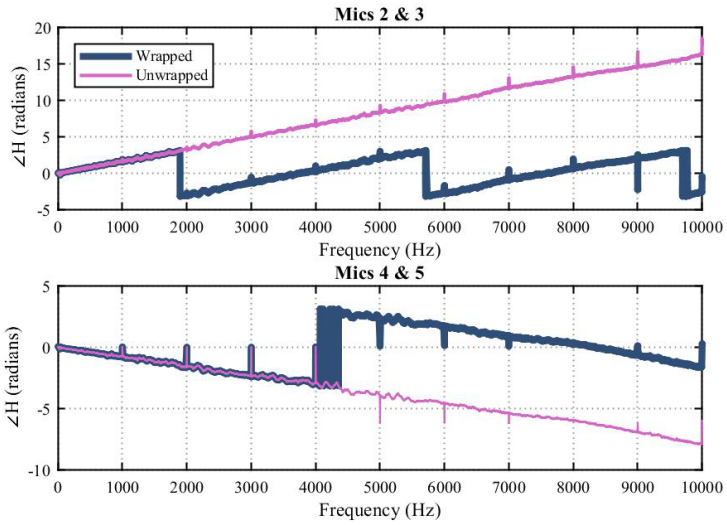

Figure 4.4: For a speaker broadcasting a 1000 Hz sawtooth wave (θ_s = 0°) and another speaker broadcasting brown noise (noise case 1, θ_n = 25°), the wrapped and unwrapped phase of the transfer function are compared.

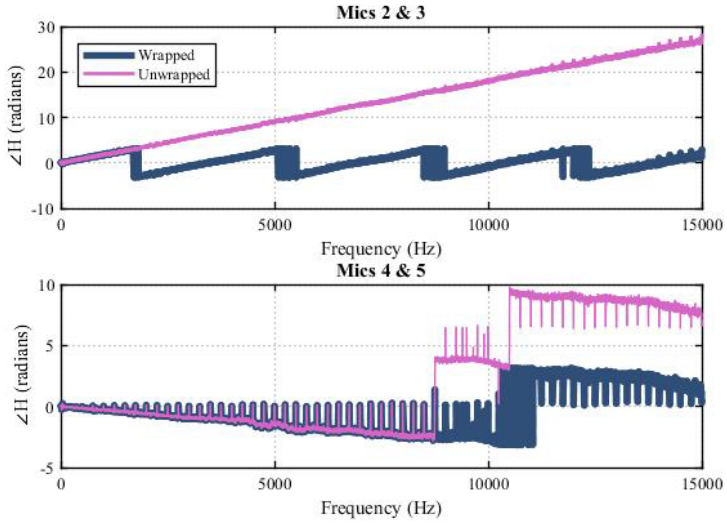

Figure 4.5: For a speaker broadcasting a 250 Hz sawtooth wave (θ_s = 0°) and another speaker broadcasting brown noise (noise case 2, θ_n = 10°), the wrapped and unwrapped phase of the transfer function are compared.

For a 1000 Hz sawtooth at $\theta_s = 0°$ and brown noise at $\theta_n = 25°$ and noise case 1 (see Table 4.1), interesting effects can be seen in the active intensity magnitude, seen in Figure 4.6. Despite the still relatively high SNR of noise case 1, the additive noise helps the intensity magnitude of the sawtooth to be correctly calculated up to 6 kHz, and is still within 0.5 dB up to at least 10 kHz. The comparison with the traditional result begins to illuminate just how valuable this method can be, as seen in Figure 4.7. The phase of the relevant transfer functions is shown in Figure 4.4. Note that the phase at the harmonics of the sawtooth jumps to a different value at those frequencies. This is the result of Eq. (8) and Eq. (9), showing that at the harmonics of the sawtooth wave, the phase of the sawtooth wave dominates. Interestingly, the magnitude seems to match the correct results even better than the phase would suggest since the phase only jumps to the correct value for both microphone pairs up to 4 kHz.

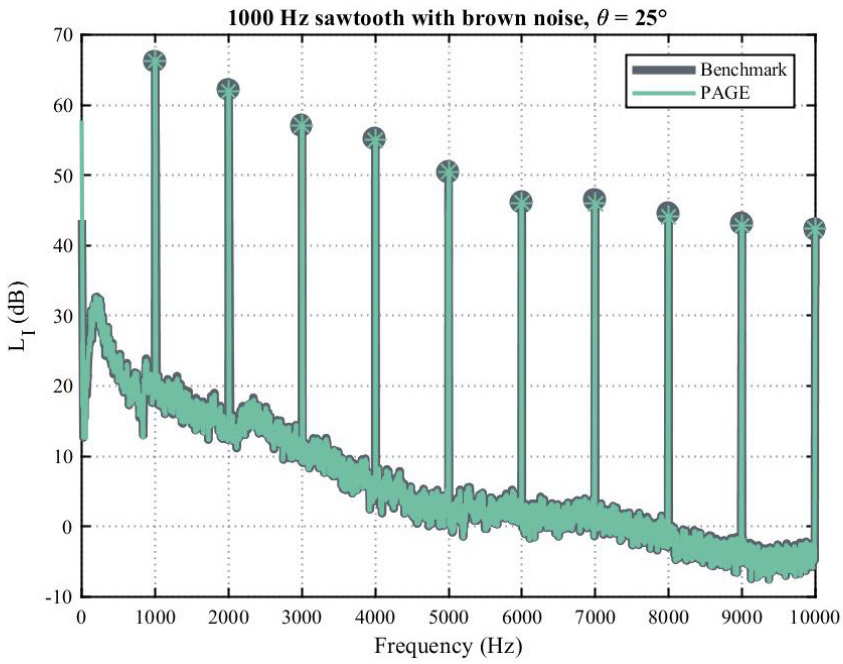

Figure 4.6: For a speaker broadcasting a 1000 Hz sawtooth wave ($\theta_s = 0°$) and another speaker broadcasting brown noise (noise case 1, $\theta_n = 25°$), a benchmark of $\boldsymbol{I} = \frac{p_{rms}^2}{\rho_0 c}$ is compared to active intensity calculated using the PAGE method. Markers on each curve are at the frequencies of the sawtooth wave.

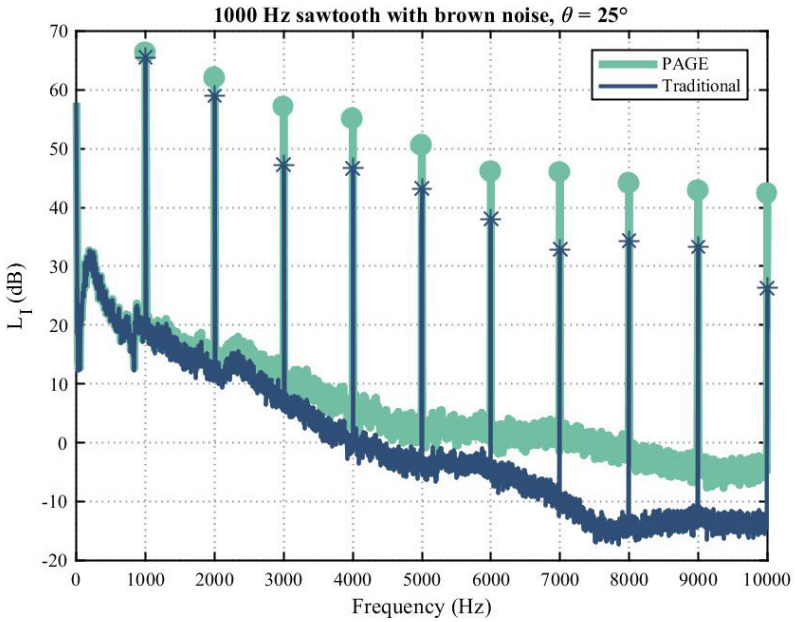

Figure 4.7: For a speaker broadcasting a 1000 Hz sawtooth wave (θ_s = 0°) and another speaker broadcasting brown noise (noise case 1, θ_n = 25°), the active intensity calculated using the PAGE method is compared to the active intensity calculated using the traditional method. Markers on each curve are at the frequencies of the sawtooth wave.

For many cases like that of the 4000 Hz sine wave in Figure 4.3, accurate intensity direction could only be obtained when the separation angle was 15° or smaller. To further explore this, the intensity direction was calculated for a 250 Hz sawtooth, rotated with 2.5° resolution. The analytical graph of this result is observed in Figure 4.8. When obtaining this analytical result, there was no difference between noise case 1 and noise case 2, but errors began to occur when the SNR decreased to less than 18 dB. The analytical result matches what would be expected from Eq. (8) and Eq. (9), because when the direction does not describe the direction of the sawtooth, it instead describes the direction of the noise. An experimental result for this case with noise case 2 (see Table 4.1) is observed in Figure 4.9. The experimental result in Figure 4.9 follows the same trends as the analytical result in Figure 4.8. Using the higher noise case of noise case 1 (see Table 4.1), Figure 4.10 was obtained. Notice that Figure 4.10 follows the trends of Figure 4.8 even more closely than Figure 4.9. The improvement over the traditional method can be seen in Figure 4.11.

As discussed earlier in this section, the frequencies for which intensity magnitude and direction calculated using the PAGE method will be accurate are described by the effective spatial Nyquist frequency equation for microphones 4 and 5 in Eq. (6). For the analytical case (see Figure 4.8), there is no intensity direction error for θ_{rotation} = 10° up to just under 10 kHz. The experimental result with noise case 2 (see Figure 4.9) has no intensity direction error for θ_{rotation} = 10° up to just under 9 kHz. The experimental result with noise case 1 (see Figure 4.10) has no intensity direction error for θ_{rotation} = 10° up to just above 11 kHz, which means this experiment is doing even better than the effective spatial Nyquist frequency calculation and therefore the analytical case.

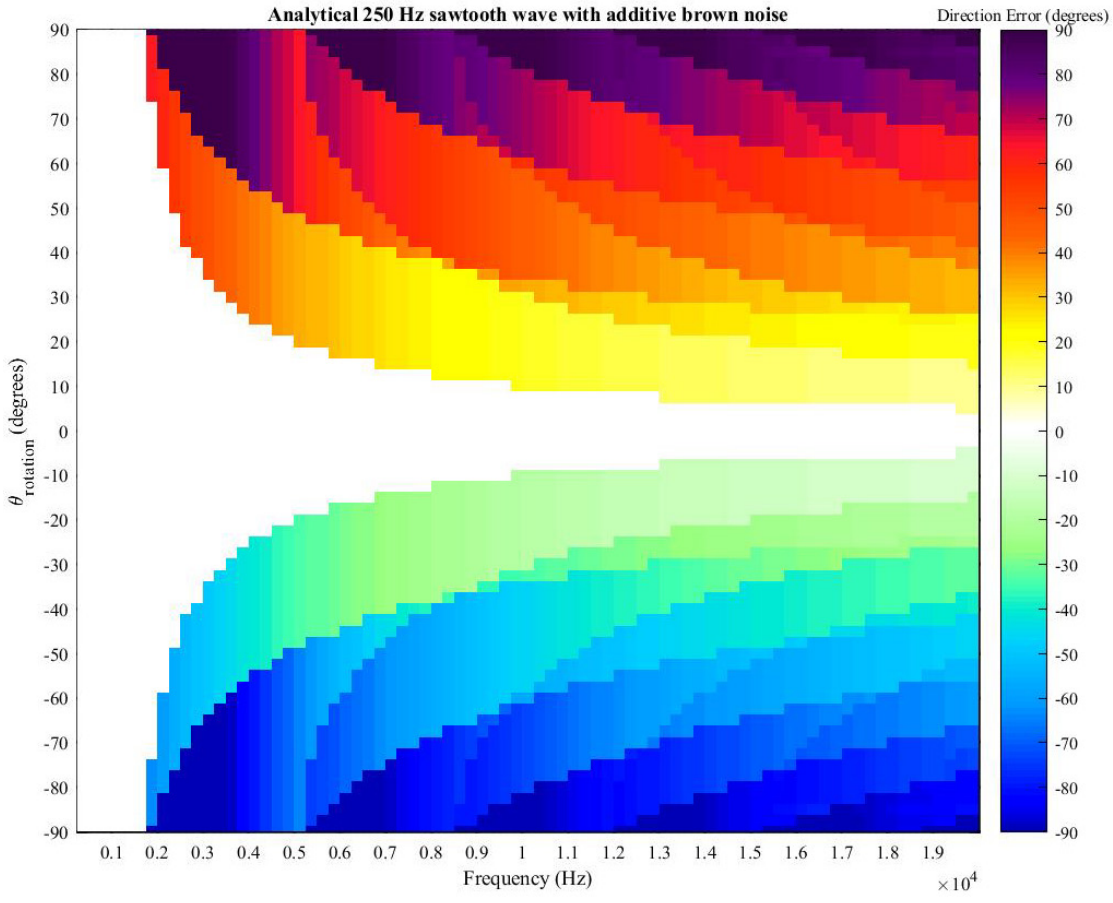

Figure 4.8: Analytical result for a speaker broadcasting a 250 Hz sawtooth wave (θ_s = 0°) and another speaker broadcasting brown noise ($\theta_n = \theta_{rotation}$), the intensity direction error for the PAGE method is shown across frequencies which correspond to the peaks of the sawtooth and rotation angle.

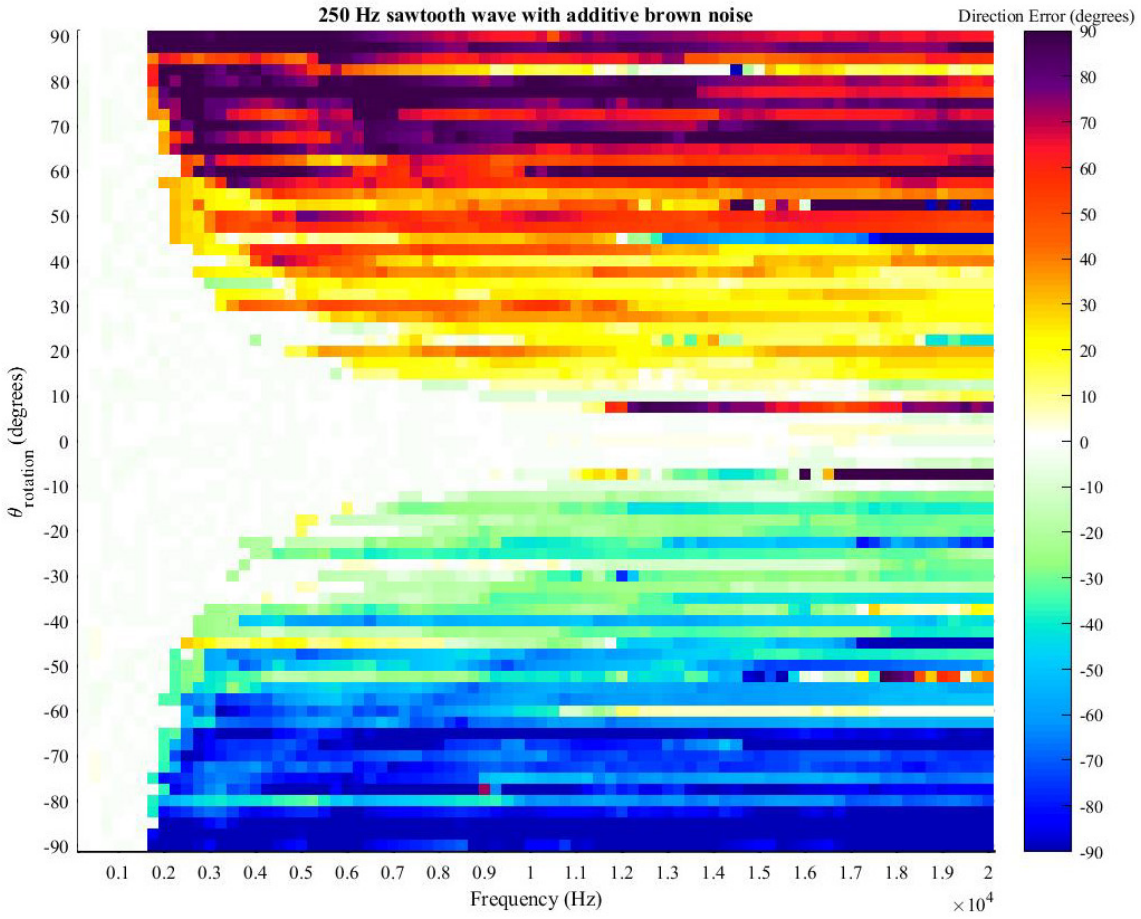

Figure 4.9: For a speaker broadcasting a 250 Hz sawtooth wave (θ_s = 0°) and another speaker broadcasting brown noise (noise case 2, $\theta_n = \theta_{rotation}$), the intensity direction error for the PAGE method is shown across frequencies which correspond to the peaks of the sawtooth and rotation angle.

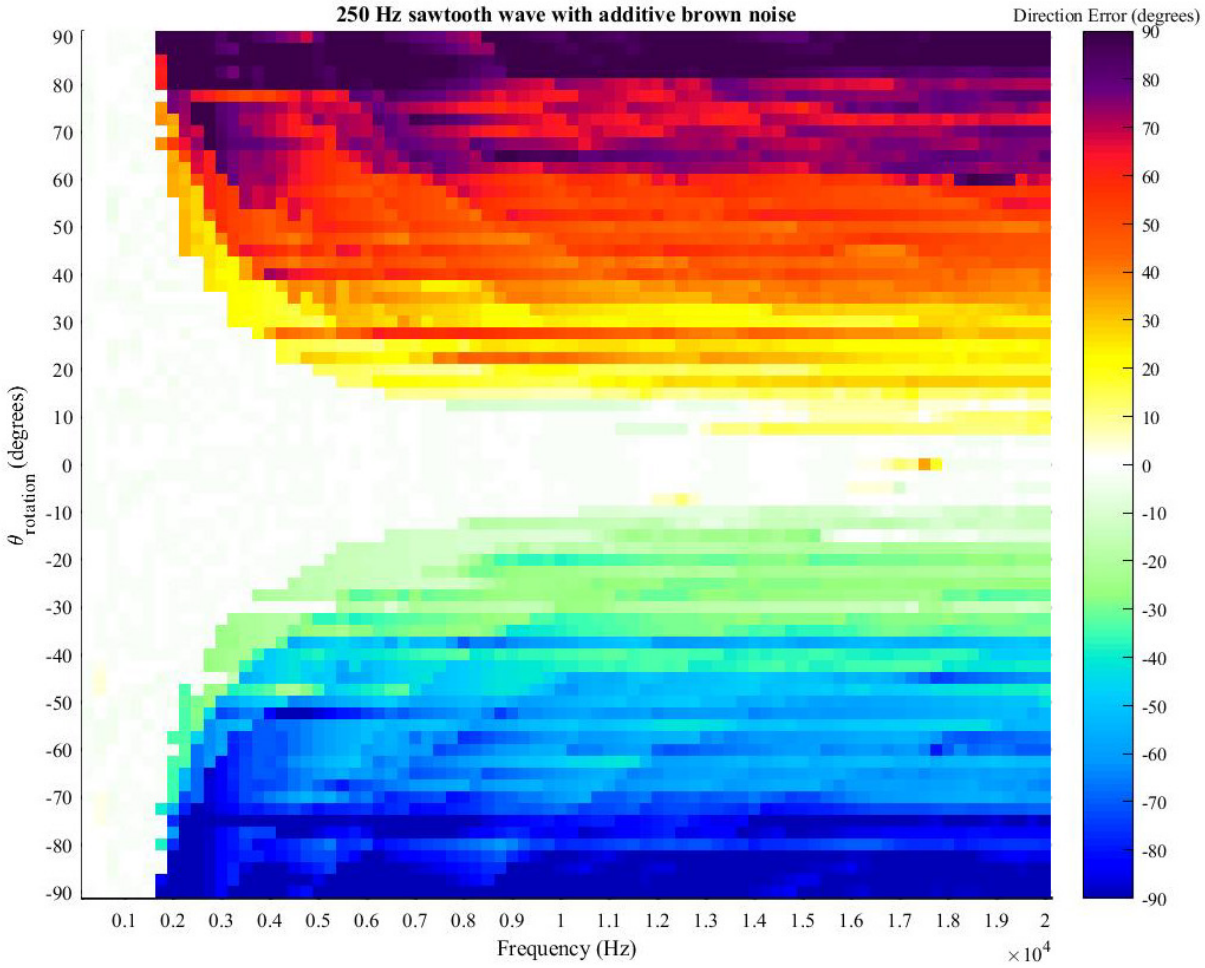

Figure 4.10: For a speaker broadcasting a 250 Hz sawtooth wave (θ_s = 0°) and another speaker broadcasting brown noise (noise case 1, $\theta_n = \theta_{rotation}$), the intensity direction error for the PAGE method is shown across frequencies which correspond to the peaks of the sawtooth and rotation angle.

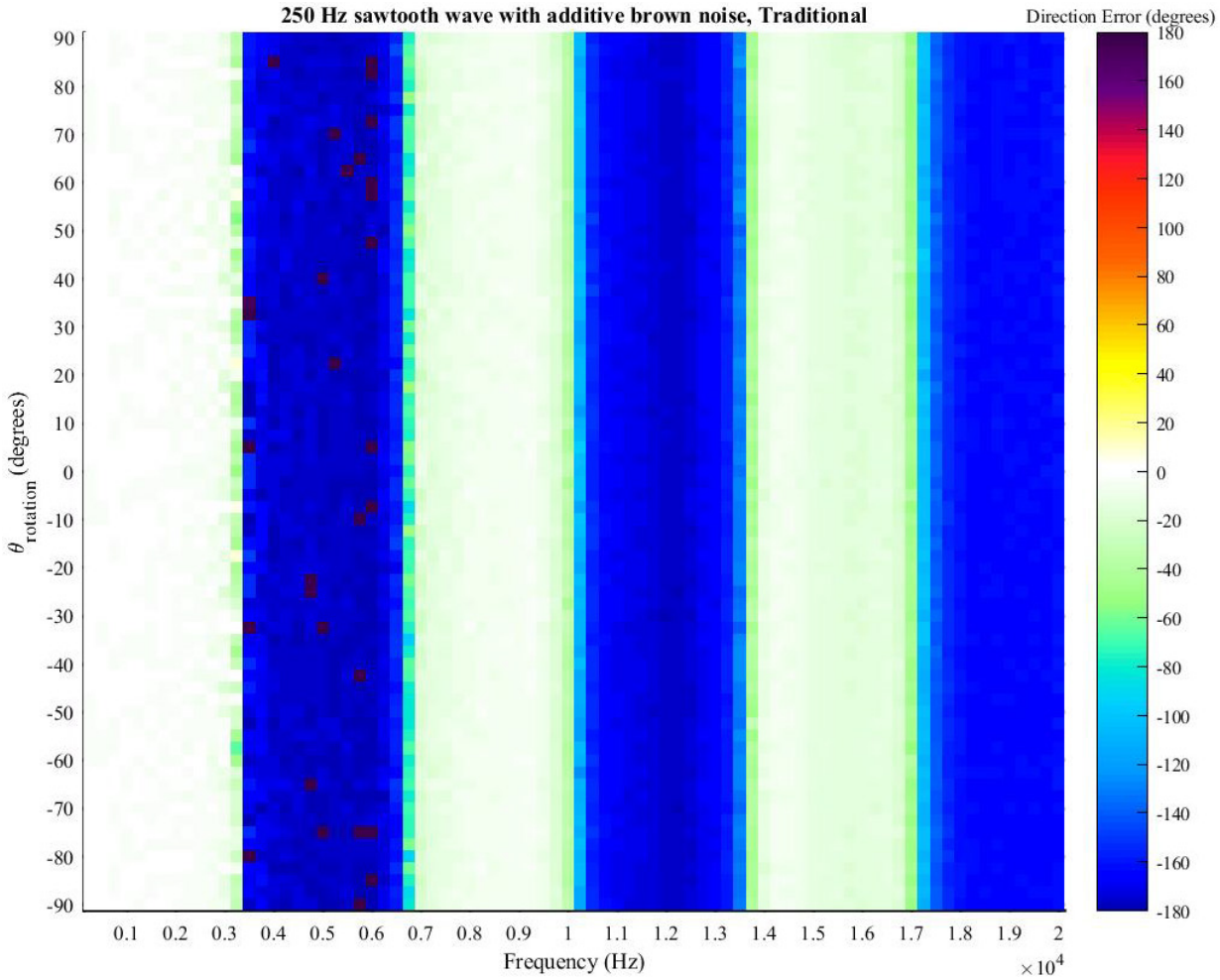

Figure 4.11: For a speaker broadcasting a 250 Hz sawtooth wave (θ_s = 0°) and another speaker broadcasting brown noise (noise case 1, $\theta_n = \theta_{rotation}$), the intensity direction error for the traditional method is shown across frequencies which correspond to the peaks of the sawtooth and rotation angle.

4.3 Fan noise application

4.3.1 Experiment

This experiment was meant to show that fan noise is a case for which broadband and narrowband noise are produced in a compact space and to test that the PAGE method could correctly calculate the intensity magnitude and direction for fan noise.

The expected spectrum from a fan involves some broadband noise and several tones that are related to the blade passage frequency. The blade passage frequency can be calculated by:

$$\text{BPF} = \frac{nb}{60}, \tag{9}$$

where BPF is the blade passage frequency, n is the rotation velocity in rpm, and b is the number of blades. The fan used for testing had a rotation velocity of about n = 7200 rpm and b = 7 blades. This results in a BPF of 840 Hz. Therefore, for this fan the spectrum is expected to have broadband noise at a relatively low level and a strong peak somewhere around 840 Hz and its harmonics. It would not be unusual for this BPF to vary slightly with time. A slender object, in this case a mechanical pencil, was placed on the inlet to create a greater obstruction and therefore enhance the tones in the spectrum.

Figure 4.12: The setup for the fan noise experiment in an anechoic chamber. The fan is on the turntable and the probe is on a stand approximately 2 meters away.

For this experiment, a small, axial fan was placed on the turntable and the probe was on a stand about 2 m away from the front of the fan. The experimental setup can be seen in Figure

4.12. The fan was a 6.9 cm by 6.9 cm, 7-blade high-speed axial fan powered by a 12 V DC power supply.

It is expected that the PAGE method will calculate both magnitude and direction very well for this scenario, because all of the generated sound is coming from a very compact source so the tones and broadband noise will be traveling together from the same source. This means that the phase data from the broadband noise should be able to unwrap properly to provide the correct phase for the narrowband peaks. Even though the turntable was rotated with the fan on it, the probe was always pointing directly at the fan. Therefore, the intensity direction would be expected to be around 0° for all test cases.

4.3.2 Results and analysis

The PAGE method was found to calculate intensity magnitude accurately. Some rotation angles provided peaks of higher amplitude than others due to the directivity of the fan. One case with pronounced peaks was when the fan had rotated 112.5°, and the results of the PAGE calculation of active intensity can be seen in Figure 4.13. The improvement over the traditional method is seen in Figure 4.14. The blade passage frequency in this case is at 842 Hz. There are more peaks in the spectrum than would necessarily be expected for a typical fan. It can be seen that these smaller peaks occur at a frequency of once/revolution and its harmonics, and thus are likely due to an imbalance in the fan motor. Regardless of why the spectrum is exactly how it is, the PAGE method was able to correctly calculate the intensity magnitude of the combined broadband and tonal sound radiated from the fan. This is due to the phase unwrapping across microphones 2 and 3 occurring accurately, and the phase difference across microphones 4 and 5 being about zero, as expected. These phase results are in Figure 4.15. All other cases worked

just as well, despite the changes in amplitude due to the directivity of the fan and a slight drift in BPF with time.

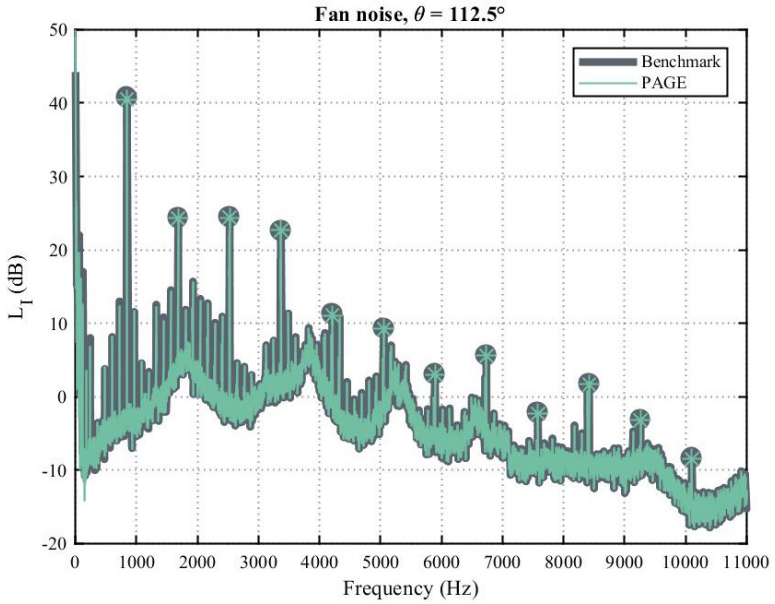

Figure 4.13: For a small axial fan in an anechoic chamber, a benchmark of $\boldsymbol{I} = \frac{p_{rms}^2}{\rho_0 c}$ *is compared to active intensity calculated using the PAGE method. Markers on each curve are at the BPF and its harmonics.*

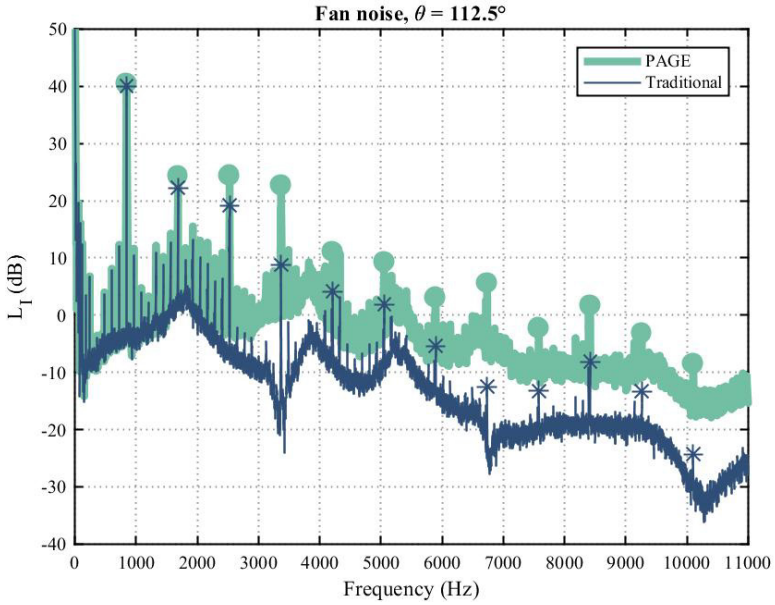

Figure 4.14: For a small axial fan in an anechoic chamber, the active intensity calculated using the PAGE method is compared to the active intensity calculated using the traditional method. Markers on each curve are at the BPF and its harmonics.

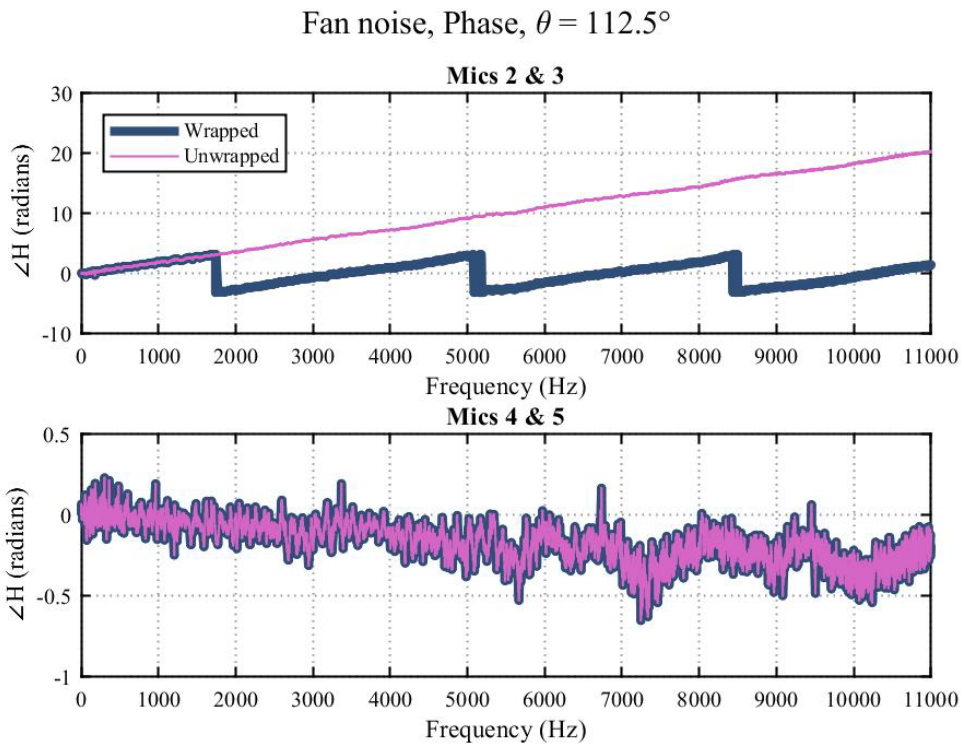

Figure 4.15: For a small axial fan in an anechoic chamber, the wrapped and unwrapped phase of the transfer function are compared for a probe at a 0° angle of rotation.

The PAGE intensity direction would be expected to be accurate for fan noise within a tolerance which accounts for errors in the experimental setup, but the traditional direction would only be expected to be accurate up to the spatial Nyquist frequency. As expected, the intensity direction obtained using the PAGE method was accurate within about 3°. This result can be seen in Figure 4.16. The direction error for the traditional method is seen in Figure 4.17, where it is seen that the traditional method has significant error over some of the frequencies above the spatial Nyquist frequency. The PAGE method provides intensity direction calculations that are more consistently accurate than the traditional method results.

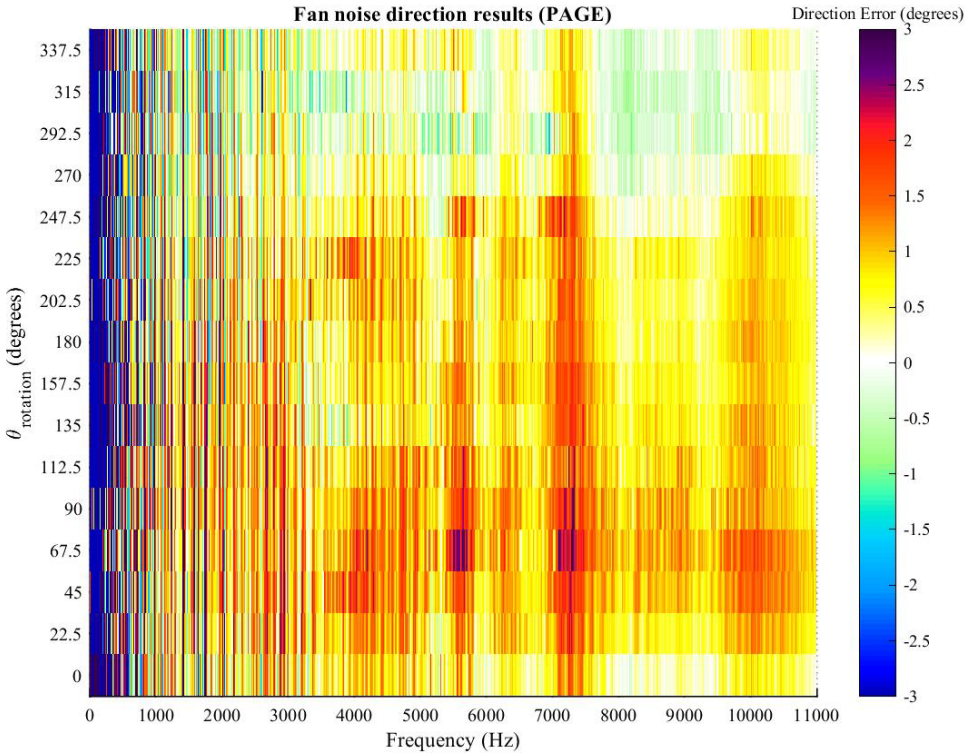

Figure 4.16: For a small axial fan in an anechoic chamber, the intensity direction for the PAGE method is shown over all rotation angles.

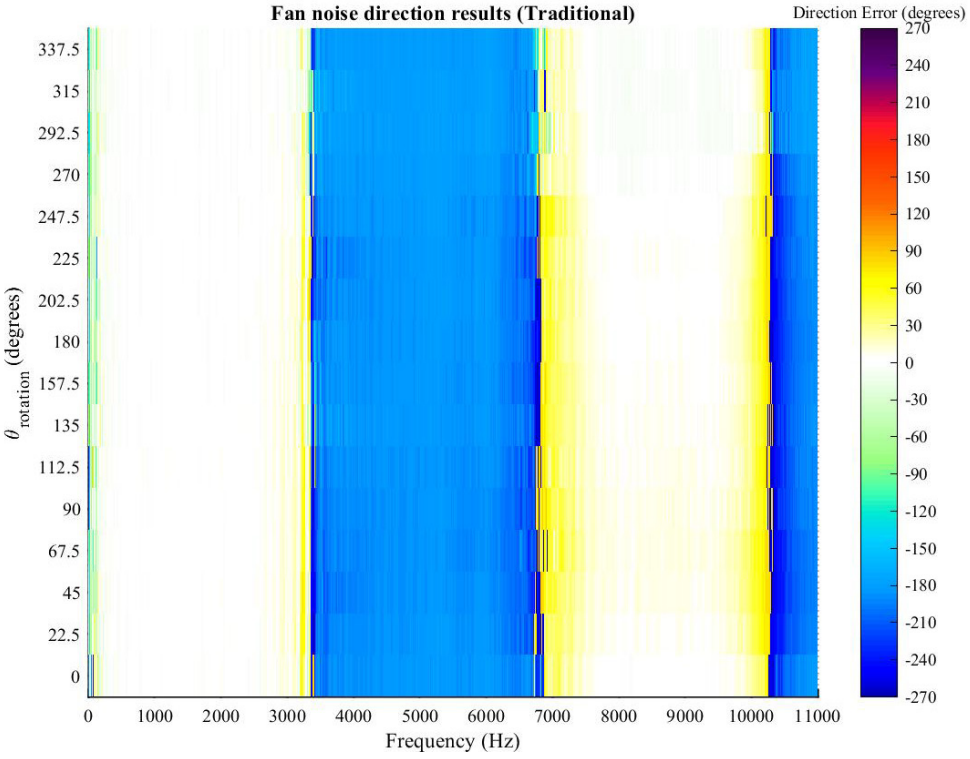

Figure 4.17: For a small axial fan in an anechoic chamber, the intensity direction for the traditional method is shown over all rotation angles.

4.4 Conclusions

For certain cases, the addition of broadband noise greatly aided the calculation of narrowband signals above the spatial Nyquist frequency. The method works best when the noise is high enough in amplitude for phase unwrapping to occur properly. More specifically, the noise must be above the ambient noise and will produce slightly better results with slightly more noise, as long as it does not approach an SNR of about 10 dB of the actual narrowband signal. Due to the experimental setup, the frequencies for which intensity magnitude and direction calculated using the PAGE method will be accurate are described by the effective spatial Nyquist frequency equation for microphones 4 and 5 in Eq. (6). This means that there is a tradeoff of frequency and rotation angle—if you want accurate intensity calculations at a high frequency, you need a low angle of rotation, or vice versa. The magnitude and direction obtained using the PAGE method are an improvement over the traditional method for cases where the PAGE method works, especially with increasing frequency.

An example of both broadband noise and tonal noise coming from a compact source is a small, axial fan. The PAGE method was able to accurately calculate the intensity magnitude and intensity of fan noise above the spatial Nyquist frequency.

Chapter 5

Conclusion

5.1 Conclusions

The PAGE method is an analysis method used to calculate energy quantities in an attempt to improve upon the p-p method that has been used traditionally. In this thesis, the limitations of the PAGE method for calculating acoustic intensity in various cases with narrowband sources was explored. Then, the PAGE results were compared to results obtained using the traditional method. Due to the narrowband nature of the sources, it was expected that typical methods of bandwidth extension above the spatial Nyquist frequency, such as phase unwrapping, would generally be ineffective. However, it was explored if there were other methods of bandwidth extension which would be effective for narrowband sources.

For all tested cases, the PAGE method was found to correctly calculate magnitude and direction of intensity of narrowband sources below the spatial Nyquist frequency. From sine wave testing, it was also found that the two-dimensional probe does have a higher effective spatial Nyquist frequency when the effective microphone spacing is smaller due to the angle of incidence on the probe. The highest frequency where accurate results were obtained was 2100 Hz at a 45° rotation angle for a planar probe with a 4” diameter. This is an improvement because the nominal spatial Nyquist frequency for that probe is 1688 Hz.

For sawtooth waves in one- and multi-dimensional environments, an extrapolated PAGE method was effectively used to calculate intensity magnitude and direction even far above the

spatial Nyquist frequency. This method is effective in free-field environments where there is at least one tone below the spatial Nyquist frequency. This method was also applied to two tones from separate sources. The correct intensity magnitude was obtained, but the direction error was equal to the separation angle between the speakers. The extrapolated PAGE method for separate sources would only be an effective method if the angular separation between two sources was small.

In a plane wave tube and an anechoic chamber, it was explored if the magnitude and direction of bandlimited white noise completely above the spatial Nyquist frequency could be calculated accurately using the phase unwrapping in the PAGE method. It was found for the plane wave tube case that with sufficient bandwidth and SNR, accurate intensity magnitude and direction could be obtained using the PAGE method for bands of noise that are completely above the spatial Nyquist frequency. However, the background noise of the setup could have aided in the success of the phase unwrapping. In the anechoic chamber, phase unwrapping could consistently be utilized to obtain the correct intensity magnitude and phase for the entire band of noise as long as there was a coherence of at least 0.1 for the band from 1500-1800 Hz ($f_N \approx 1688$ Hz). For both cases, successful phase unwrapping requires larger bandwidths for frequency bands of increasing frequency.

Two speakers playing the same signal in the anechoic chamber was another case that was explored. It was concluded that for small separation angles, the intensity magnitude could be calculated within a reasonable tolerance using the PAGE method and the intensity direction was half of the separation angle, as we expected. However, with increasing separation angles and increasing frequency the results deviated from what was expected. Possible explanations for these deviations are due to the speakers not broadcasting the signal at the same volume or over

the same path length, due to high reactive intensity at high angles of separation, and due to increasing probe size relative to a wavelength.

Narrowband sources above the spatial Nyquist frequency with added low-level broadband noise were measured to see if the low-level noise could aid in obtaining correct phase and therefore correct intensity magnitude and direction. It was found that within certain magnitude and angular constraints, the additive noise was effective in aiding the PAGE calculation. As an extension of this, fan noise was tested due to its low-level broadband noise combined with tones. It was found that the intensity magnitude and direction were both calculated very well even far above the spatial Nyquist frequency.

In almost every case, the PAGE method showed improved calculations over the traditional method. The PAGE method was shown to accurately calculate the intensity magnitude and direction of any narrowband source up to the spatial Nyquist frequency. Several techniques were employed to extend the bandwidth above the spatial Nyquist frequency as well, most notably the extrapolated PAGE method and the addition of low-level broadband noise to a narrowband source to aid in phase unwrapping. The only cases where the PAGE method did not improve on the traditional method were for intensity direction of sine waves and sawtooth waves above the effective spatial Nyquist frequency and intensity direction of two speakers playing the same tone.

5.2 Future work

As has been mentioned, all experimental work in this thesis has been done in sound fields that were mostly propagating. Future work could include repeating some of the measurements in semi-reverberant fields.

Although the extrapolated PAGE method used in this thesis was effective for some cases (see Section 2.4, Section 3.3, and Section 3.4), several improvements could be made to the extrapolated PAGE method to make it more widely applicable. The extrapolated PAGE method required some phase information below the spatial Nyquist frequency, usually in the form of a tone or fundamental of the sawtooth. Also, the assumption of a propagating field was necessary for it to work. Further, all of the frequency content above the spatial Nyquist frequency needs to be coming from approximately the same direction as the source with the tone below the spatial Nyquist frequency, or else significant errors result. One possible improvement would be to take into account all phase information below the spatial Nyquist frequency. Another, more significant improvement would be to indirectly extrapolate by using the phase information below the spatial Nyquist frequency and assumption of linear phase to make the necessary number of "unwraps," or 2π jumps, instead of imposing an unwrapped phase based on one point. The advantage of this is it is more based on the real data being taken above the spatial Nyquist frequency, and would likely increase the separation angle over which it could be effective.

There are a great many number of narrowband sources that occur in the real world. One test that could be done to extend this work would be to do tests with multiple sources, each playing a random assortment of tones above and below the spatial Nyquist frequency. Through some variation of the extrapolated PAGE method and other processing tools, it may be possible to extract which tone came from which source and the correct intensity magnitude and direction of each tone.

Near-field acoustical holography (NAH) is a method of using an array of microphones to measure a sound field, usually by measuring pressure at each sensor. Then, through analysis of the sound field, the measurement is "propagated" back to another location, such as the face of the

source. Many quantities such as particle velocity and intensity can be extrapolated to the surface of the source from the measurements, which can provide useful information such as the nature of the vibration and the regions of radiation of the source.[14] Even though pressure measurements with a single microphone at the measurement plane and a nearby reference microphone are the most common, there has been work showing that measuring different quantities can have advantages. For example, Harris[19] showed that by directly measuring the particle velocity the number of measurement points needed to get an equally accurate calculation of the other quantities at the source can be reduced. This improvement was achieved by using a spline interpolation that used both the pressure and the gradient of the pressure. Future work could use an intensity probe for measurements and use PAGE processing to obtain the estimate of the gradient of pressure required to perform the same interpolation and compare to Harris's results. Another example of a NAH method which utilizes energy quantities is broadband acoustic holography reconstruction from acoustic intensity measurements (BAHIM), which uses a multi-microphone probe for measurements and then is able to do all of the reconstruction from the intensity calculated from that probe.[18,57] However, BAHIM could potentially be improved using the PAGE method because the intensity calculations will be more accurate than traditional processing, at least up to the spatial Nyquist frequency. Previous work by Collins[58] for obtaining NAH results in semi-reverberant or reverberant fields using energy quantities could also potentially be improved using the PAGE method because it used a multi-microphone probe. Since NAH processing is done in the frequency domain, frequency by frequency, it is a form of processing narrowband signals. Through these three experiments and their analysis, it could be determined if the PAGE method can improve accuracy and possibly decrease the number of sensor positions needed for NAH.

Bibliography

1. J. A. Mann and J. Tichy, "Near-field Identification of Vibration Sources, Resonant Cavities, and Diffraction Using Acoustic Intensity Measurements," J. Acoust. Soc. Am. **90**, 720-729 (1991).

2. S. Gade, K. Ginn, O. Roth, and M. Brock, "Sound power determination in highly reactive environments using sound intensity measurements," Proc. Inter-Noise **83**, pp. 1047-1050 (1983).

3. F. Jacobsen, "Spatial sampling errors in sound power estimation based upon intensity," J. Sound Vib. **145**, 129-149 (1991).

4. F. J. Fahy, *Sound Intensity* (Thomson Press, Bury St Edmunds, Suffolk, Great Britain, 1995).

5. F. Jacobsen, "An overview of the sources of error in sound power determination using the intensity technique," Appl. Acoust. **50**, 155 - 166 (1997).

6. R. Hickling, P. Lee, and W. Wei,"Investigation of integration accuracy of sound-power measurement using an automated sound-intensity system," Appl. Acoust. **50**, 125 - 140 (1997).

7. ISO 11205:2003, Acoustics—Noise emmited by machinery and equipment - Engineering method for the determination of emission sound pressure levels *in situ* at the work station and at other specified positions using sound intensity (International Organization for Standardization, Geneva, Switzerland, 2003).

8. ISO 15186-1:2000, Acoustics—Measurement of sound insulation in buildings and of building elements using sound intensity—Part 1: Laboratory measurements (International Organization for Standardization, Geneva, Switzerland, 2000).

9. ISO 15186-1:2003, Acoustics—Measurement of sound insulation in buildings and of building elements using sound intensity - Part 1: Field measurements (International Organization for Standardization, Geneva, Switzerland, 2003).

10. ISO 9614-1:1993, Acoustics—Determination of sound power levels of noise sources using sound intensity - Part 1: Measurement at discrete points (International Organization for Standardization, Geneva, Switzerland, 1993).

11. ISO 9614-2:1996, Acoustics—Determination of sound power levels of noise sources using sound intensity - Part 2: Measurement by scanning (International Organization for Standarization, Geneva, Switzerland, 1996).

12. ISO 9614-3:2002, Acoustics—Determination of sound power levels of noise sources using sound intensity -Part 3: Precision method for measurement by scanning (International Organization for Standardization, Geneva, Switzerland, 2002).

13. ANSI/ASA S1.9:1996, Instruments for the Measurement of Sound Intensity (Acoust. Soc. Am., Melville, NY, 1996).

14. E. G. Williams, *Fourier acoustics: sound radiation and nearfield acoustical holography* (Academic press, 1999).

15. J. D. Maynard, E. G. Williams, and Y. Lee, "Nearfield acoustic holography: I. Theory of generalized holography and the development of NAH," J. Acoust. Soc. Am. **78**, 1395-1413 (1985).

16. F. Jacobsen and Y. Liu, "Near field acoustic holography with particle velocity transducers," J. Acoust. Soc. Am. **118**, 3139-3144 (2005).

17. F. Jacobsen and V. Jaud, "Statistically optimized near field acoustic holography using an array of pressure-velocity probes," J. Acoust. Soc. Am. **121**, 1550-1558 (2007).

18. T. Loyau, J.-C. Pascal, and P. Gaillard, "Broadband acoustic holography reconstruction from acoustic intensity measurements. I: Principle of the method," J. Acoust. Soc. Am. **84**, 1744-1750 (1988).

19. M. C. Harris, J. D. Blotter, and S. D. Sommerfeldt, "Obtaining the complex pressure field at the hologram surface for use in near-field acoustical holography when pressure and in-plane velocities are measured," J. Acoust. Soc. Am. **119**, 808-816 (2006).

20. S. D. Sommerfeldt and P. J. Nashif, "An adaptive filtered-x algorithm for energy- based active control," J. Acoust. Soc. Am. **96**, 300-306 (1994).

21. Y. C. Park and S. D. Sommerfeldt, "Global attenuation of broadband noise fields using energy density control," J. Acoust. Soc. Am. **101**, 350-359 (1997).

22. J. W. Parkins, S. D. Sommerfeldt, and J. Tichy, "Narrowband and broadband active control in an enclosure using the acoustic energy density," J. Acoust. Soc. Am. **108**, 192-203 (2000).

23. B. Xu, S. D. Sommerfeldt, and T. W. Leishman, "Generalized acoustic energy density," J. Acoust. Soc. Am. **130**, 1370-1380 (2011).

24. D. B. Nutter, T. W. Leishman, S. D. Sommerfeldt, and J. D. Blotter, “Measurement of sound power and absorption in reverberation chambers using energy density,” J. Acoust. Soc. Am. **121**, 2700-2710 (2007).

25. H.-E. De Bree, "An overview of microflown technologies," Acta Acust. united Ac. **89**, 163-172 (2003).

26. H.-E. De Bree, "The Microflown: An acoustic particle velocity sensor," Acoust. Aust. **31**, 91-94 (2003).

27. F. Jacobsen and H.-E. de Bree, "A comparison of two different sound intensity measurement principles," J. Acoust. Soc. Am. **118**, 1510-1517 (2005).

28. F. J. Fahy, "Measurement of acoustic intensity using the cross-spectral density of two microphone signals," J. Acoust. Soc. Am. **62**, 1057-1059 (1977).

29. G. Pavić, "Measurement of sound intensity," J. Sound Vib. **51**, 533-545 (1977).

30. J. Y. Chung, "Cross-spectral method of measuring acoustic intensity without error caused by instrument phase mismatch," J. Acoust. Soc. Am. **64**, 1613-1616 (1978).

31. F. Jacobsen, "Intensity Techniques," in *Handbook of Signal Processing in Acosutics* (Springer, New York, NY), pp. 1109-1127 (2008).

32. F. Jacobsen, "Sound Intensity," in *Springer Handbook of Acoustics* (Springer, New York, NY), pp. 1053-1075 (2007).

33. F. Jacobsen, "Random errors in sound intensity estimation," J. Sound Vib. **128**, 247-257 (1989).

34. A. F. Seybert, "Statistical errors in acoustic intensity measurements," J. Sound Vib. **75**, 519-526 (1981).

35. T. Loyau and J.-C. Pascal, "Statistical errors in the estimation of the magnitude and direction of the complex acoustic intensity vector," J. Acoust. Soc. Am. **97**, 2942-2962 (1995).

36. C. P. Wiederhold, K. L. Gee, J. D. Blotter, and S. D. Sommerfeldt, "Comparison of methods for processing acoustic intensity from orthogonal multimicrophone probes," J. Acoust. Soc. Am. **131**, 2841-2852 (2012).

37. J.-C. Pascal and J.-F. Li, "A systematic method to obtain 3D finite-difference formulations for acoustic intensity and other energy quantities," J. Sound Vib. **310**, 1093-1111 (2008).

38. C. P. Wiederhold, K. L. Gee, J. D. Blotter, S. D. Sommerfeldt, and J. H. Giraud, "Comparison of multimicrophone probe design and processing methods in measuring acoustic intensity," J. Acoust. Soc. Am. **135**, 2797-2807 (2014).

39. F. Jacobsen,"A simple and effective correction for phase mis-match in intensity probes," Appl. Acoust. **33**, 165-180 (1991).

40. T. Yanagisawa and N. Koike, "Cancellation of both phase mismatch and position errors with rotating microphones in sound intensity measurements," J. Sound Vib. **113**, 117-126 (1987).

41. T. Iino, H. Tatekawa, H. Mizukawa, and H. Suzuki, "Numerical evaluation of three-dimensional sound intensity measurement accuracies and a proposal for an error correction method," Acoust. Sci. Technol. **34**, 34-41 (2013).

42. D. C. Thomas, B. Y. Christensen, and K. L. Gee, "Phase and amplitude gradient method for the estimation of acoustic vector quantities," J. Acoust. Soc. Am. **137**, 3366-3376 (2015).

43. B. Y. Christensen, "Investigation of a New Method of Estimating Acoustic Intensity and Its Application to Rocket Noise." Master's thesis, Brigham Young University, Provo, UT, 2014.

44. J. A. Mann, J. Tichy, and A. J. Romano, "Instantaneous and time-averaged energy transfer in acoustic fields," J. Acoust. Soc. Am. **82**, 17-30 (1987).

45. J. A. Mann and J. Tichy "Acoustic intensity analysis: Distinguishing energy propagation and wave-front propagation," J. Acoust. Soc. Am. **90**, 20-25 (1991).

46. D. C. Ghiglia and M. D. Pritt, *Two-dimensional phase unwrapping: theory, algorithms, and software* (Wiley New York, 1998).

47. T. A. Stout, K. L. Gee, T. B. Neilsen, A. T. Wall, and M. M. James, "Source characterization of full-scale jet noise using acoustic intensity," Noise Control Eng. J. **63**, 522-536 (2015).

48. D. K. Torrie, E. B. Whiting, K. L. Gee, T. B. Neilsen, and S. D. Sommerfeldt, "Initial laboratory experiments to validate a phase and amplitude gradient estimator method for the calculation of acoustic intensity," Proc. Mtgs. Acoust. **23**, 030005 (2015).

49. K. L. Gee, T. B. Neilsen, S. D. Sommerfeldt, M. Akamine, and K. Okamoto, "Experimental validation of acoustic intensity bandwidth extension by phase unwrapping," J. Acoust. Soc. Am. **141**, EL357-EL362 (2017).

50. K. L. Gee, T. B. Neilsen, E. B. Whiting, D. K. Torrie, M. Akamine, K. Okamoto, S. Teramoto, and S. Tsutsumi, "Application of a Phase and Amplitude Gradient Estimator to Intensity-Based Laboratory-Scale Jet Noise Source Characterization," in *Berlin Beamforming Conference Paper BeBeC-2016-D3* (2016).

51. K. L. Gee, M. Akamine, K. Okamoto, T. B. Neilsen, M. R. Cook, S. Teramoto, and T. Okunuki, "Characterization of Supersonic Laboratory-Scale Jet Noise with Vector Acoustic Intensity," submitted to AIAA Aviation (2017).

52. E. B. Whiting, J. S. Lawrence, K. L. Gee, T. B. Neilsen, and S. D. Sommerfeldt, "Bias error analysis for phase and amplitude gradient estimation of acoustic intensity and specific acoustic impedance," J. Acoust. Soc. Am. **142**, 2208-2218 (2017).

53. E. B. Whiting, "Energy quantity estimation in radiated acoustic fields," Master's thesis, Brigham Young University, Provo, UT, 2016.

54. J. S. Lawrence, K. L. Gee, T. B. Neilsen, and S. D. Sommerfeldt, "Higher-order estimation of active and reactive acoustic intensity," Proc. Mtgs. Acoust. **30**, 055004 (2017).

55. M. R. Cook, K. L. Gee, S. D. Sommerfeldt, and T. B. Neilsen, "Coherence-based phase unwrapping for broadband acoustic signals," Proc. Mtgs. Acoust. **30**, 055005 (2017).

56. C. B. Goates, B. M. Harker, T. B. Neilsen, and K. L. Gee, "Extending the bandwidth of an acoustic beamforming array using phase unwrapping and array interpolation," J. Acoust. Soc. Am. **141**, EL407-EL412 (2017).

57. J.-C.Pascal, T. Loyau, and J. Mann III, "Structural intensity from spatial Fourier transformation and BAHIM acoustical holography method," Proc. Cong. On Structural Intensity and Vibrational Energy Flow, 197-204 (1990).

58. Z. A. Collins, K. L. Gee, S. D. Sommerfeldt, and J. D. Blotter, "Interior Fourier Near-field Acoustical Holography Using Energy Density," J. Acoust. Soc. Am. **9**, 040007 (2015).